e-HIGHWAY 2050

Modular Development Plan of the Pan-European Transmission System 2050

Contract number	308908	**Instrument**	Collaborative Project
Start date	1st of September 2012	**Duration**	40 months
WP4	**Modular development and operations**		
D4.1	**Operational validation of the grid reinforcements by 2050**		

		Date & Visa
Written by	R. Jankowski, M. Wilk (IEN) M. Haller, P. Centeno (Swissgrid) D. Petrescu (Transelectrica) P. Ziółek, M. Małecki (PSE) J. Setreus, K. Elkington (SvK) K. Máslo (Ceps) J. Warichet (Elia) C. Strotmann (Amprion) R. Pestana, N. Machado (REN) E. Carlini, S. Moroni (Terna) T. K. Vrana (Sintef) N. Grisey (RTE)	2015-12-23
Checked by	Rui Pestana, REN	2015-12-28
Validated by	Gérald Sanchis, Nathalie Grisey	2015-12-30

Project co-funded by the European Commission within the Seventh Framework Programme		
Dissemination Level		
PU	Public	X
PP	Restricted to other programme participants (including the Commission Services)	
RE	Restricted to a group specified by the consortium (including the Commission Services)	
CO	Confidential, only for members of the consortium (including the Commission Services)	

Document Information

General purpose

Task 4.1 assesses the operability of the 2050 scenarios and grid architectures. Deliverable D4.1 describes the four types of studies performed:

- Voltage levels for N-1
- Short circuit current levels
- Frequency stability
- Small signal stability

Change status

Revision	Date	Changes description	Authors
V1.0	21.09.2015	Contribution from report T.4.1.1 – Definition of strategy and framework to perform case studies for operational validation	M. Haller, P. Centeno, R. Jankowski, M. Wilk, D. Petrescu, M. Małecki, P. Ziółek, K. Elkington, J. Setreus, S. Moroni
V1.1	23.09.2015	Contribution from report T.4.1.2 • Assessment on tools and data formats to use in case studies • Preparation of grid data for system dynamic analysis	K. Máslo, P. Centeno, R. Jankowski, M. Wilk, J. Warichet, S. Moroni
V1.2	25.09.2015	Contribution from report T.4.1.5 – Curative remedial actions and technology performances to restore Pan-European Transmission System 2050 to normal operation after disturbances	E. Carlini
V1.3	29.09.2015	Contribution for the Executive Summary and Conclusion	S. Moroni
V1.4	29.09.2015	Contribution for the Frequency stability calculation: scenario X-7 strategy 3	K. Máslo
V1.5	30.09.2015	Contribution from report T.4.1.3 – Small signal stability	R. Jankowski, B. Sobczak, M. Wilk
V1.6	5.10.2015	Contribution for the Frequency stability calculation: scenario X-10 strategy 3 and X-16	K. Máslo
V1.7	13.10.2015	Contribution for the Small signal stability calculation.	M. Wilk, R. Jankowski
V1.8	13.10.2015	Contribution for the voltage analysis	R. Pestana, N. Machado
V1.9	16.10.2015	Contribution for the Short Circuit Current	R. Pestana, N. Machado
V1.10	19.10.2015	Contribution for the Short Circuit Current – 220 Kv	R. Pestana, N. Machado
V1.11	22.10.2015	Contribution for the Executive Summary and Conclusions	S. Moroni
V1.12	26.10.2015	Small remarks	R. Pestana
V1.13	20.11.2015	Endorsement of RTE comments	S. Moroni
V1.14	23.11.2015	Endorsement of comments	R. Pestana
V2.0	04.12.2015	Complete reorganisation of the document (incomplete)	T. K. Vrana
V2.1	10.12.2015	Complete reorganisation of the document (complete)	T. K. Vrana
V3.0	15.12.2015	Re-reorganisation of the document	T. K. Vrana
V4.0	18.12.2015	Significantly shortening the report	N. Grisey
V4.1	21.12.2015	Fixing formatting issues and minor improvements	T. K. Vrana
V4.2	21.12.2015	Corrections in chapters 2, 6 and appendix C and D	K. Máslo, M. Wilk, R. Jankowski, S.Moroni
V4.3	28.12.2015	Final remarks	N. Grisey
V4.4	28.12.2015	Final comments	R. Pestana

Executive Summary

The work package WP4 - Task T4.1 - received from WP2 a portfolio of possible scenarios and grid architectures capable of overcoming weak points and congestions of the future 2050 pan-European transmission grid. The e-Highway2050 **scenarios** are:

- X-5 (Large Scale RES)
- X-7 (100%RES)
- X-10 (Big & Market)
- X-13 (Fossil & Nuclear)
- X-16 (Small & Local)

Under task 4.1, two **regimes** are considered for each scenario:

- Winter Peak
- Summer Low

All of the analysed scenarios have been prepared with two possible grid development **strategies** suggested by WP2:

- Strategy 2 - which consists of grid development using HVAC overhead lines
- Strategy 3 - that uses HVDC cable lines

The set of a scenario, regime and strategy forms a **configuration**, which is subject to assessments.

AC power flow models of the continental European system is provided by WP2 (see deliverable 2.4). The calculated power flows, as well as the corresponding outputs from the system simulations (see deliverable 2.3) are used as inputs to the task.

To completely assess the operability of the system, different phenomena should be assessed. These phenomena are listed in Table I. To study such complex phenomena 35 years ahead is unrealistic due to the uncertainty on the detailed datasets, which influence the results significantly. However, exploratory studies can be performed on some test cases to highlight possible phenomenon and anticipate the challenges and solutions. In that perspective, the following issues were considered in the task 4.1 of the e-Highway2050 project:

- Short circuit current levels
- Voltage drop
- Short-term frequency stability
- Small signal stability

Regarding short circuit currents, the maximal value appeared to be within acceptable range. However, the contribution of power electronics to short circuit currents should be further investigated and especially the impact on the minimal short circuit currents.

For voltage stability, the analyses did not show any un-manageable voltage drop in the considered configurations. Only one unstable situation was identified but it can be avoided by limiting the maximal capacity of a single line. However, some configurations could not be considered, as they were not convergent, these situations face very likely significant voltage issues. This should be further investigated with methodologies and tools suitable for the analysis of very different power flow configurations.

In all the situations analysed, the frequency was kept within acceptable range after significant disturbance. This was achieved thanks to the participation of wind farms to primary control. More-detailed studies of the behaviour of the system with significant penetration of power electronics are planned in the European Migrate project.

Regarding small signal stability, only one case showed a negative damping, but it is still on the range of power system stabilisers.

To fully assess the impacts of the current changes in the power system, further studies are required. To do so, improvements in the quality of the available data, in the modelling of new technologies and in the methods will be necessary.

Table I. Operational validation phenomena and their consideration in the project

Phenomena considered for operational validation		**Consideration within e-Highway2050**
Current limits	Line loading	Addressed in task 2.4
	Short-circuit current levels	Addressed in task 4.1
Voltage limits	Steady-state voltage levels: within limits in N situation	Addressed in task 2.4
	Voltage stability: risk of voltage collapse	Addressed in task 4.1
	Temporary voltage deviations: temporary overvoltages following an event	No dedicated studies as part of the project
Frequency stability	Long-term frequency stability	No dedicated studies as part of the project
	Short-term frequency stability	Addressed in task 4.1
Rotor angle stability	Small signal stability	Addressed in task 4.1
	Transient stability	No dedicated studies as part of the project

Abbreviations

CCGT	Combined Cycle Gas Turbine
CE	Continental Europe
CIM	Common Information Model
CSP	Concentrated Solar Power
DER	Distributed Energy Resource
DFIG	Double Fed Induction Generator
DoW	Description of Work
DSR	Demand Side Response
ESS	Energy Storage System
FACTS	Flexible AC Transmission Systems
FC	Full Converter connected generator
FPC	Full Power Converter
FSM	Frequency Sensitive Mode
HVDC	High Voltage Direct Current
IIDS	Improved Interface and Decision Support
LFC	Load Frequency Control
LFSM-O	Limited Frequency Sensitive Mode – Over frequency
LFSM-U	Limited Frequency Sensitive Mode – Under frequency
MV	Medium voltage (distribution level)
NC RfG	Network Code - Requirements for Grid Connection
PMG	Permanent Magnet synchronous Generators
PSP	Pumped Storage hydro Plant
PV	Photovoltaic
RAW	abbreviation for power flow input data in PSS/E data format
RES	Renewable Energy Sources
RoR	Run of River hydro plant
SDC	System Development Committee
SMES	Superconducting Magnetic Energy Storage
SPD	System Protection & Dynamic ENTSO-E group (under regional group CE)
TES	Thermal Energy Storage
TYNDP	Ten Years Network Development Plan
(U)HVAC	(Ultra) High Voltage Alternating Current
UPFC	Unified Power Flow Controller
VSC	Voltage Source Converter
WP	Work Package

Glossary

Common Model	Data set, which can be used by participants of WP4 for particular studies
Grid Architecture	Network topology including HVDC connections
Scenario	e-Highway2050 scenario prepared by WP1 and described in [37] is one alternative image of how the future of European Electricity Highways [37] could unfold
Regime	A specific operational situation subject to analysis. This is either Summer Low or Winter Peak
Strategy	A specific way to reinforce the grid. This is either Strategy 1 (HVAC) Strategy 2 (HVAC with detour) or Strategy 3 (HVDC)
Configuration	A set of scenario, regime and strategy, which is subject to analysis
SPD Standard Model	Simple dynamic models for exciter and prime movers system with initial or tuned parameters

Table of Contents

List of Tables

List of Figures

1. Introduction

1.1. Scope

The significant changes in the localisation and types of generation, as well as the new grid architectures foreseen by the e-Highway2050 project can create significant challenges for the operation of the grid. The following key impacting factors can be mentioned:

- The increasing penetration of renewable energy sources
- The increasing power exchanges
- The increasing number of connections realised with HVDC

The task 2.3 of the e-Highway2050 project studied the European power flows only on a zonal level (100 clusters) with an equivalent grid model. This approach cannot identify all the overloads that could occur in the real complete network. In addition, the zonal power flows are done under the DC approximation, hiding possible voltage issues. That is why task 2.4 performed some AC power flows on a complete network model. The analysis was limited to continental Europe due to data availability. It showed that only limited overloads occur during N-1 contingencies and they could be overcome by local reinforcements. Moreover, no major voltage problem was highlighted.

To completely assess the operability of the system, even more phenomenon should be assessed, they are listed in the table below. To study such complex phenomena 35 years ahead is unrealistic due to the uncertainty on the detailed datasets, which influence the results significantly. However, exploratory studies can be performed on some test cases to highlight possible phenomena and anticipate the challenges and solutions. In that perspective, the following issues are considered in the task 4.1 of the e-Highway2050 project:

- Short circuit levels
- Voltage stability
- Short-term frequency stability
- Small signal stability

For each type of study, a theoretical background is given in this report. The assumptions and models are described and the simulation results are presented.

The general purpose of task 4.1 is not to conclude definitely on the above-mentioned phenomenon up to the year 2050, but more to pave the way for further in-depth analysis. Indeed, to consider them completely requires a dedicated project and is out of the scope of the e-Highway2050 project.

Table 1.1. Operational validation phenomena and their consideration in the project

Phenomena considered for operational validation		Consideration within e-Highway2050
Current limits	Line loading	Addressed in task 2.4
	Short-circuit current levels	Addressed in task 4.1
Voltage limits	Steady-state voltage levels: within limits in N and N-1 situations	Addressed in task 2.4
	Voltage stability: risk of voltage collapse	Addressed in task 4.1
	Temporary voltage deviations: temporary overvoltages following an event	No dedicated studies as part of the project
Frequency stability	Long-term frequency stability	No dedicated studies as part of the project
	Short-term frequency stability	Addressed in task 4.1
Rotor angle stability	Small signal stability	Addressed in task 4.1
	Transient stability	No dedicated studies as part of the project

1.2. Inputs from WP2

Five representative **scenarios** were selected in WP1 and quantified in WP2:

- X-5 (Large Scale RES)
- X-7 (100% RES)
- X-10 (Big & market)
- X-13 (Large Fossil Fuel & Nuclear)
- X-16 (Small and Local)

Scenario X-5 is mostly based on centralised RES, but also nuclear power plants are included. X-7 is purely based on RES, both centralised and decentralised. X-10 is based on a broad mix of generation technologies. X-13 relies mostly on conventional sources. X-16 represents a decentralised solution based on local embedded RES generation and does not require a huge transmission system development. More details on the scenarios can be found in Appendix I and [37]. The scenarios are detailed in deliverables D1.2 and D2.1 of the project.

Two operational **regimes** are considered (see Table 1.2)

- Winter Peak
- Summer Low

Table 1.2. Scenarios and corresponding regimes

Scenario	Winter Peak	Summer Low
X-5	Nov. 27th – 6 pm	Jun. 23rd – 2 pm
X-7	Jan. 9th – 6 pm	Jun. 23rd – 1 pm
X-10	Nov. 26th – 6 pm	Jun. 24th – 1 pm
X-13	Nov. 27th – 6 pm	Jun. 6th – 2 am
X-16	Nov. 27th – 6 pm	Jun. 23rd – 1 pm

All of the four analysed scenarios have been prepared with two possible grid development **strategies** suggested:

- Strategy 2 - which consists of grid development using HVAC overhead lines
- Strategy 3 - that uses HVDC cable lines

The set of a scenario, regime and strategy forms a **configuration**, which is subject to assessments.

AC power flow models of the continental European system were created by WP2 (see deliverable 2.4). AC power flows were run within the task 2.4 of the project and serve as the basis of the work for the task 4.1 described in this report. It should be noted that for three cases: X-5 winter peak, X-5 summer low and X-7 winter peak, no convergent power flows could be created. Indeed, the flows in these situations are extremely different from the starting case (2030) and need more-advanced methods to be studied. As a result, those three cases could not be considered either during the task 4.1 (except for frequency stability, which does not require a convergent power flow).

To create the power flows, task 2.4 scaled up the generation and demand from the starting case (2030) to match the results of the system simulations performed in task 2.3. This approach was chosen due to the difficulty to localise the generation and demand in all the European substations at the 2050 horizon. The consequence is that the types of generation are not matching the results of the system simulations where the generation and demand adequacy was considered with details. This does not influence the power flow calculations but is critical for the analyses of task 4.1 when the types of generation have impact on the results. However, except for frequency stability, the generation types were not corrected in task 4.1.

2. Short-Circuit Current Level Calculations

The short-circuit current contribution provided by the new renewable sources and the HVDC network components could create challenges for the future system. Indeed, an important amount of the generation units, based on conversion through power electronics, are presently characterised by low short-circuit currents. HVDC network might connect large amounts of power to single points, with zero fault level in-feed. These new technical solutions challenge selective isolation of faults by protection systems, with potential impacts on safety, generation and network equipment damage and possible extension of incidents on wider areas.

2.1. Tool and Models

PSS/E computation software was chosen to perform the analysis.

The short circuit current depends of the amount of generation and the generation type since the contribution for the short circuit current depends of the internal impedance. Synchronous machines, asynchronous machine and full decoupled machine for wind and solar have different response.

The AC power flow models from WP2 were used as inputs of the short circuit calculation. It should be noted that the generation types in these power flows are not 100% correct (see explanations in the introduction), influencing the short circuit calculations.

Although short circuit are dynamic phenomena, they are commonly analysed with steady state tools. Their analysis requires additional data compared to a simple power flow: the reactance of the synchronous machines are required, as well as the short circuit contribution of power electronic devices (RES generation and HVDC). For task 4.1, the following assumptions were taken:

- The reactances of the synchronous machines come from the dataset provided.
- The short circuit contribution of PV and wind generations is similar has other generation. In the PSS/E model we are not able to describe the type of generation. It's expected for 2050 that PV and Wind can provide the same amount of short circuit contribution.
- The short circuit contribution of HVDC is neglected.

2.2. Test Cases

For scenarios X-10, X-13, and X-16 the two strategies (AC or DC reinforcements) and the two regimes (Summer Low and Winter Peak) were analysed. For X-7, only the Summer Low was analysed and no situation for X-5 as the simulation requires a convergent power flow.

2.3. Methodology

As usually for this type of analysis, only 3-phase short circuits are analysed.

Short-circuit currents must not exceed the breaking capacity of all the devices installed in the respective node or designed to eliminate the fault. As a result, the maximal short circuit currents are discussed for each case.

2.4. Results

2.4.1. 380, 400 and 500 kV System

Based on the cases that converge for Continental Europe, PSS/E computation software was used to compute the total short circuit current in every Very High Voltage bus. The results for 380, 400 and 500 kV is showed in Figure 2.1.

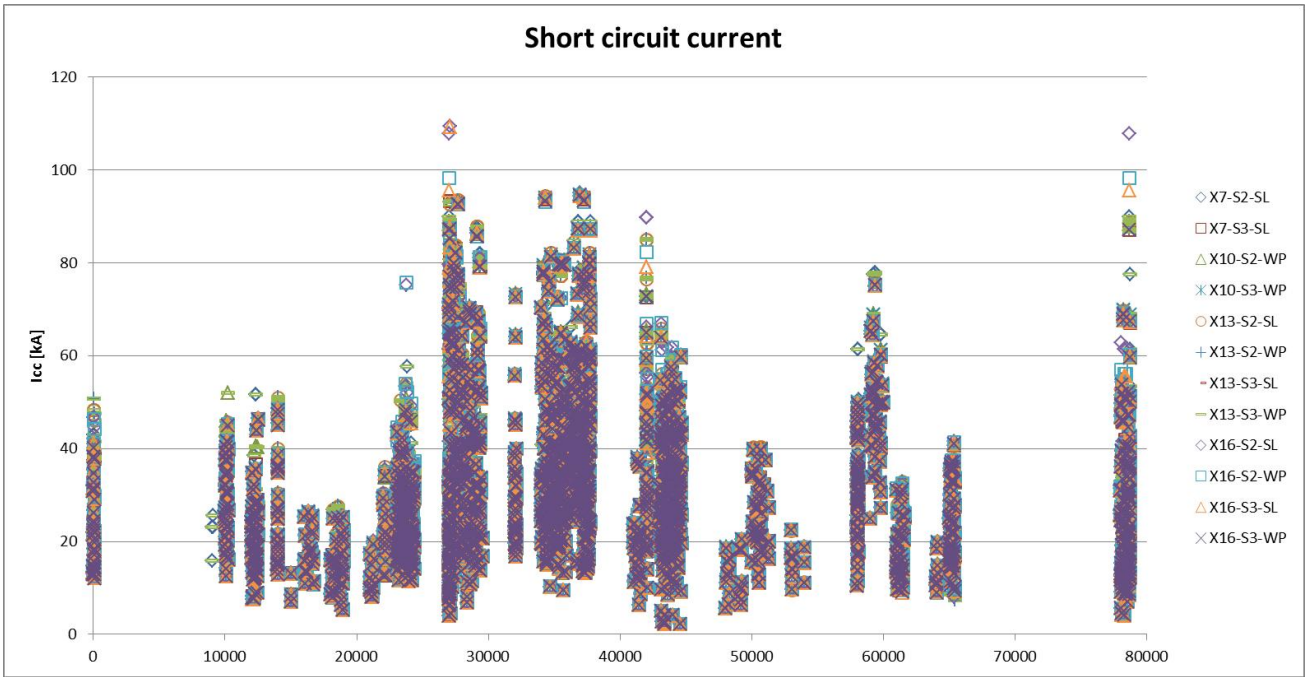

Figure 2.1. Short circuit current for 380, 400 and 500 kV nodes

In all cases, the maximum Icc is 95 kA, with the exception of X-16 scenario were the maximum values reach 109 kA. The results are summarised in Table 2.1. The maximum Icc that the circuit breakers are able to deal is 80 kA.

Table 2.1. Maximum Icc results

Scenario	Regime	Strategy	Maximum Icc (kA)	Country
X-7	Summer Low	2	95.1	DE
		3	94.4	DE
X-10	Winter Peak	2	94.8	DE
		3	94.7	DE
X-13	Summer Low	2	94.6	DE
		3	94.6	DE
	Winter Peak	2	95.0	DE
		3	94.9	DE
X-16	Summer Low	2	**109.3**	**FR**

		3	**109.2**	**FR**
	Winter Peak	2	98.2	FR
		3	94.5	DE

This Icc is the total short-circuit current at the busbar. Of course, the circuit breaker will cut its contribution to the Icc that is less than the total. The short circuit histogram is displayed in Figure 2.2.

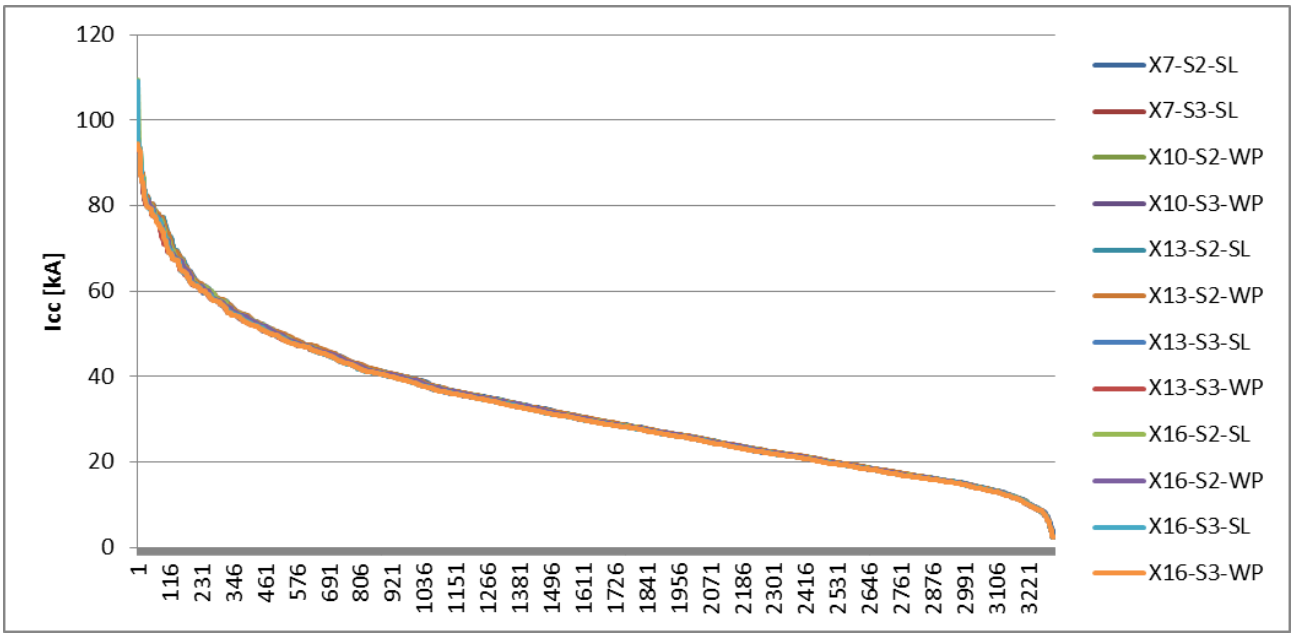

Figure 2.2. Short circuit histogram for 380, 400 and 500 kV nodes

There is no big difference of the Icc related to the scenario. To see the details of the higher values, Figure 2.3 shows the top 200 nodes in CE.

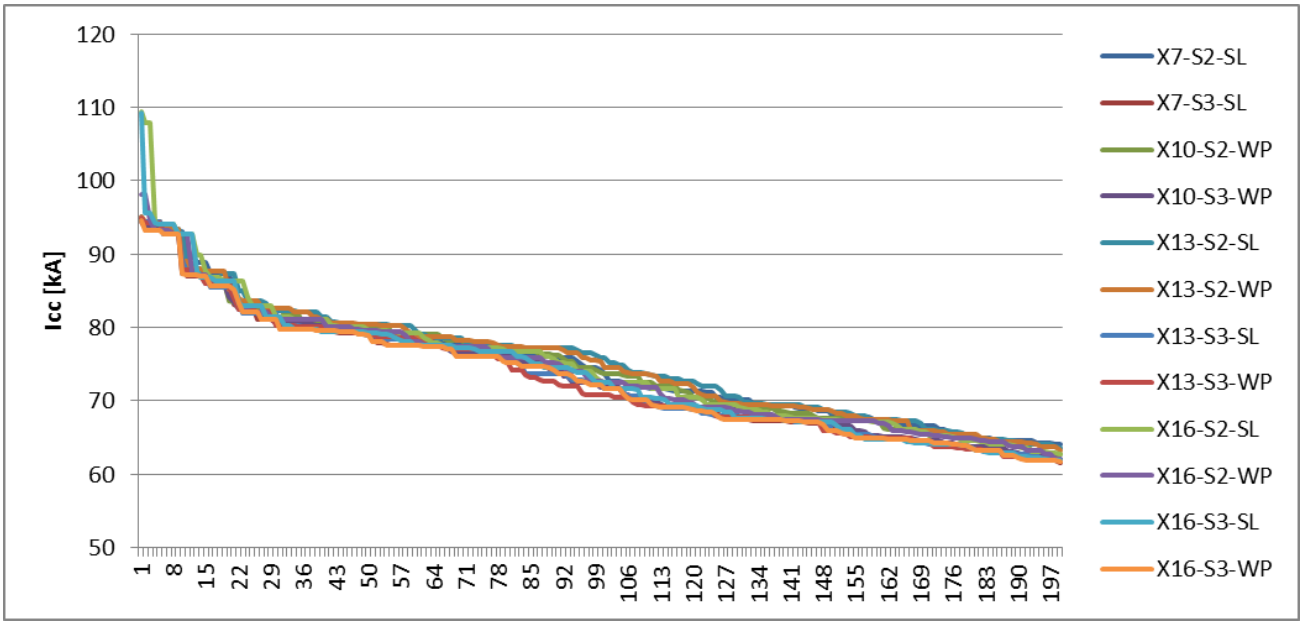

Figure 2.3. Top short circuit histogram for 380, 400 and 500 kV nodes

2.4.2. 220 kV System

Based on the configurations that converge for Continental Europe, PSS/E computation software was used to compute the total short circuit current in every HVH bus. The for 220 kV is showed in Figure 2.4.

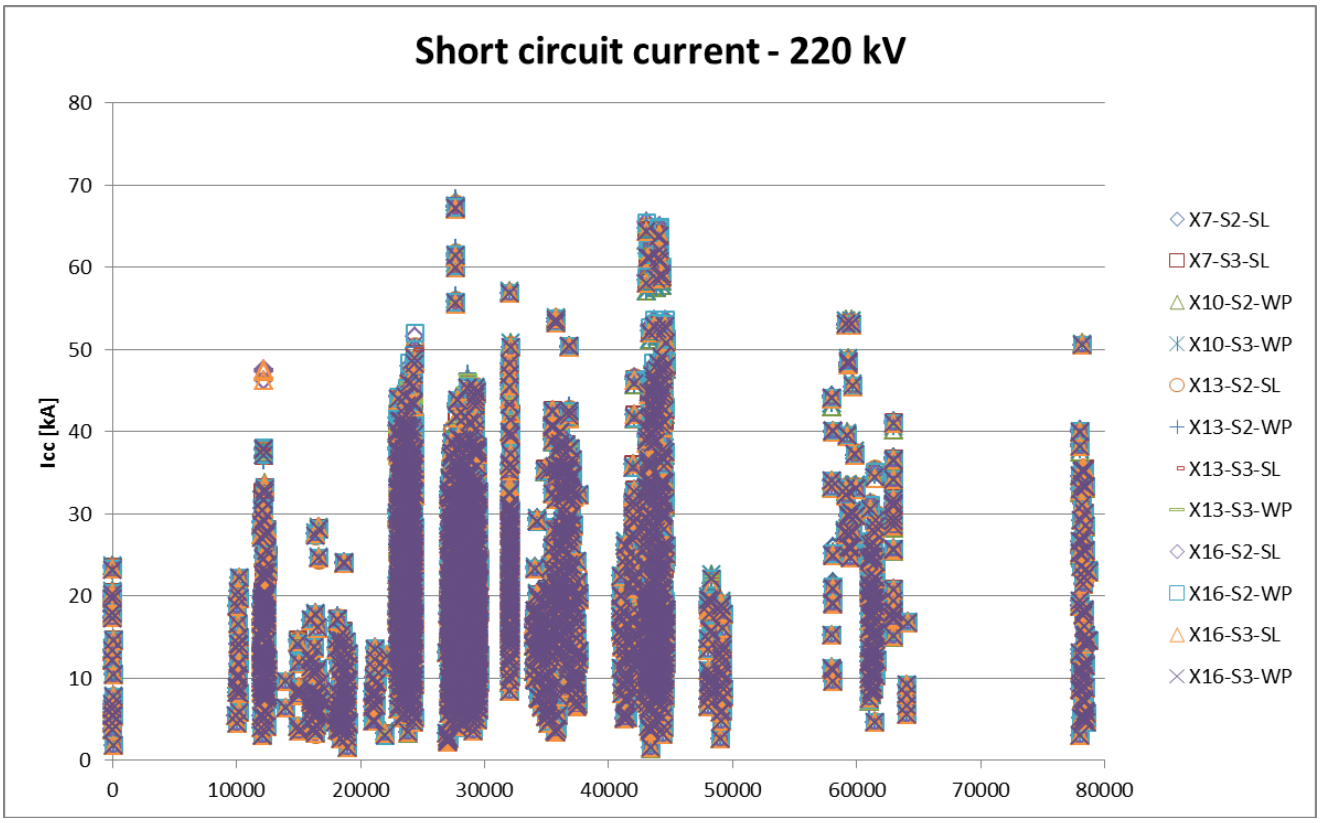

Figure 2.4. Short circuit current for 220 kV nodes

In all cases, the maximum Icc is 68 kA and is observed in France. The results are summarised in Table 2.2. The normal values are in the range of 40 to 50 kA now, but in 2050 since we will have more install capacity this level of 60 to 70 kA is acceptable.

Table 2.2. Maximum Icc results for 220 kV

Scenario	Regime	Strategy	Maximum Icc (kA)	Country
X-7	Summer Low	2	67.4	FR
		3	67.1	FR
X-10	Winter Peak	2	67.9	FR
		3	67.4	FR
X-13	Summer Low	2	67.6	FR
		3	66.9	FR

	Winter Peak	2	**68.4**	FR
		3	67.7	FR
X-16	Summer Low	2	67.2	FR
		3	67.0	FR
	Winter Peak	2	67.3	FR
		3	67.1	FR

There is no big difference of results due to the scenario. The short circuit histogram is displayed in Figure 2.5.

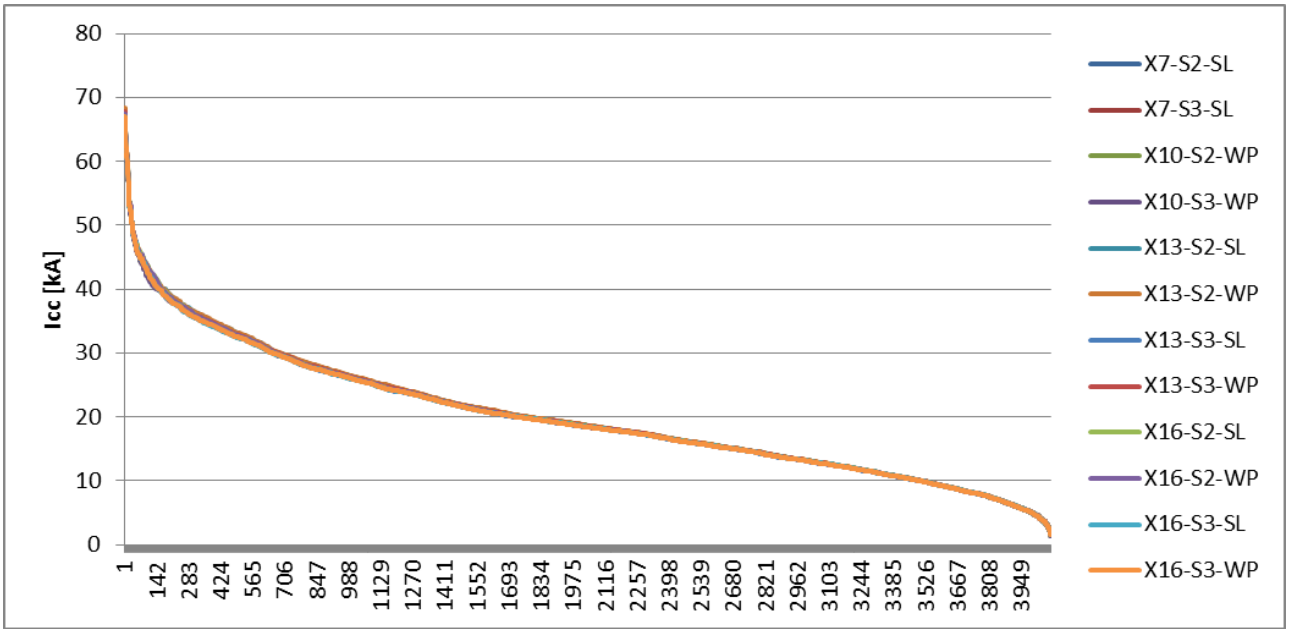

Figure 2.5. Short circuit histogram for 220 kV nodes

To see the details of the higher values, Figure 2.6 shows the top 200 nodes in CE.

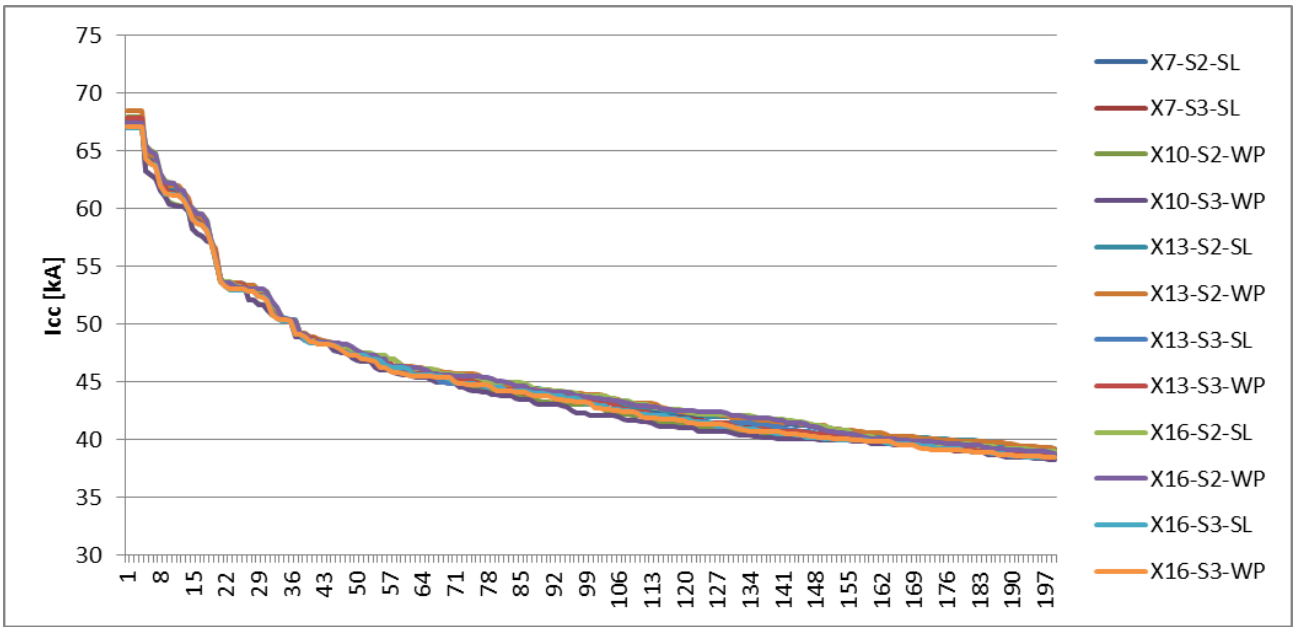

Figure 2.6. Top short circuit histogram for 220 kV nodes

2.5. Conclusion

The test cases analysed under T2.4 did not show any major issue regarding the maximal short circuit currents. However, the contribution of power electronics to short circuit currents should be further investigated and especially the impact on the minimal short circuit currents. Indeed, they may become even more critical due to the limited short-circuit contribution of power electronics. As a result, some faults could be missed by the protection devices.

3. Voltage Stability

One of the basis of the Network Code on Operational Security [14] is the responsibility of TSOs to keep voltages within Operational Security Limits. The origin of the requirement of keeping network voltages within a range is the limitation of operating voltage conditions of the equipment connected to the power system. This results in providing these elements with under- and over-voltage protective systems. Tripping these elements may lead to unacceptable voltage deviations and finally to cascading outages. The reasons to consider the voltage conditions for the period up to 2050 are:

- A strong development in electricity system infrastructures in the recent years, especially increasing volume of lines
- Implementation of internal electricity market. Technical functions necessary for stable system operation that today are provided by large synchronous generators will be delivered by the new players and will be significantly based on the provisions established by the Grid connection Network Codes. Market decisions leading to highly fluctuating allocation of generation will also affect regional system dynamics.
- Low carbon future of Europe, which involves increasing levels of non-synchronously connected RES while decreasing level of synchronous generators. Displacement of conventional generation in favour of non-synchronously connected RES directly affects the system in terms of all voltage limits phenomena. There is a reduction of reactive reserves from synchronous generation and a reduction in the number of voltage stabiliser devices. Emergence of converter-based generators will put emphasis on concerns related to voltage control capabilities.
- Distributed generation. The structure of generation is evolving and there will be an increase in the share of distributed generation that is usually connected to OSDs grid and on the other hand, a decrease in the share of high capacity combustion plants equipped with synchronous machines connected mostly to EHV grid.
- Long distance bulk power-flows will put emphasis on voltage stability issues and will further stress the reduction of reactive reserves from synchronous generation. The long distance bulk power flows are due to concentration of RES in areas with low power consumption and RES power needs to be transmitted to areas with high load. The connections between areas with high wind and high load (which are often very distant) usually need to be developed.
- New capabilities, devices and solutions such as Demand Side Response, FACTS and HVDC connections will provide significant changes to network performance
- As demand still grows, the voltage stability conditions are weakened unless the power network is developed.
- As RES generation level is weather (wind) determined, fast fluctuations of RES power require appropriate system response, which includes also voltage response.
- Increased use of underground cables
- Three assessments of voltage limits are usually performed: steady-state voltage levels, voltage stability and temporary voltage deviations. The first one was addressed within task 2.4 whereas task 4.1 addressed the second one.

3.1. Tool and Models

PSS/E computation software was chosen to perform the analysis.

A DC power flow model on an equivalent grid is not suitable for voltage analysis thus the AC power flow models provided by task 2.4 were directly used for the analysis. It should be noted that the mapping of generation types in the models from task 2.4 is not completely correct and thus cannot reflect with precision the real behaviour of the system in terms of voltage (provision of reactive power can depend on the type of generators).

The provision of reactive power by generators follows the 2030 model by ENTSOE. The provision of reactive power by HVDC is not considered.

3.2. Test Cases

Only converging configurations in N situation could be studied. These converging configurations are reminded in the table below.

Table 3.1. Nodal configurations analysed

Scenario	Regime	Strategy 2	Strategy 3
X-5	Summer Low	Not converged	Not converged
	Winter Peak	Not converged	Not converged
X-7	Summer Low	Converged	Converged
	Winter Peak	Not converged	Not converged
X-10	Summer Low	Not converged	Not converged
	Winter Peak	Converged	Converged
X-13	Summer Low	Converged	Converged
	Winter Peak	Converged	Converged
X-16	Summer Low	Converged	Converged
	Winter Peak	Converged	Converged

3.3. Methodology

The objective was to perform voltage analysis of the nodal network with the reinforcements selected for the strategies 2 and 3, by comparing the voltage difference when the grid losses one of the reinforcements (N-1). It was assumed that the existing lines, cables and transformers meet the N-1 security rule.

According to Article 10 [14] Voltage control and Reactive Power management of Network Code on Operational Security, Operation Security Limits are specified in Table 3.2 and Table 3.3.

Table 3.2. Voltage ranges for reference voltages defined by TSOs between 110 kV to 300 kV

Synchronous Area	Voltage range
Continental Europe	0.90 pu – 1.118 pu
Nordic	0.90 pu – 1.050 pu
Great Britain	0.90 pu – 1.100 pu
Ireland	0.90 pu – 1.118 pu
Ireland offshore	0.90 pu – 1.100 pu
Baltic	0.90 pu – 1.120 pu

Table 3.3. Voltage ranges for reference voltages defined by TSOs between 300 kV and 400 kV

Synchronous Area	Voltage range
Continental Europe	0.90 pu – 1.05 pu
Nordic	0.90 pu – 1.05 pu
Great Britain	0.90 pu – 1.05 pu
Ireland	0.90 pu – 1.05 pu
Ireland offshore	0.90 pu – 1.10 pu
Baltic	0.90 pu – 1.10 pu

Within task 4.1, it was decided to classify a case as unstable if the voltage drop following a N-1 contingency was above 25%.

3.4. Results

Below are presented the results of the voltage analysis by simulating the loss of each transmission grid reinforcements, using the base case (N) voltage as the normalised voltage. Analysing the results for the 12 configurations shows that only in one there is a voltage collapse since the voltage drop is 25%. The results are displayed in Table 3.4.

Table 3.4. Voltage level analysis results

Scenario	Regime	Strategy	Maximum voltage drop [pu)	Assessment
X-7	Summer Low	2	-0.0307	Stable
		3	-0.0331	Stable
X-10	Winter Peak	2	-0.0200	Stable
		3	**-0.0421**	Stable
X-13	Summer Low	2	-0.0191	Stable
		3	**-0.0456**	Stable
	Winter Peak	2	**-0.0961**	Stable
		3	**-0.2525**	**Not Stable**
X-16	Summer Low	2	-0.0191	Stable
		3	-0.0187	Stable
	Winter Peak	2	-0.0177	Stable

		3	-0.0837	Stable

In the scenario X-13 Strategy 3 regime Winter Peak both contingency R1 and R2 that represent HVDC link to France with 6519 MW, causes a voltage drop in France. It proves that the integration of link of more than 6 GW between UK and France seems inoperable. A better solution is to consider different parallel lines to realise transmission requirements of significant power. This will prevent this type of issues.

Plots with details on the voltage level analysis can be found in Appendix H.

3.5. Conclusion

The analyses performed in task 4.1 did not show any un-manageable voltage drop in the considered configurations. Only one unstable situation was identified but it can be avoided by limiting the maximal capacity of a single line. However, some configurations could not be considered as they were not convergent, these situations face very likely significant voltage issues. This should be further investigated with methodologies and tools suitable for the analysis of very different power flow configurations.

4. Frequency Stability Assessment

Frequency stability deals with the ability of a power system to maintain steady frequency following a disturbance resulting in a significant imbalance between generation and load Three main causes for frequency instability exist:

- large generation or load outage
- forecast errors (especially in connection with the variable RES generation)
- separation of part of network (islanded operation)

According to ENTSO-E [2]:

"Frequency Stability means the ability of the Transmission System to maintain stable Frequency in N-Situation and after being subjected to a Disturbance."

According to [8]:

"Frequency Stability is concerned with the ability of a power system to maintain steady frequency within a nominal range following a severe system upset resulting in a significant imbalance between generation and load. It depends on the ability to restore balance between system generation and load, with minimum loss of load. Instability that may result occurs in the form of sustained frequency swings leading to tripping of generating units and/or loads."

In normal operation, the electric power system is characterised by the balance between the electrical power consumed by the loads and the power provided by the prime movers (turbines) of the generators. In case there is a sudden disconnection of load or generation, this balance is no longer kept, leading the system frequency to deviate from its nominal value.

In the first instants after the disturbance, the kinetic energy stored in the rotating masses of the generators is used in order to provide the energy required by the loads (in case of a generation trip). The energy consumed by the loads will therefore be supplied at the expense of reducing the system frequency. Therefore, a control system is required in order to arrest the frequency decay, keep it within acceptable values, and in the end bring it back to its nominal value. The control loop in charge of providing the initial response of the turbines required to stop the frequency decay is the Primary control. The loop responsible for bringing the frequency back to its nominal value is the secondary control. There is an additional loop, called Tertiary control, which is responsible for restoring the reserve band of the secondary control.

Figure 4.1 shows the structure of the different control loops responsible for restoring the frequency after a disturbance according to [1].

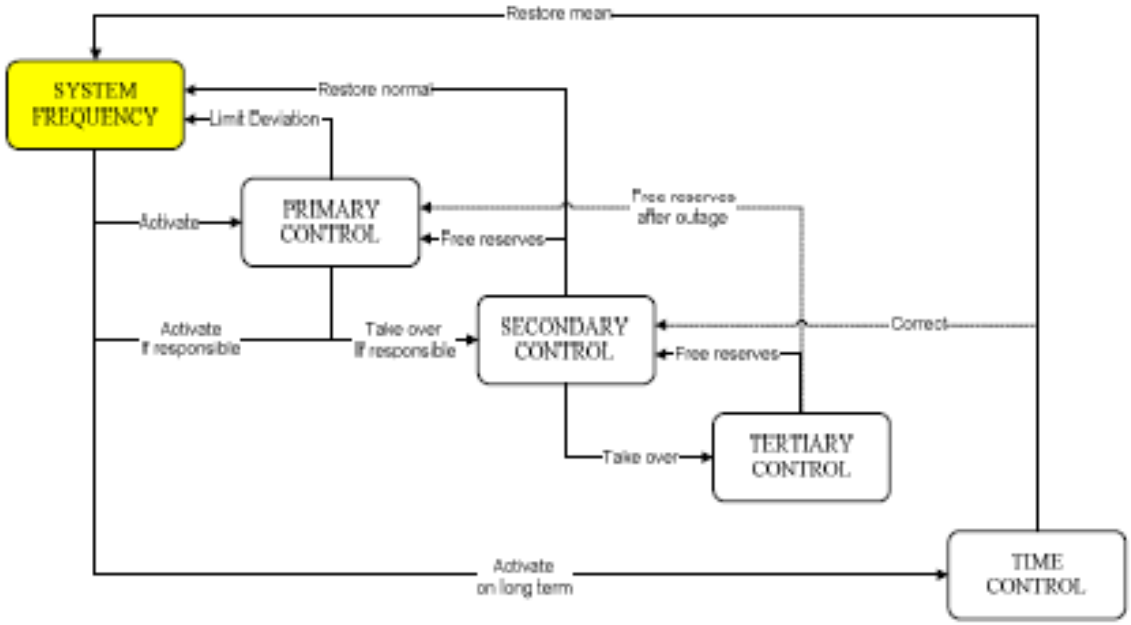

Figure 4.1. Overview of the structure of the different frequency control loops [1]

The time frame of each of the control loops is shown in Figure 4.2.

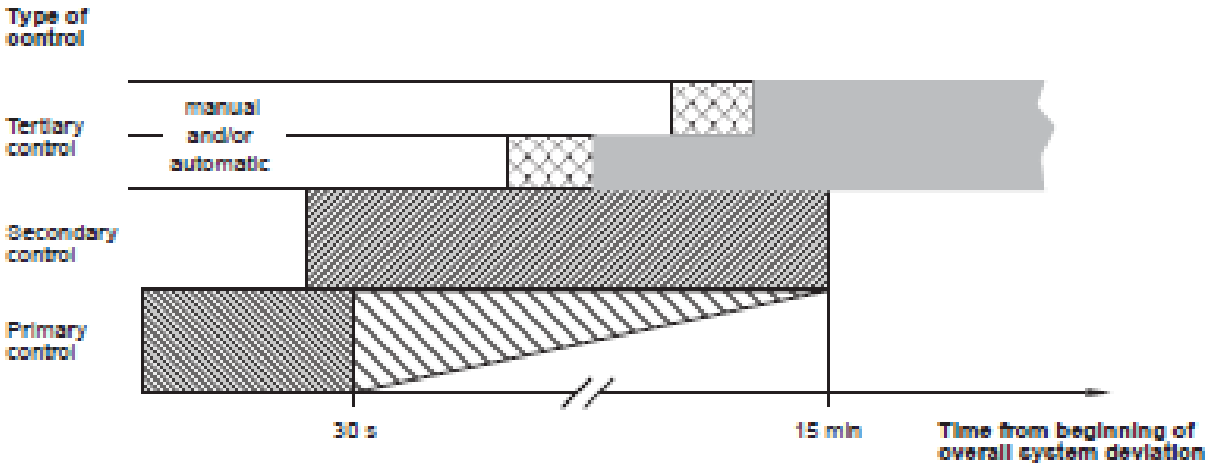

Figure 4.2. Time frame of each of the frequency control loops [1]

Frequency stability is sometimes also referred to as short-term adequacy.

The initial rate of change of the frequency can be calculated according to the following expression, already proposed in [6]:

$$\frac{df}{dt} = f_{base} \cdot \frac{\Delta P_{step}}{2 \cdot H_{eq}}$$

where $\frac{df}{dt}$ is the derivative of the frequency in [Hz/s], f_{base} is the system base frequency in [Hz], ΔP_{step} is the magnitude of the disturbance in [pu] and H_{eq} is the equivalent inertia constant of the system in [s]. the magnitude of the disturbance and the equivalent inertia constant are referred to the same base power. For convenience, the base power can be

chosen as the sum of the nominal powers of the generating units that remain connected. Therefore, and according to the previous equation, the main variables influencing the initial rate of decay of the system frequency are:

- Size of the disturbance: the larger the disturbance the faster the frequency will initially vary
- System inertia: the larger the inertia the slower the frequency will initially vary

With the trend of connection of RESs to the Transmission system, the conventional units will be gradually replaced by wind or solar power plants. The reduction of inertia provided by conventional generation (synchronous generators) will be significant in the future. Therefore, under scenarios with a large penetration of renewables, the inertia of the system can be significantly reduced, leading to faster and larger frequency deviations, namely:

- When a large loss of generation or load occurs the frequency will vary faster than in the current situation due to the lower inertia
- Besides, when the tripped generator is a conventional unit the inertia will be additionally reduced and the system state become even worse.

Once the frequency starts to change, the Primary Control will try to increase/decrease the power of the generating units in order to restore the balance between the generation and the load. The Primary control consists basically of a proportional control, so that when the balance is restored and a steady state is reached, there will be a frequency error. The size of the error depends on the gain of the proportional control. The inverse of this gain is called *droop* and defines a linear relationship on how the power of a generating unit will change depending on the frequency variations (see Figure 4.3). The Primary control response time is in the order of seconds.

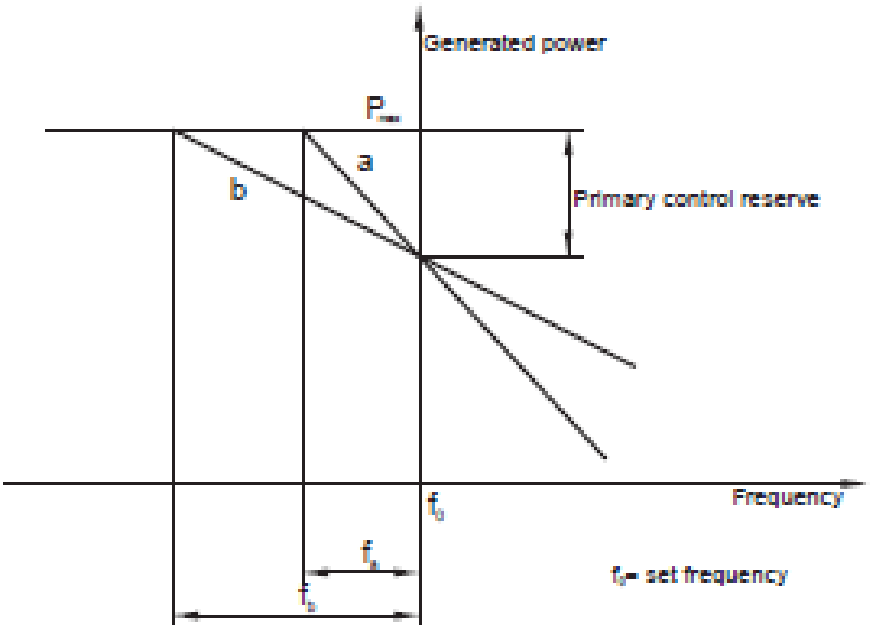

Figure 4.3. Droop characteristic of a generating unit [1]

The speed at which the Primary control reacts depends very much on the type of generation unit: Hydro, Thermal, Combined Cycle, etc., some of them being very fast and the others

slower. The minimum value reached by the frequency depends on how fast the Primary control is able to restore the balance between generation and load by acting on the generators output. The slower they are the large will be the minimum value reached by the frequency. This is of crucial importance, since large frequency deviations can trigger protection schemes, which can lead to the disconnection of additional generating units, eventually leading to a system blackout. This may occur even if there is enough spinning reserve but the disturbance is so large that the Primary control cannot arrest the frequency deviation before it starts to cause additional generation trips.

The frequency deviations can be classified in two types, depending on its sign:

- Under-frequency: due mainly to the trip of generating units.
- Over-frequency: due mainly to the trip of large loads.

In order to protect the system against under-frequency situations, the power systems are equipped with additional schemes, which disconnect load when the frequency reaches predefined values. These schemes are called load shedding. As an example in Figure 4.4 are shown the ENTSO-E recommendations for such defence plans.

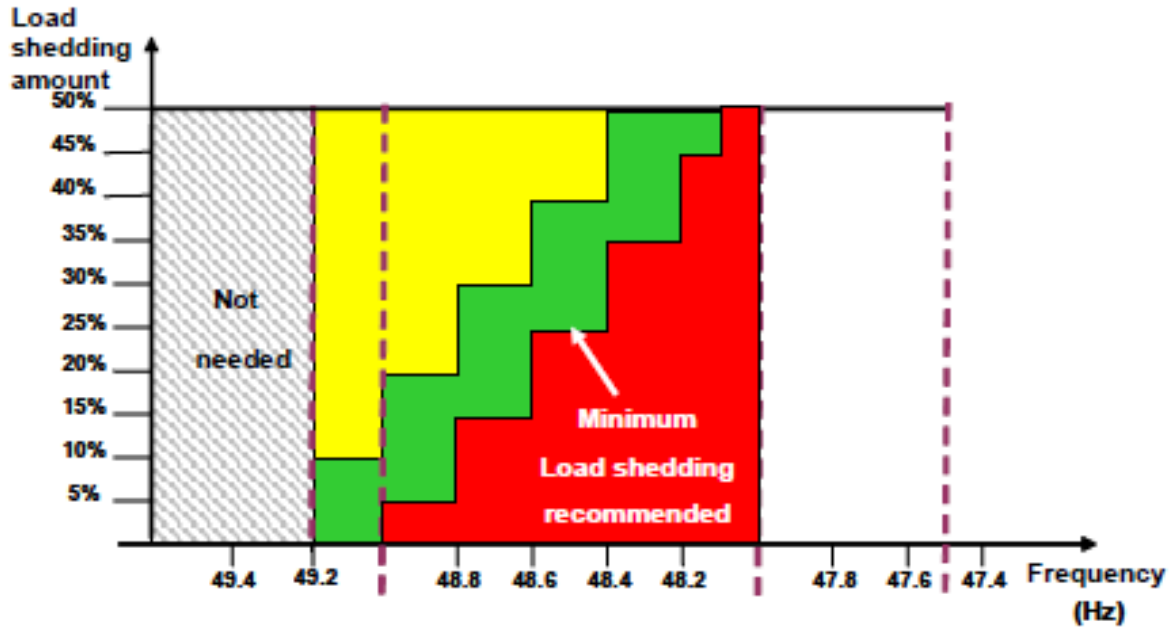

Figure 4.4. Load shedding recommendations as per [3]

Under large frequency deviations, the power delivered by some generating units may not remain constant and may be reduced due, for instance, to the different performance of the auxiliary services of the power plant. This means that when a large disturbance occurs, the frequency drop can be so significant to make the available spinning reserve not enough in order to arrest the frequency decay. In such circumstances, the system may experience a frequency collapse [5]. This fact can even be aggravated since the loads behave more and more like constant power loads, thus reducing the natural damping of the loads, which can be helpful during under-frequency situations.

On the other hand, in over-frequency situations there are additional phenomena that can aggravate the system state (over-frequency protection can be triggered leading to the

disconnection of conventional generators). This can produce the opposite phenomena of under-frequency [7], eventually leading to the system collapse

After the Primary Control has acted, the Secondary Control takes over and attempts to restore the frequency to its nominal value (not only that, but also to keep the power exchanges between the different control areas to their scheduled values). The secondary control is basically an integral control, thus producing zero error when reaching the steady state. The secondary control is much slower than the primary control, and it highly depends on the generation technology. For instance, hydro power plants are much faster than typical thermal units. Typical response times of the Secondary control are in the range of minutes.

In the past, when the penetration of renewables was not relevant, it was relatively "simple" for the secondary control to restore the frequency, since there were not random factors affecting to the frequency behaviour. Nowadays, the increase number of renewables and its random characteristic makes it a challenge to operate the system when unexpected wind or sun conditions occur. In such cases, the power system should be able to control the frequency and keep it within acceptable ranges.

This might impose very demanding requirements to the secondary control. Therefore, scenarios with a large percentage of renewable generation and its random variations and its impact on the system frequency behaviour should be analysed. Moreover, the coordination between the different types of frequency control and reserves should also be investigated in order to assess possible problems derived from such scenarios.

Therefore, under scenarios with significant percentages of renewable generation, as it is foreseen in the future for the European power system, the analysis of the system frequency behaviour must be addressed by means of the adequate studies. These studies should focus on the following issues:

- *Frequency deviations following generation contingencies or tripping of an HVDC connecting a different synchronous area*
- *Ability of the system to cope with unexpected variations of renewable power*
- *Ability of the system to cope with very high ramps of generation implied by RES (especially solar)*

Within the task 4.1 of the e-Highway2050 project, only the issue of frequency deviation following a contingency was analysed.

4.1. Tools and Models

For the frequency stability, a reduced power flow data based on available TYNDP 2030 model was used. With combination of simple (initial) dynamic models the reduced model enables to carry out calculations of frequency stability.

Since the reduced model contains plugin nodes (corresponding to the switching substations of the cluster model prepared by WP2) it can be easily expanded.

Initial power flow data is based on TYNDP 2030 model. This model contains full data for continental Europe including X nodes for HVDC inside Continental Europe model – see right side of figure below.

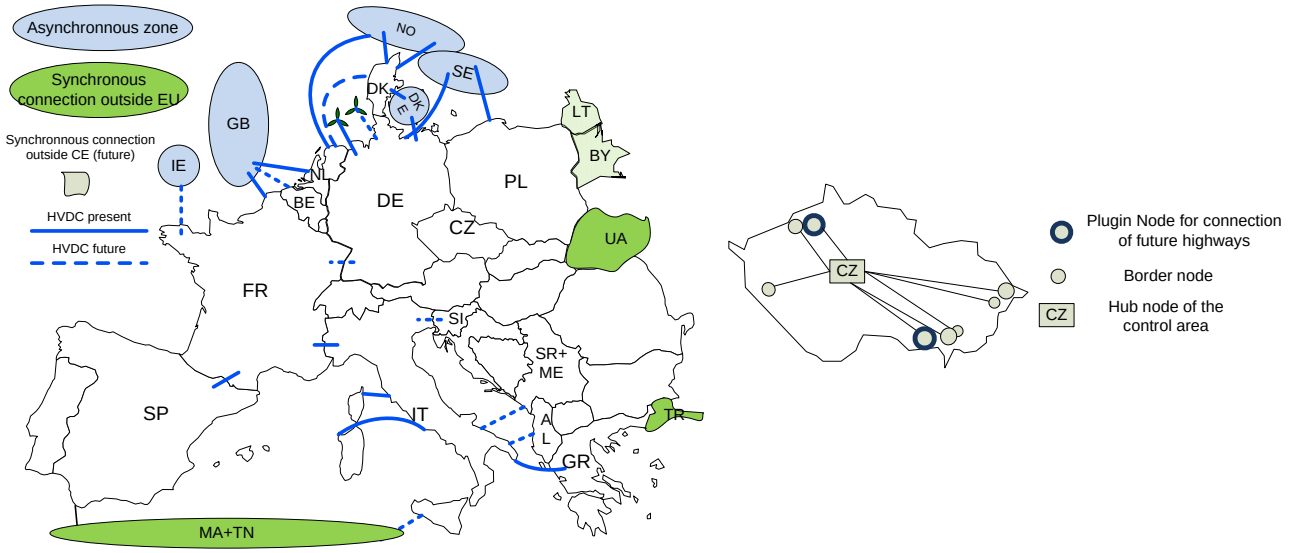

Figure 4.5. Scheme of CE synchronous zone with HVDC and example of reduction of CZ control area

Each control area in the initial model is reduced into:

- one hub node with concentrated all generation and consumption of the control area
- all border nodes with the neighbouring control areas in order to preserve all tie lines
- internal X HVDC nodes (with HVDC terminals in CE)
- external X HVDC nodes (terminals of HVDC in GB, NO, SE and TN) – list of these HVDC is in table 4.2)

An example of the reduced control area is depicted on the left side of figure 4.5.

Following table compares numbers of objects of the initial (full) and reduced model:

Table 4.1. Number of objects in the full and reduced models

Model	Numbers of		
	Nodes	Branches + Transformers	Generators
Full model	15575	21426+1157	888
Reduced model	576	1485	53

Reduced model significantly speeds up dynamic calculations. For example, one minute simulation of unit outage takes nearly 180 second for full model, but only two seconds for reduced model (using the MODES network simulator).

Table 4.2. List of identified HVDC outside the CE

HVDC Name	Node name (internal CE)	Area	Node name (external CE)	Area
NorNed	ORNED2NL	NL	ORNED2NO	NO
	XEE_FE1N	NL	XEE_FE1O	NO
	XMA_SE11	FR	XSE_FR42	GB
KontiSkan	XVH_L21K	DK	XVH_L11S	SE
	XBE_GB1B	BE	XBE_GB1G	GB
SwePol	XSL_SW11	PL	XSL_ST1S	SE
	XFR_GB1F	FR	XFR_GB1G	GB
Nord.Link	XBR_ER1D	DE	XBR_ER1N	NO
Skagerrak	XTJ_K41K	DK	XTJ_K41N	NO
	XTJ_K23K	DK	XTJ_K23N	NO

	XTJ_K31K	DK	XTJ_K31N	NO
	XTJ_K31K	DK	XTJ_K31N	NO
	XMA_SE2F	FR	XMA_SE12	GB
Baltic Cable	XHW_KR1D	DE	XHW_KR1S	SE
	XGR_MA1N	NL	XGR_MA1G	GB
	XIE_FR42	FR	XIE_FR41	IE
	XPA_EL9I	IT	XEL_PA9I	TN

Reduced power flow data was complemented by simple dynamic models for sub-transient round rotor generator and simpler models for excitation, PSS, turbine and governor (SEXS, PSS2A and TGOV1) with tuned parameters from Appendix C.

The validation of the reduced model can be found in Appendix II.

4.2. Test Cases

From the WP2 configurations, the following ones have been selected to capture a wide scope of possible frequency stability:

- X-7 (100% RES)
  - Summer Low
  - Reinforcement strategy 3
- X-7 (100% RES)
  - Winter Peak
  - Reinforcement strategy 3
- X-10 (Big & market)
  - Winter Peak
  - Reinforcement strategy 3
- X-16 (Small & Local)
  - Summer Low
  - Reinforcement strategy 2

As explained before, the reduced models consist of all border buses (all tie lines were observed), so called plugin nodes for clusters, X nodes to external systems (terminals of HVDC or AC connection outside continental Europe) and so called hub nodes (one hub for each control area). Initial dynamic model was created by combining this reduced power flow data with dynamic data from Appendix C (C.4 wind parks and Tab. C.1-4 for conventional units). Turkish power system was substituted by 50 GW load and generation.

The second step was adjustment of the **initial dynamic model** according to market model simulation. The generation was adjusted to correspond with the ANTARES results and conventional generation was replaced by appropriate dynamic models for non-synchronous generation (connected to the network through converters). An overview of the utilised models is given in Table 4.3.

Table 4.3. Overview of the models

Scenario		X-7 adjusted		X-10 adjusted	X-16 adjusted
Regime		Sommer Low	Winter Peak	Winter Peak	Sommer Low
Load [MW]		449111	547243	554705	347702
Generation [MW]	Synchronous	193871	326916	434857	112925
	Pumping	-2849	0	0	-8499
	Wind	53732	106811	69907	17414
	PV	127369	0	0	176576
	Admittance	78180	111300	50995	38177
Inertia [GJ]		1195	2071	2038	773
K-factor [MW/Hz]		20088	33889	40944	11918

The share of synchronous generation as part of total generation is given in Table 4.4.

Table 4.4. Share of synchronous generation

Scenario	Regime	Share of synchronous generation
X-7	Summer Low	42%
	Winter Peak	59%
X-10	Winter Peak	78%
X-16	Summer Low	32%

Figure 4.6, Figure 4.7, Figure 4.8 and Figure 4.9 show country balances and power flows show difference between the clusters.

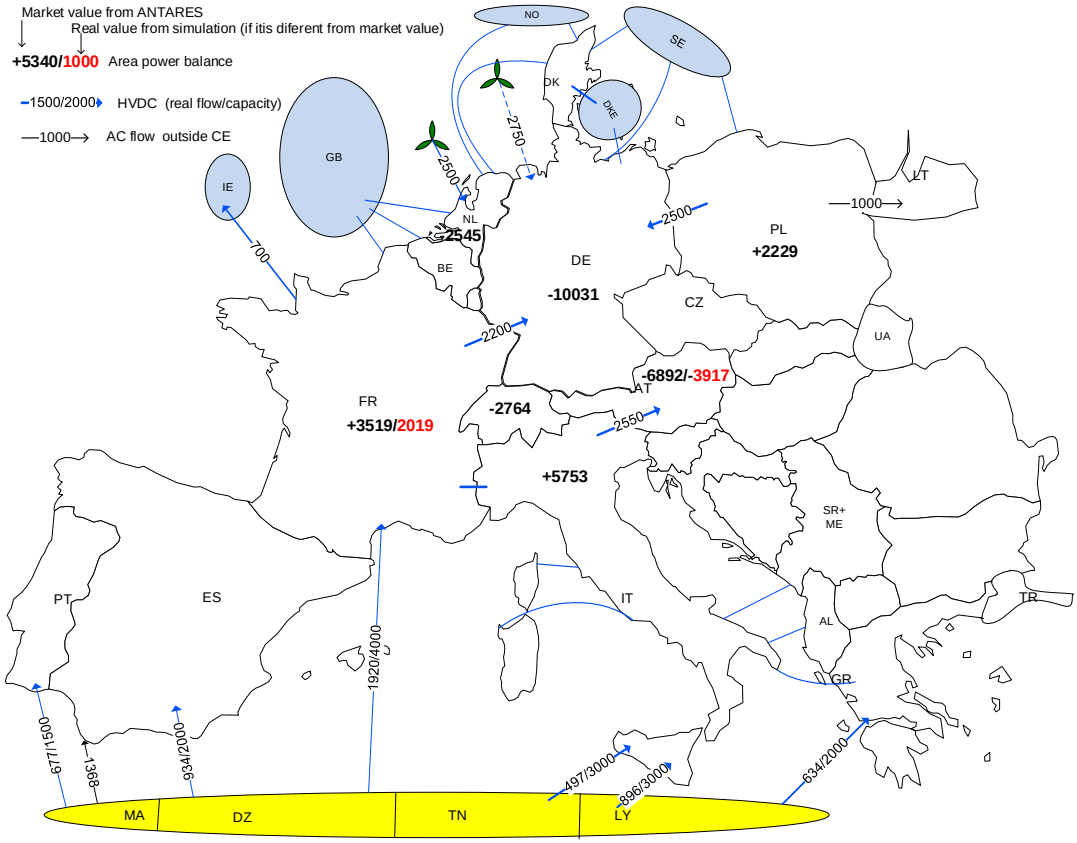

Figure 4.6. Overview scenario X-7, regime Summer Low

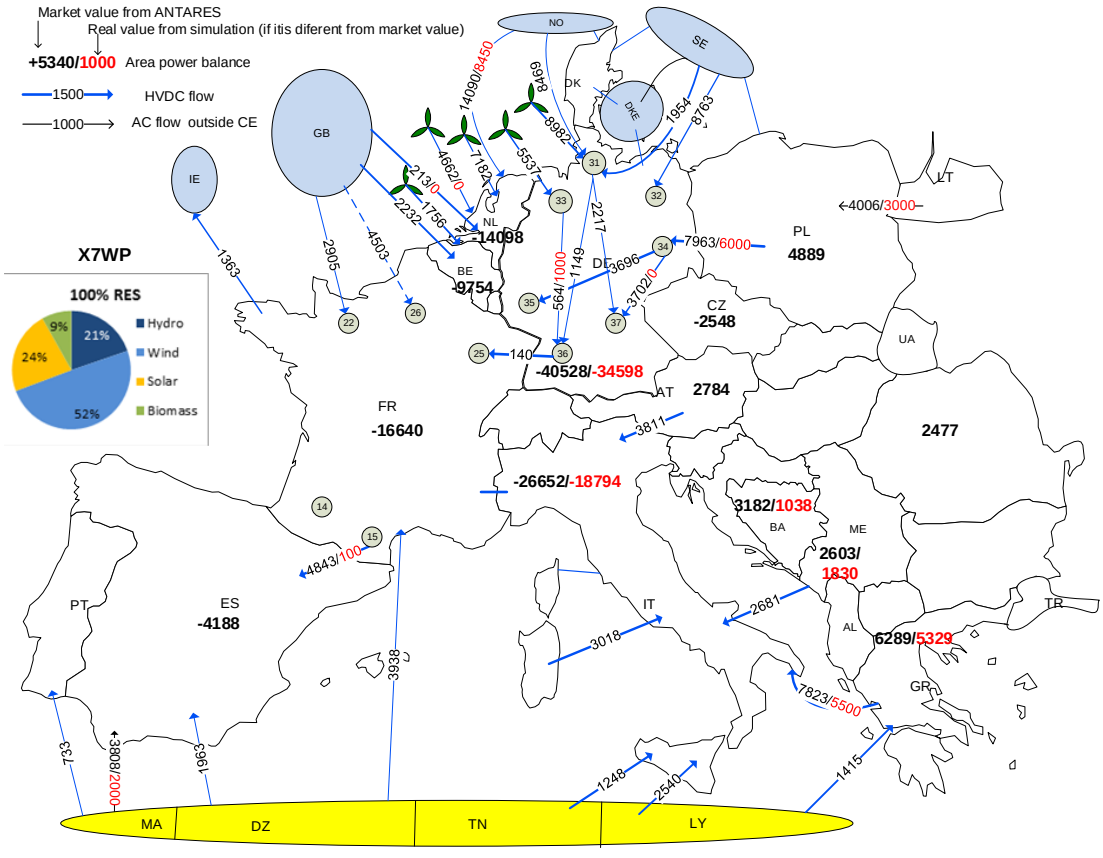

Figure 4.7. Overview scenario X-7, regime Winter Peak

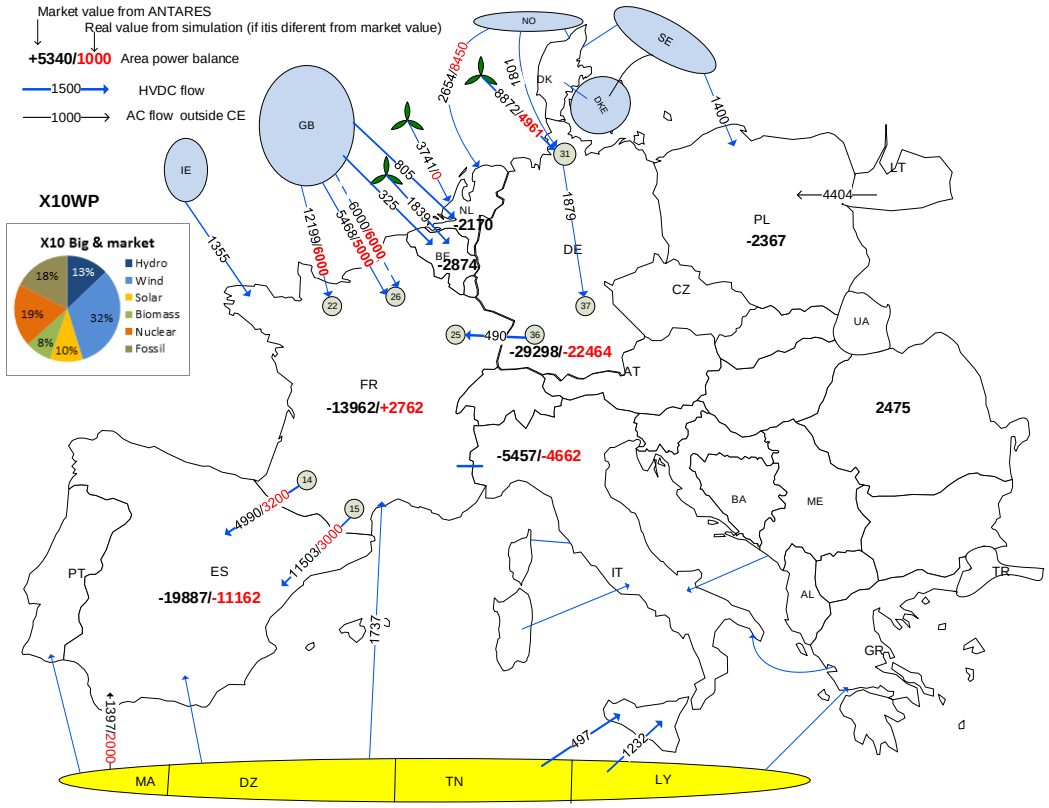

Figure 4.8. Overview scenario X-10, regime Winter Peak

The main importing countries are DE and ES with significant import from GB in X-10 Winter Peak.

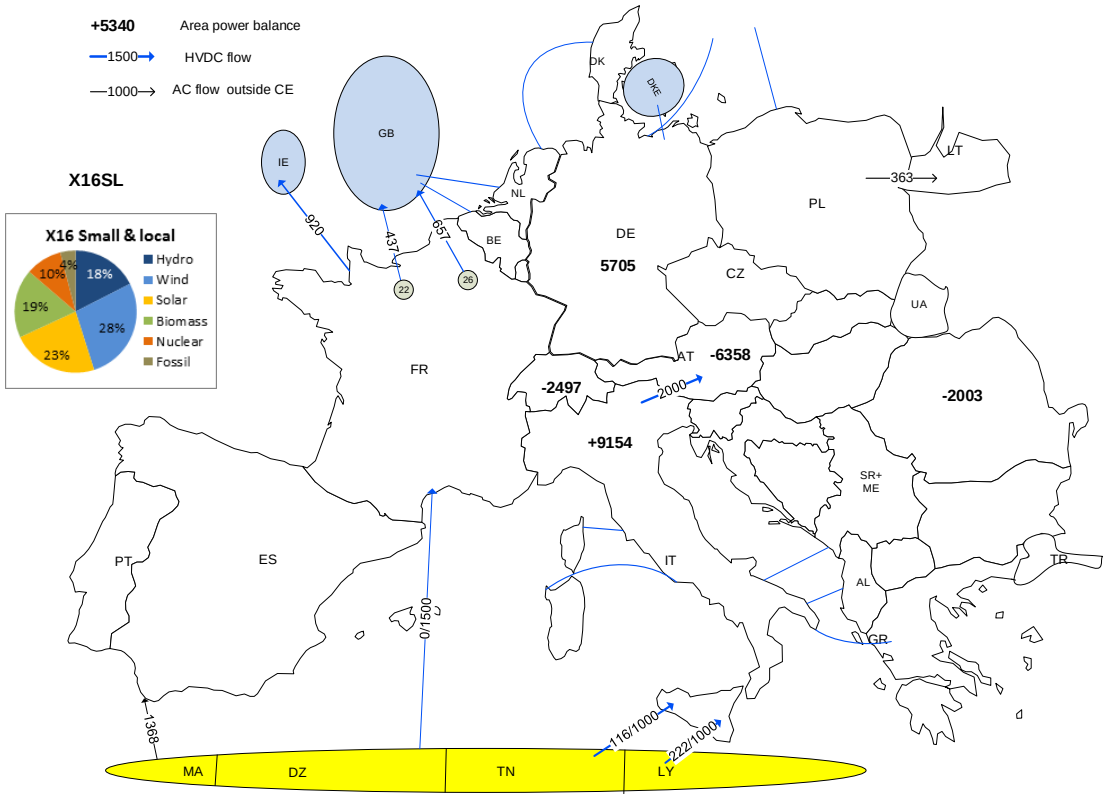

Figure 4.9. Overview scenario X-16, regime Summer Low

Power exchange outside continental Europe is small in X-7 Summer Low (the main export comes from IT to AT) to the contrary with X-7 Winter Peak, when exchanges are very large: imports from GB, NS, NO, SE and North Africa (DE stays very large importer, but there are large imports to IT and FR). The main importing country is AT in X-16 Summer Low, power exchange outside the continental zone is very small.

4.3. Methodology

The criteria for frequency stability are based on the following references:

- In case a simulation shows stable behaviour but the frequency experiences large deviations, the rejection will be based on the following:
  - *ENTSO-E Policy 3 [2] and*
  - *ENTSO-E Network Code on Load-Frequency Control and Reserves [4]*
- If a scenario shows instability during the simulations, the scenario will be rejected

Table 4.5. and Table 4.6. show frequency requirements as per [1] and [4]. The proposed criteria are based on current codes and policies, and they may of course differ from those that will be operative in 2050. Using them may lead to some conservative results, but they can be used as a starting point. Besides, the studies carried out in the scope of this project may help to identify and propose changes in the operational criteria based on the evolution of the system and the proposed architectures.

Table 4.5. Values defined in [1] and used for system operation

Reference	Subject	Value	dated
P1-A-D1	Nominal Frequency	50 Hz	Fixed
P1-A-D2.1	Activation of PRIMARY CONTROL	±20 mHz	Fixed
P1-A-D2.5	Full Activation of PRIMARY CONTROL RESERVES	±200 mHz	Fixed
P1-A-D3.1	Reference Incident	3000 MW	Fixed
P1-A-D4.1	SELF-REGULATION of Load	1 %/Hz	Fixed
	Highest load in the system (from 03.12.2008)	412000 MW	2009
	Contribution by SELF-REGULATION of Load	4120 MW/Hz	2009
P1-A-D4.3	Minimum NETWORK POWER FREQUENCY CHARACTERISTIC of PRIMARY CONTROL	15000 MW/Hz	Fixed
P1-A-D4.4	Avarage NETWORK POWER FREQUENCY CHARACTERISTIC of PRIMARY CONTROL	19500 MW/Hz	2009
	Mean generation power (in the system)	306000 MW	2009
P1-A-D4.5	SURPLUS-CONTROL OF GENERATION (50% of mean generation power in the system / 50 Hz)	3060 MW/Hz	2009
P1-A-D4.6	Overall NETWORK POWER FREQUENCY CHARACTERISTIC	26680 MW/Hz	2009
P1-A-D4.7	Overall PRIMARY CONTROL RESERVE	3000 MW	Fixed

Table 4.6. Frequency Quality Defining Parameters of the Synchronous Areas [4]

	CE	GB	IRE	NE
Standard Frequency Range	±50 mHz	±200 mHz	±200 mHz	±100 mHz
Maximum Instantaneous Frequency Deviation	800 mHz	800 mHz	1000 mHz	1000 mHz
Maximum Steady-state Frequency Deviation	200 mHz	500 mHz	500 mHz	500 mHz
Time to Recover Frequency	not used	1 minute	1 minute	not used
Frequency Recovery Range	not used	±500 mHz	±500 mHz	not used
Time to Restore Frequency	15 minutes	10 minutes	20 minutes	15 minutes
Frequency Restoration Range	not used	±200 mHz	±200 mHz	±100 mHz
Alert State Trigger Time	5 minutes	10 minutes	10 minutes	5 minutes

4.4. Results

The frequency stability was checked by power outage. Four cases were simulated:

- 2750 MW wind power plant outage in the North sea (X-7, Summer Low)
- 4503 MW HVDC outage between France and Great Britain (X-7, Winter Peak)
- 6000 MW HVDC outage between France and Great Britain (X-10, Winter Peak)
- 1700 MW unit outage in the Czech Republic (X-16, Summer Low)

Figure 4.10., Figure 4.11., Figure 4.12. and Figure 4.13. present simulation results – frequency deviations in different parts of the continental Europe synchronous zone.

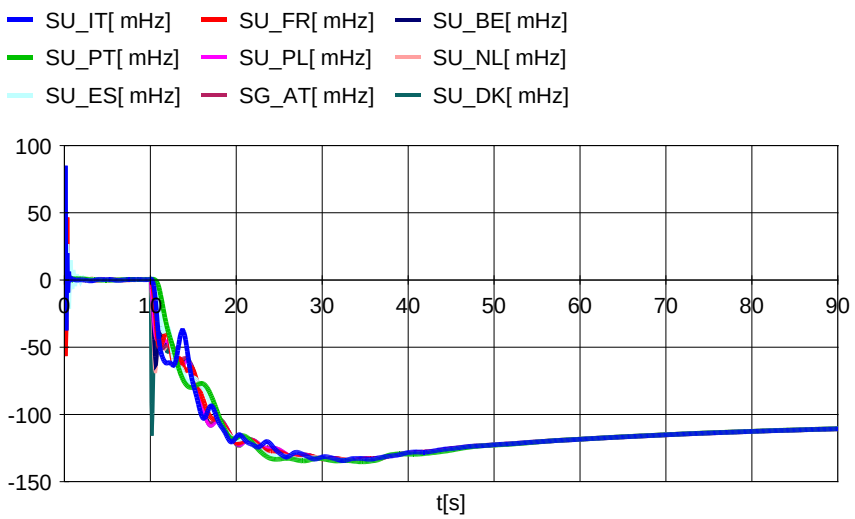

Figure 4.10: Frequency deviation waveforms for 2750 MW outage (Wind power plant in NS) in X-7 Summer Low

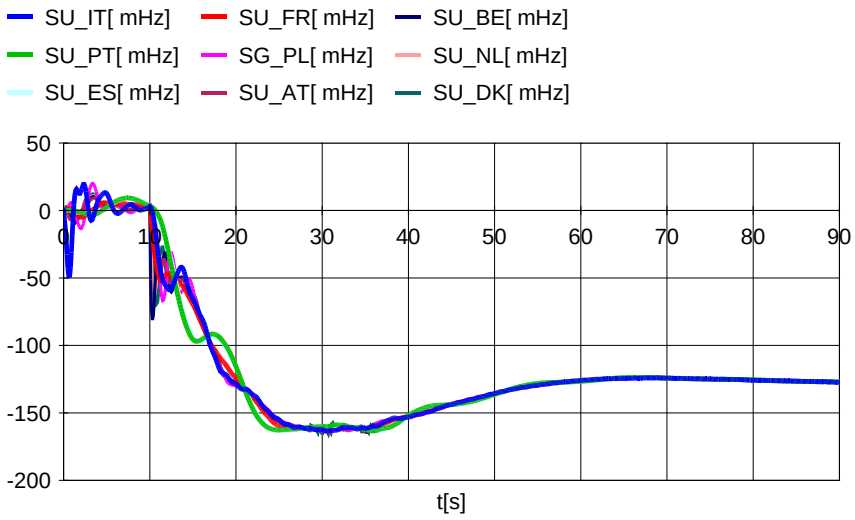

Figure 4.11: Frequency deviation waveforms for 4503 MW outage (HVDC GB -FR) in X-7 Winter Peak

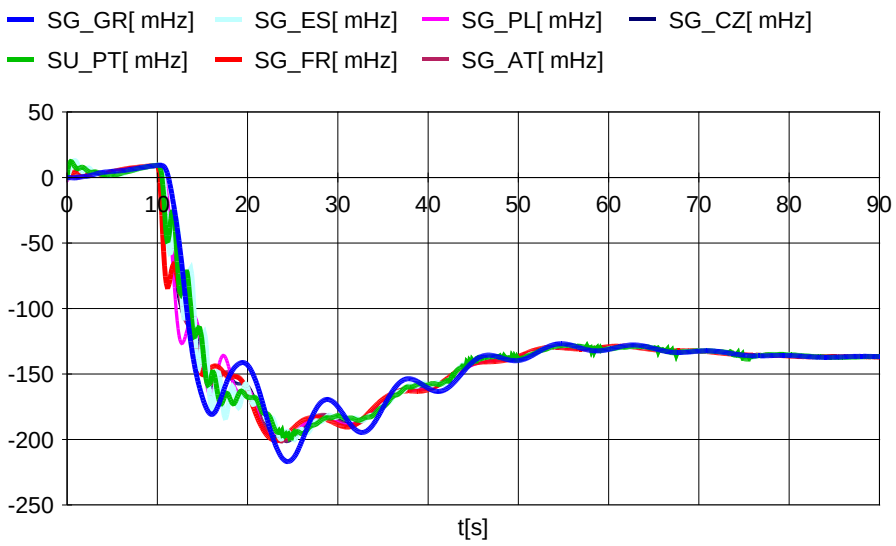

Figure 4.12: Frequency deviation waveforms for 6000 MW outage (HVDC GB -FR) in X-10 Winter Peak

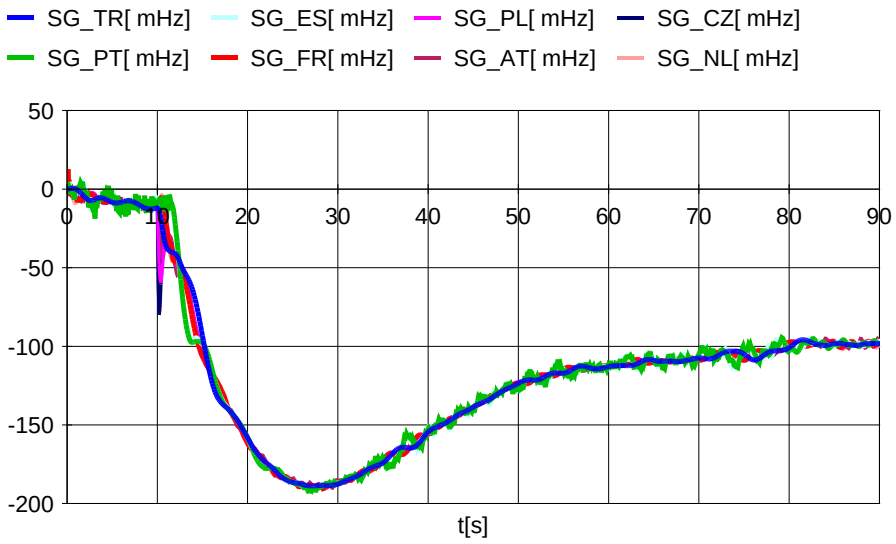

Figure 4.13: Frequency deviation waveforms for 1700 MW unit outage (CZ) in X-16 Summer Low

All cases are stable.

4.5. Conclusion

The reduced dynamic models were prepared for selected scenarios X-7, X-10 and X-16. Four cases of large HVDC import, wind power plant infeed and unit outages were simulated and CE interconnection stayed stable.

The maximum frequency deviation should not reach value -200 mHz provided that wind power plants enable the primary frequency control (similar like conventional units with synchronous generators). It means that power system is able to withstand an outage of large source with power unbalance from 1700 to 6000 MW (depending on scenario).

5. Small-Signal Stability Assessment

Rotor angle stability deals with the ability of synchronous machines of an interconnected power system to remain in synchronism after being subjected to a disturbance. It depends on the ability to maintain/restore equilibrium between electromagnetic torque and mechanical torque of each synchronous machine in the system [16]. Rotor angle stability is one of the criteria taken into account during the assessment of power system stability. The definitions, theoretical background and recommendations presented here are based on [16], [9], [10] and [5]. It is common to divide rotor angle stability into:

- Transient stability
- Small signal stability

Within task 4.1 of the e-Highway2050 project, only small signal stability is considered.

Small signal stability deals with inter-area oscillations caused by interactions among large groups of generators and that have widespread effects. They involve oscillations of a group of generators in one area swinging against a group of generators in another area. They are characterised by small deviations between the rotor angles of generators located in different areas. Small signal stability is defined as an ability of the system to maintain stability under small disturbances [16]. If no control equipment is involved in this process, it is described as natural steady-state stability, otherwise as artificial steady-state stability [2].

Small disturbances occur continuously in the normal operation of a power system due to small variations in load and generation. A disturbance is considered to be small if the equations that describe the resulting response of the system may be linearised for the purpose of analysis [9]. Instability that may result can be of two forms:

- steady increase in generator rotor angle due to lack of synchronizing torque, or
- rotor oscillations of increasing amplitude due to lack of sufficient damping torque.

In today's practical power systems, the small-signal stability problem is usually one of insufficient damping of system oscillations. Small signal analysis using linear techniques provides valuable information about the inherent dynamic characteristics of the power system and assists in its design.

In large power systems, small-signal stability problems may be either local or global in nature.

Local problems involve a small part of the system. They may be associated with rotor angle oscillations of a single generator, or a single plant against the rest of the power system. Such oscillations are called local plant mode oscillations. The stability problems related to such oscillations are similar to those of a single-machine infinite bus system. Most commonly encountered small-signal stability problems are of this category.

Local problems may also be associated with oscillations between the rotors of a few generators close to each other. Such oscillations are called inter-machine or inter-plant mode oscillations. Usually, the local plant mode and interplant mode oscillations have frequencies in the range of 0.7 to 2.0 Hz.

Other possible local problems include instability of modes associated with controls of equipment such as generator excitation systems, HVDC converters, and static VAR compensators. The problems associated with control modes are due to inadequate tuning of the control systems. In addition, these controls may interact with the dynamics of the turbine-generator shaft system, causing instability of torsional mode oscillations.

Analysis of local small-signal stability problems requires a detailed representation of a small portion of the complete interconnected power system. The rest of the system representation may be appropriately simplified by use of simple models and system equivalents. Usually, the complete system may be adequately represented by a model having several hundred states at most.

Global small-signal stability problems are caused by interactions among large groups of generators and have widespread effects. They involve oscillations of a group of generators in one area swinging against a group of generators in another area. Such oscillations are called inter-area mode oscillations.

Large interconnected systems usually have two distinct forms of inter-area oscillations:

- A very low frequency mode involving all the generators in the system. The system is essentially split into two parts, with generators in one part swinging against machines in the other part. The frequency of this mode of oscillation is in the order of 0.1 to 0.3 Hz.
- Higher frequency modes involving subgroups of generators swinging against each other. The frequency of these oscillations is typically in the range of 0.4 to 0.7 Hz.

The characteristics of inter-area modes of oscillation are very complex and in some respects significantly differ from the characteristics of local plant modes. Load characteristics, in particular, have a major effect on the stability of inter-area modes. The manner in which excitation systems affect inter-area oscillations depends on the types and locations of the exciters, and on the characteristics of loads.

Speed-governing systems normally do not have a very significant effect on inter-area oscillations. However, if they are not properly tuned, they may decrease damping of the oscillations slightly. In extreme situations, this may be sufficient to aggravate the situation significantly. In the absence of any other convenient means of increasing the damping, adjustment or blocking of the governors may provide some relief.

A mode of oscillation in one part of the system may interact with a mode of oscillation in a remote part due to mode coupling. This occurs when the frequencies of the two modes are nearly equal. Care should be exercised in interpreting results of analysis in such cases.

The controllability of inter-area modes with PSS is a complex function of many factors:

- Location of unit with PSS
- Characteristics and location of loads
- Types of exciters on other units

Other effective means of stabilizing inter-area modes of oscillation include modulation of HVDC converter controls and static VAR compensator controls. Analysis of inter-area oscillations requires detailed representation of the entire interconnected power system (or power system model reduced to maintain inter-area oscillations). Models for excitation

systems and loads, in particular, should be accurate, and the same level of modelling detail should be used throughout the system.

Small-signal stability problems may be either local or global in nature. Local problems are related to a small part of the system and require a detailed representation of this portion of the complete interconnected power system. On the other hand, global small-signal stability problems are caused by interactions among large groups of generators and have widespread effects. For global problems these kind of studies, transmission system model seems to be the most important part of the simulation process. It is very important to use coherent reduction methods to generate reduced order transmission system models for this type of study. Classical generator models, which assume ideal controls holding an internal voltage constant behind the transient reactance of the generator used as part of a large system model generally, give simulated oscillation frequencies close to those calculated using detailed models. Alternatively, controls with default dynamic data can also be used. All of the gathered information as well as the long term experience in preparing these kind of studies let us presume, that small signal stability studies could be prepared in detail, bearing in mind the limitations of applied simplifications and reduction methods. This does not apply to local small-signal stability problems. Structure of the model to be provided by WP2, allows making the assumption that it will not be suitable for studying local problems but will be sufficient for identification of the inter-area mode oscillations.

5.1. Test Cases

In order to utilise power flow models obtained from WP2 for purpose of dynamic analysis, they had to be modified. Special set of procedure (tools) which included generators aggregation and netting was prepared to prepare power flow model (from any scenario) for dynamic calculations. Moreover, installed synchronous capacity was modified in each region in order to meet results coming directly from market simulation results from WP2. Also a tool for automatic creation of dynamic model was developed.

As a result modified power flow and dynamic models for scenarios X-16, X-13 and X-10 have been prepared, where X-16 stands for Small & Local, X-13 - Fossil & Nuclear, X-10 Big & Market. All of the analysed scenarios have been prepared with 2 possible grid development strategies - strategy 2 which stands for grid development using HVAC overhead lines and strategy 3 - using HVCD cable lines. Moreover, two operational regimes have been taken into consideration:

- Winter Peak - characterised by a very high load and thus a high production in the system
- Summer Low - characterised by a high infeed of renewable energy sources and a low load

The scope of analysed configurations was presented in Figure 5.1. Scenarios X-5 and X-7 where not analysed due to lack of proper power flow model coming from WP2. Details on this can be found in deliverable 2.4. [1]

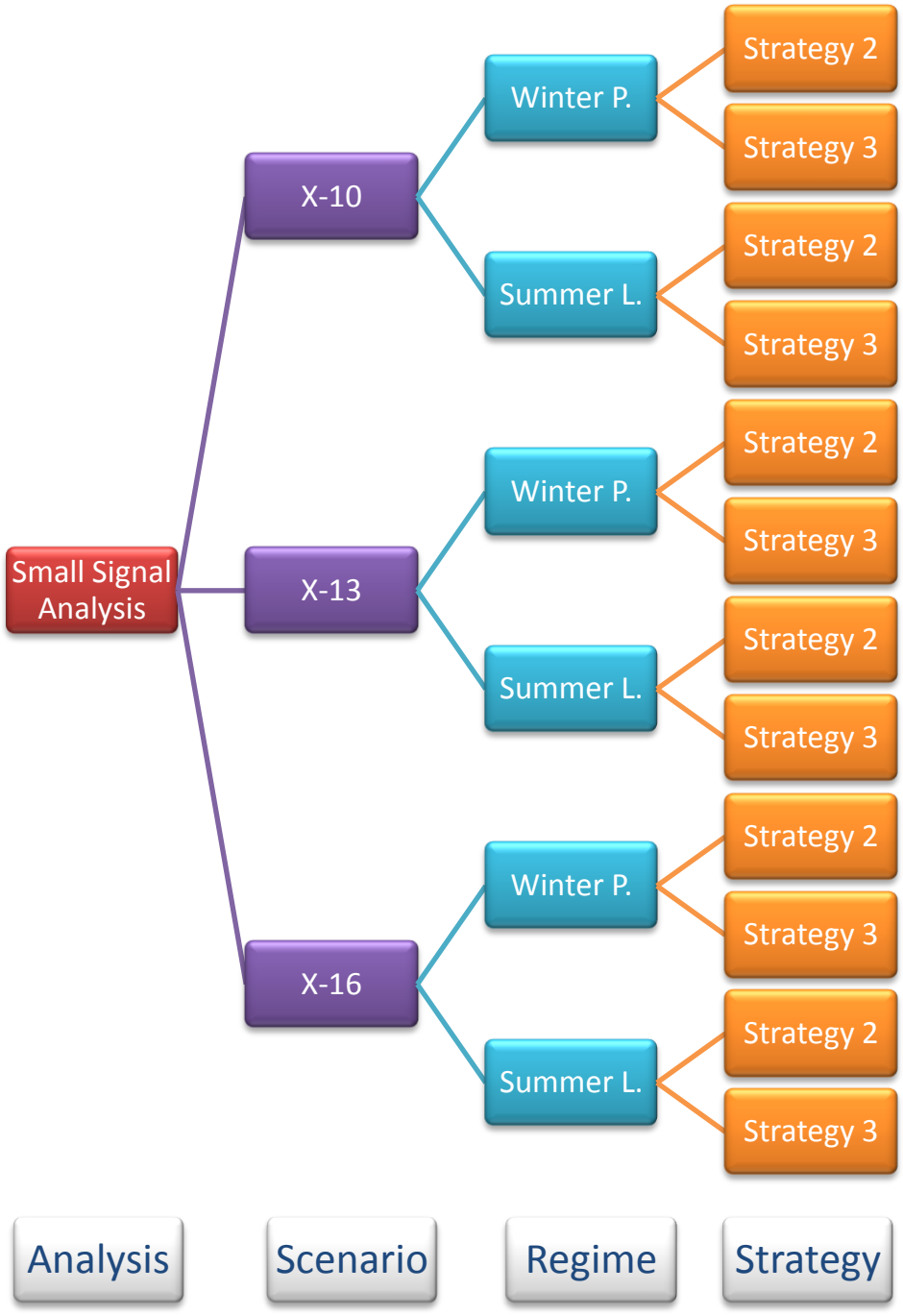

Figure 5.1. Scope of analysed configurations

[1] According to deliverable 2.4 "It is not said, that Scenarios X-5 and X-7 are not feasible for the transmission system. The implementation of such amounts of renewable production is technically feasible, but it requires new planning standards and concepts in grid development."

5.2. Methodology

According to Operational Security Network Code (2nd edition from 24th September 2013) one of the explanations for a need for dynamic stability management are continuously increasing power flows in Transmission System due to changes in the market and the increasing amount of intermittent generation. These changes together with long distance transmission paths from generation to load centres can increase the risk of wide area oscillations or other dynamic stability problems in transmission systems.

In the foreseen 2050 scenarios, future system architecture will be not less demanding than is nowadays. For the purpose of proper evaluation of potential risk of inter-area oscillation, it is proposed to perform small signal stability analysis of power systems with comprehensive analysis function based on modal analysis calculating eigenvalues and participation factors.

For the purpose of the small signal stability evaluation, it proposed to calculate eigenvalues corresponding to the analysed power system.

$$\lambda = \sigma \pm j\omega$$

Where:

σ - real part

ω - imaginary part

The real component of the eigenvalues gives the damping (ξ), and the imaginary component gives the frequency of oscillation (*f*). A negative real part represent a damped oscillation whereas a positive real part represents oscillation of increasing amplitude.

$$\xi = \frac{-\sigma}{\sqrt{\sigma^2 + \omega^2}}$$

$$f = \frac{\omega}{2\pi}$$

A real eigenvalue (λ) corresponds to a non-oscillatory mode. A negative real eigenvalue represents a decaying mode. The larger its magnitude, the faster the decay. A positive real eigenvalue represents aperiodic instability. Complex eigenvalues occur in conjugate pairs, and each pair corresponds to an oscillatory mode.

The very useful tool of searching for power system elements (generators, devices) influencing identified inter-are oscillations the most, is calculation of so-called participation factors. This is a standard feature of programs dedicated to small signal analysis.

In analysis of low frequency (inter-area) oscillations in interconnected power systems, it is desired that modes are damped not less than 5%. Swing modes with damping lower than 3% are generally not acceptable. Those values were applied during the study Synchronisation of the Turkish Power System with the UCTE Power System [17]. The proposed approach represents a first attempt to set up criteria for the operational validation of dynamic phenomena. Future developments shall need to adapt the envisaged clusters to avoid «YES/NO» closed answers.

5.3. Results

Calculations results for all analysed scenarios are presented in Table 5.1., using eigenvalue representation based on:

- frequency of oscillation *f*
- damping ξ

Presented eigenvalues are limited only to those of frequency lower than 0.5 Hz.

Table 5.1. Combined results for calculated eigenvalues.

X-16							
Strategy 2				**Strategy 3**			
Winter Peak		**Summer Low**		Winter Peak		**Summer Low**	
f	ξ	*f*	ξ	*f*	ξ	*f*	ξ
0.2026	3.33	0.3648	1.35	0.1937	3.80	0.3816	2.15
0.4060	0.48	-	-	0.3753	0.63	-	-
-	-	-	-	0.4325	1.07	-	-
X-13							
Strategy 2				**Strategy 3**			
Winter Peak		**Summer Low**		Winter Peak		**Summer Low**	
f	ξ	f	ξ	*f*	ξ	*f*	ξ
0.2147	3.51	0.3187	1.83	0.1576	5.04	0.2600	3.59
0.3794	1.48	0.4333	1.82	0.3382	-0.50	0.3628	1.87
0.4053	2.02	-	-	0.3439	1.91	0.4665	0.51
X-10							
Strategy 2				**Strategy 3**			
Winter Peak		**Summer Low**		Winter Peak		**Summer Low**	
f	ξ	*f*	ξ	*f*	ξ	*f*	ξ
0.2331	2.08	0.3458	2.51	0.1864	3.28	0.2935	2.72
0.3764	0.62	-	-	0.3626	1.33	-	-
0.3842	2.70	-	-	0.3836	2.67	-	-

In order to better understand the character and geographical structure of the identified oscillations modes, the ones with lowest frequencies are presented below on a European

map. This kind of presentation is called mode shape scatter. Each pictogram on the map represents single synchronous machine that has high participation factor in analysed mode. The individual generating units are positioned according to the representative cluster, so their location on the map is not exact, but detailed enough to see the geographical structure of the mode.

The contribution of synchronous generation to the total generation (based on results from ANTARES) in each model is presented in Table 5.2. These values help better understand why some modes vanished in Summer Low regimes (smaller amount of synchronous generation is not sufficient to excite the modes) or create more complex dependencies (greater number of generators creates more possibilities for interactions).

Table 5.2. Contribution of synchronous generation in total generation.

Scenario	Model	Synchronous generation	
		Power [GW]	Share [%]
X-16	Winter Peak	226	74
	Summer Low	42	10
X-13	Winter Peak	427	90
	Summer Low	244	64
X-10	Winter Peak	317	77
	Summer Low	116	34

A few representative mode shape scatter plots for modes with frequencies below 0.5Hz for the analysed configurations are presented here. The complete list of mode shape scatter plots can be found in Appendix G.

5.3.1. Mode 1

Mode 1, the lowest frequency mode, resembles the known east against west oscillation. It is observed in each scenario and strategy. In this mode, the Iberian Peninsula oscillates against the rest of Europe, with the border of the two areas located somewhere in France. The model in the study does not comprise Turkish power system so frequency of this oscillation is higher than it could be expected. The involvement of generators in southern France (in conjunction with the Iberian Peninsula) is higher in Strategy 2 than in Strategy 3. An example of a geographical mode shape scatter plot of Mode 1, where the border is located in south-western France, is shown in Figure 5.2.

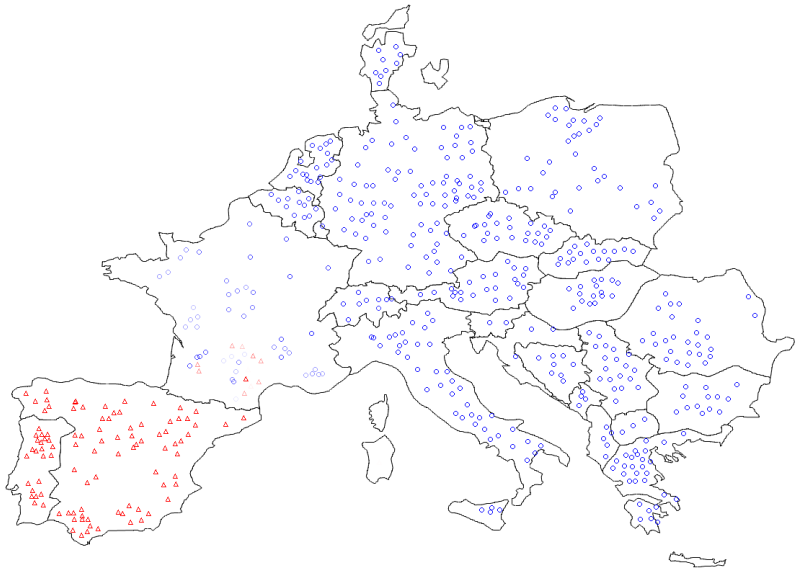

Figure 5.2 Geographical mode shape scatter plot for Mode 1, scenario X-13, strategy 3, Winter Peak

An example of a geographical mode shape scatter plot of Mode 1, where the border is located in north-eastern France, is shown in Figure 5.3.

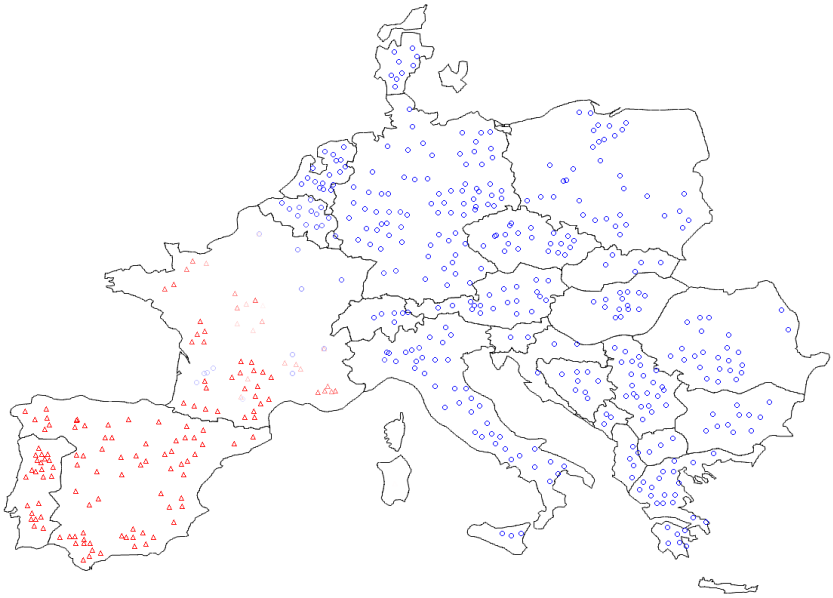

Figure 5.3 Geographical mode shape scatter plot for Mode 1, scenario X-10, strategy 2, Winter Peak

5.3.2. Mode 2

Mode 2, the second lowest frequency mode, resembles a south-east and south-west against central-north oscillation. It is observed in each Winter Peak regime but only in one Summer Low regime (scenario X-13). This mode involves usually generators in Balkan countries (also in Portugal, Spain but with smaller participation factors) oscillating against generators in Belgium, Netherlands and Northern France. In some cases, the east-central-west component is more distinct, while in other cases the north-south component is dominating. Italy's role is this mode is complex, as it sometimes is affiliated with the central area (east-west-east oscillation) and it sometimes is affiliated with the Balkan area (north-south oscillation). An

example of a geographical mode shape scatter plot of Mode 2, where the north-south component is dominant, is shown in Figure 5.4.

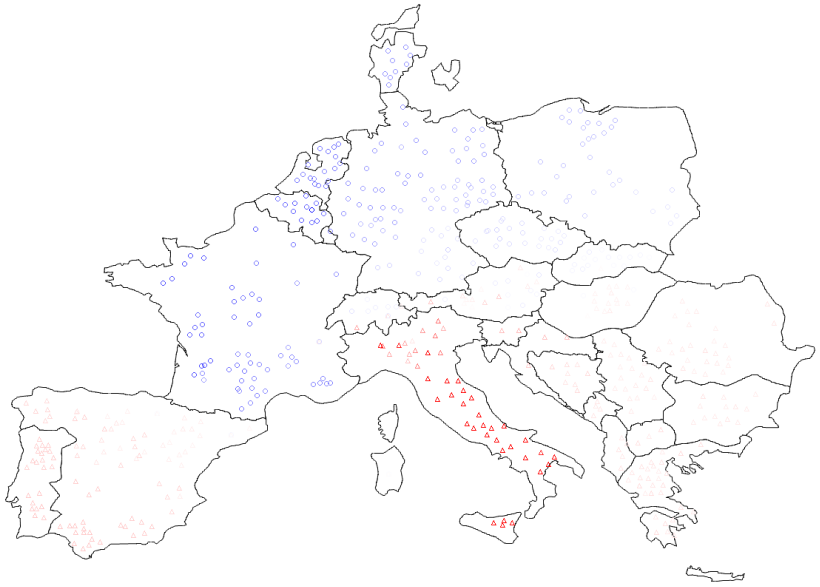

Figure 5.4 Geographical mode shape scatter plot for Mode 2, scenario X-13, strategy 3, Winter Peak

An example of a geographical mode shape scatter plot of Mode 2, where the east-central-west component is dominant, is shown in Figure 5.5.

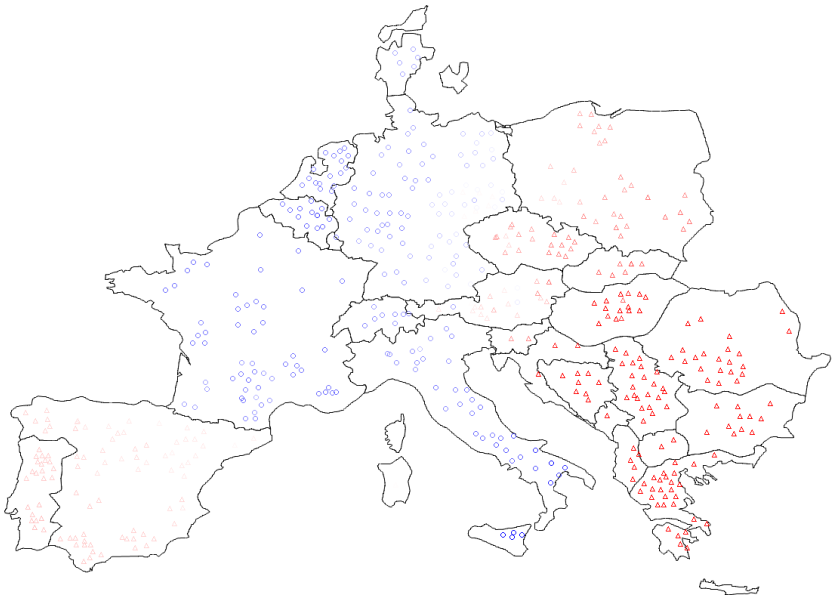

Figure 5.5 Geographical mode shape scatter plot for Mode 2, scenario X-16, strategy 3, Winter Peak

5.3.3. Mode 3

Mode 3, the third lowest frequency mode, can have a variety of shapes. It is observed in each Winter Peak regime but only in one Summer Low regime (scenario X-13). This mode involves usually generators in Italy oscillating against mostly generators in Balkan countries. An example of a geographical mode shape scatter plot of Mode 3, where the constellation can be clearly observed, is shown in Figure 5.6.

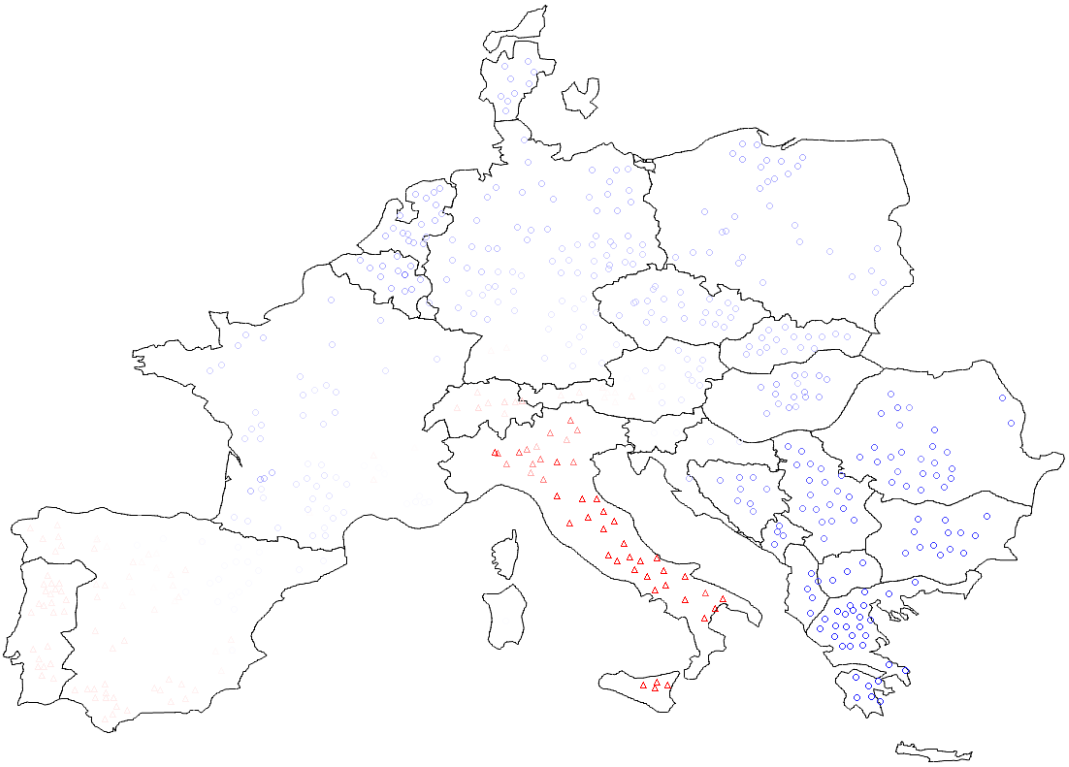

Figure 5.6. Geographical mode shape scatter for Mode 3, scenario X-13, strategy 2, Winter Peak

The mode can also have a more complex shape with four distinct areas, as shown in Figure 5.7.

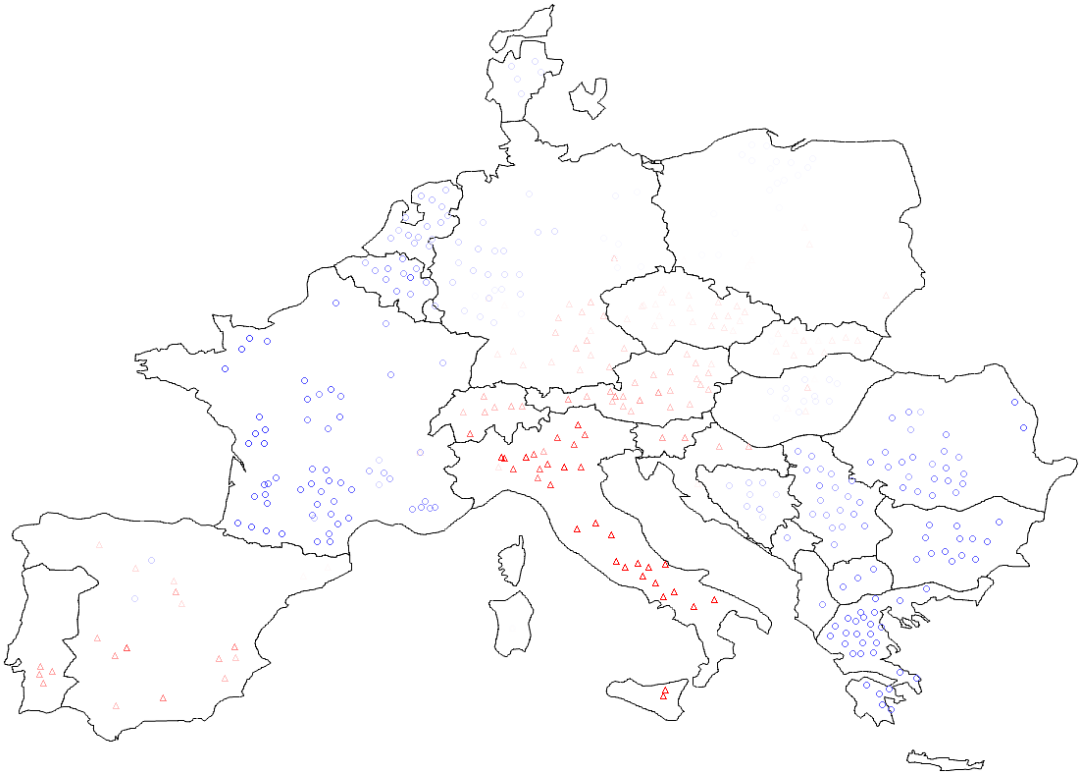

Figure 5.7. Geographical mode shape scatter for Mode 3, scenario X-13, strategy 3, Summer Low

However, it is also possible that Italy and the Balkan countries are not oscillating against each other, but together against northern Europe, as shown in Figure 5.8.

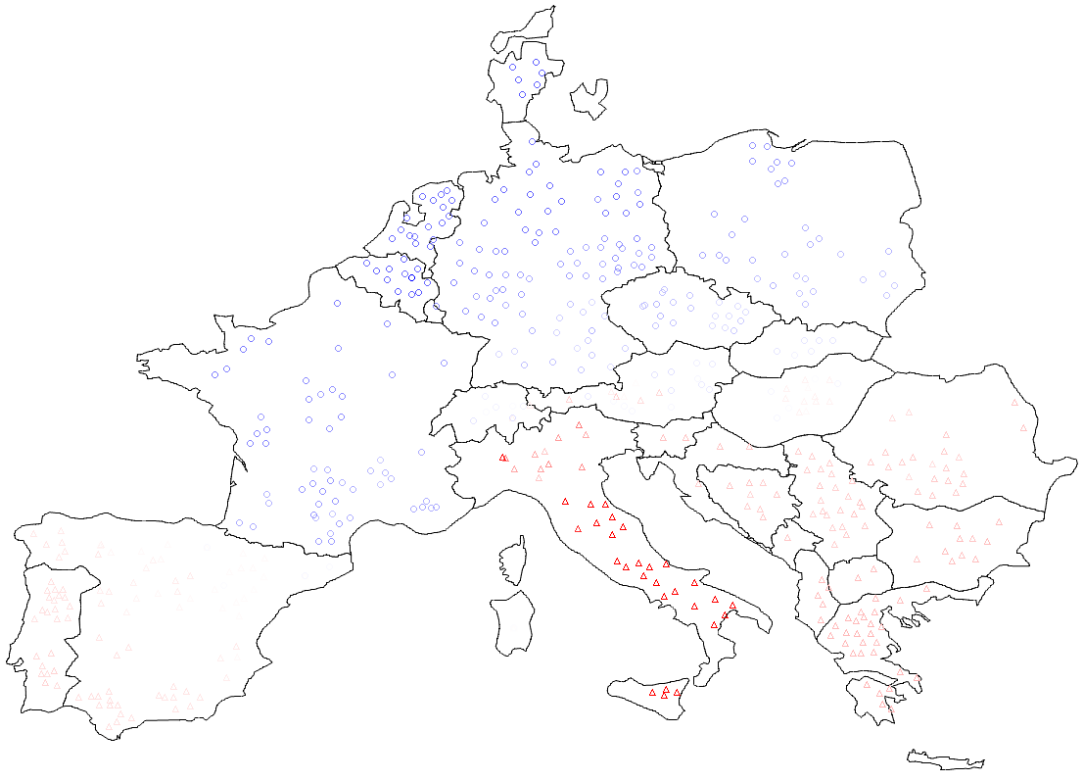

Figure 5.8 Geographical mode shape scatter plot for Mode 3, scenario X-16, strategy 3, Winter Peak

5.4. Conclusion

Elaboration of a dynamic model accurately reproducing inter-area oscillations in a large power system is a rather difficult and labour intensive task. An attempt to apply for this purpose a typical dynamic model used for transient stability study gives usually very optimistic results i.e. damping of inter-area oscillations can be much better than observed in the real power system.

The dynamic model prepared for this study involves some inevitable simplifications. One of important simplifications is of course only default dynamics for the whole model. Nevertheless, there are also further, may be less obvious simplifications resulting from time and source data constraints of the Study, which influence calculated modes of inter-area oscillations. The following simplifications have influence on obtained results:

- using of uniform static load model for all loads,
- neglecting motor load dynamics,
- replacing renewable generation by negative loads,
- using default PSS structure and parameters for all generators,
- using default structure and parameters governors,
- lack of some parts of synchronous areas (e.g. Turkey).

In large area small signal stability study, especially involving analysis of some future grid scenarios it is practically impossible to calculate accurate damping of inter-area oscillations. One reason is high accuracy of wide area modelling required in such studies. The other

reason is great dependency of low frequency modes on widely understood power system conditions like power transfers, load levels, a subset of actually used generation and so on. It is only direction of changes that can be treated as credible outcome of the study. Considering the present situation in ENTSO-E CE with small damping of some low frequency oscillations any visible deterioration of damping of these modes should attract special attention.

Due to all above-mentioned facts, the results obtained should not be treated as acceptance or rejections criteria, but rather as indication of possible problems. The goal of these calculations was more to show a trend between different analysed scenarios and grid development strategies, rather than give exact frequencies and damping values for identified modes.

Nevertheless, some conclusions from obtained results can be drawn:

- The damping of all (except one) identified interarea oscillation modes is positive (above 0), which means, that there is no instability risk for all of the analysed scenarios.
- Although the damping is positive, obtained values according to operational acceptance criteria described in the report are too low. In analysis of low frequency (inter-area) oscillation in interconnected power systems, it is desired that modes are damped not less than 5%. Swing modes with damping lower than 3% are generally not acceptable. Damping of the modes identified in the study are in range 0.48 - 5.04%.
- The damping is generally better when more synchronous generation is present in the model (scenarios X-13) rather than where more dispersed RES generation is dominant in the model (scenario X-16). The same phenomenon can be observed when comparing Winter Peak and Summer Low regimes, with poorer damping in the latter. However in the case of Scenario X-10 total synchronous generation is higher than in the Scenario X-16, but damping of the lowest frequency modes in Winter Peak model is lower. This is the case when not only amount of synchronous generation is important but also its areal distribution.
- Usually the damping gets higher for strategy 3, than for strategy 2. The situation is the other way round when it comes to oscillation frequency, which gets lower for strategy 3, than for strategy 2.
- The geographical mode shape scatter picture for lowest frequency modes is close to present situation (with except lack of Turkey). Lowest frequency mode tend to actuate generators on the ends of the interconnected power systems - Portugal and Spain is oscillating against Eastern and South-Eastern Europe, however the participating units vary among scenarios, due to differences in generation pattern. Higher involvement of generators in Southern France is observed in strategy 2.

6. Conclusions

Based on the inputs delivered by the WP2, the task 4.1 of the e-Highway 2050 project studied four types operational issues:

- Short circuit current
- Voltage stability
- Frequency stability
- Small signal stability

Regarding short circuit currents, the maximal value appeared to be within acceptable range. However, the contribution of power electronics to short circuit currents should be further investigated and especially the impact on the minimal short circuit currents.

For voltage drop, the analyses did not show any un-manageable voltage deviation in the considered configurations. Only one unstable situation was identified but it can be avoided by limiting the maximal capacity of a single line. However, some configurations could not be considered as they were not convergent, these situations face very likely significant voltage issues. This should be further investigated with methodologies and tools suitable for the analysis of very different power flow configurations

In all the situations analysed, the frequency was kept within acceptable range after significant disturbance. This was achieved thanks to the participation of wind farms to primary control. More detailed studies of the behaviour of the system with significant penetration of power electronics are planned in the European Migrate project.

Regarding small signal stability, only one case showed a negative damping but is still on the range of power system stabilisers.

To fully assess the impacts of the current changes in the power system, further studies are required. To do so, improvements in the quality of the available data, in the modelling of new technologies and in the methods will be necessary.

References

[1] *UCTE OH – Policy 1: Load-Frequency Control - Final Version* (approved by SC on 19 March 2009)

[2] *UCTE OH – Policy 3: Operational Security - Final Version* (approved by SC on 19 March 2009) Operation Handbook, Policy 3

[3] ENTSO-E RG CE OH 2nd release – *Policy 5: Emergency Operations*

[4] ENTSO-E, *Network Code on Load-Frequency Control and Reserves*, 28-June-2013

[5] J. Machowski, J.W. Bialek and J.R. Bumby, Wiley*, Power System Dynamics-Stability and Control*

[6] M. S. Baldwin and H.S. Schenkel, *Determination of frequency decay rates during periods of generation deficiency*, IEEE Transactions on Power Apparatus and Systems, vol. PAS-95, no. 1, pp. 26-36, 1976

[7] VDE, *The 50.2 Hz Problem, http://www.vde.com/en/fnn/pages/50-2-hz-study.aspx*

[8] IEEE Power & Energy Society, *Tutorial Course–Power System Stabilization via Excitation Control, IEEE* 09TP250

[9] Small Signal Stability Analysis Program Package: Version 3.0 Volume 3 Application Guide; EPRI TR-101850 Volume 3; Project 2447-01; February 1993; prepared by Ontario Hydro

[10] Small Signal Stability Analysis Program Package: Version 3.0 Volume 1 Final Report; EPRI TR-101850 Volume 1; Project 2447-01; February 1993; prepared by Ontario Hydro

[11] ENTSO-E, IMPLEMENTATION GUIDELINE FOR NETWORK CODE "Requirements for Grid Connection Applicable to all Generators", 16 October 2013

[12] Multi-terminal VSC HVDC for the European supergrid: Obstacles, Dirk Van Hertem, Mehrdad Ghandhari, Renewable and Sustainable Energy Reviews, 2010.

[13] ENTSO-E Draft Network Code on High Voltage Direct Current Connections and DC-connected Power Park Modules

[14] ENTSO-E Network Code on Operational Security, 24 September 2013

[15] ENTSO-E Supporting Document for the Network Code on Operational Security, 24 September 2013

[16] P. Kundur *Power System Stability and Control* McGraw-Hill, Inc.

[17] Complementary Studies for the Synchronization of the Turkish Power System with the UCTE Power System, Final Report, Stability Studies 2007

[18] J. Quintero, V. Vittal, G. T. Heydt, H. Zhang *The Impact of Increased Penetration of Converter Control-Based Generators on Power System Modes of Oscillation*, IEEE Transactions on Power Systems Issue 99, February 2014

[19] Y. Sun, L. Wang, G. Li, J. Lin *A Review on Analysis and Control of Small Signal Stability of Power Systems with Large Scale Integration of Wind Power* 2010 International Conference on Power System Technology (POWERCON 2010) October 2010, Zhejiang, China

[20] IEEE Committee Report, *Dynamic Performance Characteristics of North American HVDC Systems for Transient and Dynamic Stability Evaluations*, IEEE Transactions on Power Apparatus and Systems., Vol. PAS-100, July 1981

[21] H. F. Wang, F.J. Swift, M. Li, A unified model for the analysis of FACTS devices in damping power system oscillations. II. Multimachine power systems. IEEE Transactions on Power Deliv. Vol 3, no. 4, pp. 1355-1362, 1998.

[22] iTesla Project, *Deliverable D1.1. Formalization of the overall problem encountered by TSOs*

[23] Definition and Classification of Power System Stability IEEE/CIGRE, Joint Task Force on Stability Terms and Definitions, 2002

[24] GARPUR project, *Deliverable D1.1 State of the art on reliability assessment in power systems*

[25] ENTSO-E, IMPLEMENTATION GUIDELINE FOR NETWORK CODE *"Requirements for Grid Connection Applicable to all Generators"*, 16 October 2013

[26] Carson Taylor, *Power System Voltage Stability*, McGraw-Hill, Inc, ISBN 0-07-063184-0

[27] *Voltage Stability/Security Assessment and On line Control Volume 1* Final Control, EPRI TR-101931, April 1993

[28] ENTSO-E, IMPLEMENTATION PLAN 2015 – 2017

[29] Technical background and recommendations for defence plans in the continental Europe synchronous area, ENTSO-E report prepared by the sub group "System protection and dynamics" under - regional group continental Europe , 31.01.2011

[30] http://w3.siemens.com/smartgrid/global/en/products-systems-solutions/software-solutions/planning-data-management-software/planning-simulation/Pages/PSS-E.aspx

[31] http://www.energy.siemens.com/hq/en/services/power-transmission-distribution/power-technologies-international/software-solutions/pss-netomac.htm

[32] http://www.neplan.ch/html/e/e_home.htm

[33] IEC 61970: Energy Management System Application Program Interface (EMS-API) – Part 457: Common Information Model (CIM) for Dynamics Profile Draft Edition 1.00 Based on release IEC61970CIM16v24, 2013-08-31

[34] Documentation on controller tests in test grid configurations, ENTSO-E SG SPD Report, 2.10.2013

[35] SDC Consultation for European clustering related to the e-Highway2050 project, Report of WP2 task2 (Developing the grid architecture options as a function of the retained scenarios),, approved 28.06.2013

[36] European grid clustering for 2050 studies, WP2 External Workshop – clustering process 2013-10-10

[37] The selection of energy scenarios for e-Highway2050 project, public report available on-line http://www.e-highway2050.eu/uploads/media/The_selection_of_energy_scenarios_for_e-Highway2050.pdf

[38] 2014_04_23_Country and cluster results New, Excel sheet prepared by WP2

[39] D4.1.1 – Definition of strategy and framework to perform case studies for operational validation report

[40] Draft IEC 61970: Energy Management System Application Program Interface –Part 457: Common Information Model for Dynamics Profile Edition 1.00, Based on release IEC61970CIM16v24,
2013-08-31

[41] IEEE Std. 421.5-2005, IEEE Recommended Practice for Excitation System Models for Power System Stability Studies, 2006

[42] Chaoyong Hou ; Xuehao Hu ; Dong Hui: Plug and play power electronics interface applied in microgrid, 2011 4th International Conference on Electric Utility Deregulation and Restructuring and Power Technologies ,719 - 723

[43] Biczel, P. ; Jasinski, A. ; Lachecki, J.: Power Electronic Devices in Modern Power Systems The International Conference on "Computer as a Tool" EUROCON, 2007.
Huang, A.Q. ; Bhattacharya, S. ; Baran, M. ; Bin Chen ; Chong Han: Active Power Management of Electric Power System Using Emerging Power Electronics Technology, 2007. IEEE Power Engineering Society General Meeting

[44] Special Issue on Modeling and Control of Power Electronics for Renewable Energy and Power Systems, IEEE journal of emerging and selected topics in power electronics, Vol. 2, No. 4, Dec. 2014

[45] Xiongfei Wang ; Blaabjerg, F. ; Weimin Wu: Modeling and Analysis of Harmonic Stability in an AC Power-Electronics-Based Power System, IEEE transactions on power electronics, Vol. 29, No. 12, Dec. 2014 ,6421 – 6432

[46] Special Issue on Power Electronics in Emerging Applications,IEEE transactions on power electronics, Vol. 28, No. 4, Apr. 2013, 1927 - 1928

[47] Chakraborty, M. G. Simões and W. E. Kramer: Power Electronics for Renewable and Distributed Energy Systems, Springer-Verlag, London, 2013, ISBN: 978-1-4471-5103-6

[48] Kroposki, B. ; Pink, C. ; DeBlasio, R. ; Thomas, H. ; Simões, M. ; Sen, P.K. : Benefits of Power Electronic Interfaces for Distributed Energy Systems, IEEE Transactions on Energy Conversion, Vol.25 (2010),, 901 - 908

[49] Blaabjerg, F. ; Ke Ma: Future on Power Electronics for Wind Turbine Systems IEEE Journal of Emerging and Selected Topics in Power Electronics, Vol. 1 (2013), No. 3, 139 - 152

[50] Blaabjerg, F.; Chen, Z.; Kjaer, S.B. "Power Electronics as Efficient Interface in Dispersed Power Generation Systems.'' IEEE Transactions on Power Electronics; Vol. 19. Sept. 2004

[51] S. Wijnbergen, and S. W. H. de Haan, Power electronic interface with independent active and reactive power control for dispersed generators to support grid voltage and frequency stability, in Proc. European Conference on Power Electronics and Applications (EPE'03

[52] Z. Huang, Y.Ni, C.M.Shen, F.F.Wu, S. Chen, B. Zhang: Application of UPFC in Interconnected Power Systems – Modeling, Interface, Control Strategy and Case Study, IEES Transaction on Power Systems, Vol. 15, No2, May 2000

[53] N Dizdarevic, G. Anderson: Power flow regulation by use of UPFC's injection model, IEEE Power Tech 1999 Conference, 1999 Budapest

[54] P. Kundur: Power System Stability and Control; McGraw-Hill; 1993

[55] H.F. Latorre, M. Ghandhari, L. Söder: Active and reactive power control of a VSC-HVDC, Electric Power Systems Research, Volume 78, Issue 10, October 2008, 1756–1763

[56] Yao Shujun ; Bao Mingran ; Hu Ya'nan ; Han Minxiao ; Hou Junxian ; Wan Lei: Modeling for VSC-HVDC electromechanical transient based on dynamic phasor method, Renewable Power Generation Conference (RPG 2013)

[57] Moustafa, M.M.Z. ; Filizadeh, S. : A VSC-HVDC model with reduced computational intensity 2012 IEEE Power and Energy Society General Meeting, 1 - 6

[58] H.F. Latorre, M.Ghandahari: Improvement of power system stability by using a VSC-HVDC, Electrical Power and Energy Systems 33 (201), 332-339

[59] Wang, W. ; Barnes, M. ; Marjanovic, O. : Droop control modelling and analysis of multi-terminal VSC-HVDC for offshore wind farms, 10th IET International Conference on AC and DC Power Transmission (ACDC 2012), 1 - 6

[60] Cole, S. ; Belmans, R. : Modelling of VSC HVDC using coupled current injectors, 2008 IEEE Power and Energy Society General Meeting - Conversion and Delivery of Electrical Energy in the 21st Century, 1 - 8

[61] Imhof, M. ; Andersson, G. : Dynamic modeling of a VSC-HVDC converter, 2013 48th International Universities Power Engineering Conference (UPEC), 1 - 6'

[62] Jieqiu Bao ; Zhenguo Gao ; Li Yu ; Chuiyi Meng: Research on dynamic model and decoupling control strategy of VSC-HVDC system, 2011 International Conference on Electrical Machines and Systems (ICEMS), 1 - 4

[63] Teng Song ; Li Guangkai ; Song Xinli ; Ding Hui ; Ye Xiaohui: A novel method for VSC-HVDC electromechanical transient modeling and simulation, 1 - 4

[64] Lidong Zhang ; Harnefors, Lennart ; Nee, H.-P.: Modeling and Control of VSC-HVDC Links Connected to Island Systems

[65] e-Highway 2050 D 1.2 Structuring of uncertainties, options and boundary conditions for the implementation of EHS

[66] Jintao Cui, Kejun Li, Ying Sun, Zhenyu Zou, Yue Ma : Distributed energy storage system in wind power generation, 2011 4th International Conference on Electric Utility Deregulation and Restructuring and Power Technologies, 1535 – 1540

[67] Rasmussen, C.N.: Energy storage for improvement of wind power characteristics, 2011 IEEE PowerTech, Trondheim

[68] Dong-Jing Lee, Li Wang: Small-Signal Stability Analysis of an Autonomous Hybrid Renewable Energy Power Generation/Energy Storage System Part I: Time-Domain Simulations , IEEE Transactions on Energy Conversion, Volume: 23/1 (2008), 311 - 320

[69] Molina, M.G.: Distributed energy storage systems for applications in future smart grids Transmission and Distribution, 2012 Sixth IEEE/PE Latin America Conference and Exposition

[70] Babazadeh, H., Wenzhong Gao, Jin Lin, Lin Cheng: Sizing of battery and supercapacitor in a hybrid energy storage system for wind turbines , 2012 IEEE PES Transmission and Distribution Conference and Exposition (T&D)

[71] Chowdhury, M.M., Haque, M.E., Gargoom, A., Negnevitsky, M.: Performance improvement of a grid connected direct drive wind turbine using super-capacitor energy storage, 2013 IEEE PES

[72] Smith, S.C., Sen, P.K., Kroposki, B.: Innovative Smart Grid Technologies Advancement of energy storage devices and applications in electrical power system, 2008 IEEE Power and Energy Society General Meeting - Conversion and Delivery of Electrical Energy in the 21st Century

[73] Boyes, J.D., Clark, N.H.: Technologies for energy storage. Flywheels and super conducting magnetic energy storage, 2000 IEEE Power Engineering Society Summer Meeting, 1548 - 1550 vol. 3

[74] Chunlian Jin, Ning Lu, Shuai Lu, Makarov, Y., Dougal, R.A.: Coordinated control algorithm for hybrid energy storage systems ,2011 IEEE Power and Energy Society General Meeting

[75] Huang Youwei, Zhang Xu, He Junping, Qin Yi: The improvement of micro grid hybrid energy storage system operation mode, 2014 IEEE PES T&D Conference and Exposition,

[76] Bo Yang, Makarov, Y., Desteese, J., Viswanathan, V., Nyeng, P., McManus, B., Pease, J.: On the use of energy storage technologies for regulation services in electric power systems with significant penetration of wind energy, 2008 5th International Conference on European Electricity Market

[77] Usama, M.U., Kelle, D., Baldwin, T.: Utilizing spinning reserves as energy storage for renewable energy integration, 2014 Clemson University Power Systems Conference

[78] Xinda Ke, Ning Lu, Chunlian Jin: Control and size energy storage for managing energy balance of variable generation resources, 2014 IEEE PES General Meeting | Conference & Exposition,

[79] Ibrahima, K. ; Chengyong Zhao: Modeling of wind energy conversion system using doubly fed induction generator equipped batteries energy storage system, 2011 4th International Conference on Electric Utility Deregulation and Restructuring and Power Technologies, 1780 - 1787

[80] Shimizukawa, J. ; Iba, K. ; Hida, Y. ; Yokoyama, R.: Mitigation of intermittency of wind power generation using battery energy storage system , 2010 45th International Universities Power Engineering Conference

[81] Hatta, H. ; Shima, W. ; Kawakami, T. ; Kobayashi, H. ; Sueyoshi, N. ; Nakama, H. ; Oshiro, Y. ; Toguchi, M. : Demonstration test of PV output reduction method using battery energy storage system and customer equipment 2013 4th IEEE/PES Innovative Smart Grid Technologies Europe (ISGT EUROPE)

[82] Takeda, K. ; Takahashi, C. ; Arita, H. ; Kusumi, N. ; Amano, M. ; Emori, A.: Design of hybrid energy storage system using dual batteries for renewable applications, 2014 IEEE PES General Meeting | Conference & Exposition

[83] Amano, H. ; Shima, W. ; Kawakami, T. ; Inoue, T. ; Uehara, Y. ; Nakama, H. ; Oshiro, Y.: Field verification of control performance of a LFC system to make effective use of existing power generation and battery energy storage system, 2013 4th IEEE/PES Innovative Smart Grid Technologies Europe (ISGT EUROPE)

[84] Meng Liu ; Wei-Jen Lee ; Lee, L.K. : Wind and PV hybrid renewable system dispatch using battery energy storage, 2013 North American Power Symposium (NAPS)

[85] Soong, T. ; Lehn, P.W.: Evaluation of Emerging Modular Multilevel Converters for BESS Applications, IEEE Transactions on Power Delivery, Vol.29, No. ,5 ,2086 - 2094

[86] Leung, K.K.; Sutanto, D.: Using Battery Energy Storage System in a Deregulated Environment to Improve Power System Performance, International Conference on Electric Utility Deregulation and Restructuring and Power Technologies. April 2000

[87] Li, Y., Zhang, Z., Yang, Y., Chen, H., Xu, Z. : Coordinated control of wind farm and VSC-HVDC system using capacitor energy and kinetic energy to improve inertia level of power systems, International Journal of Electrical Power and Energy Systems 55 (2014), 79-92

[88] ENTSO-E Network Code for Requirements for Grid Connection Applicable to all Generators, final version (March 2013)

[89] IEC 61400-27-1 Electrical simulation models -Wind turbines

[90] K. Clark, N. W. Miller, J. J. Sanchez-Gasca: Modeling of GE Wind Turbine-Generators for Grid Studies, GE Energy report Version 4.5, 2010

[91] D. Gautom, L. Goel, R. Ayyanar, V. Vittal, and T. Harbour: Control strategy to mitigate the impact of reduced inertia due to doubly fed induction generators on large power systems, IEEE Trans. Power Syst., Vol. 26, No. 1, pp. 214–224, Feb. 2011.

[92] D. Gautam, V. Vittal, and T. Harbour: Impact of increased penetration of DFIG-based wind turbine generators on transient and small signal stability of power system, IEEE Trans. Power Syst., Vol. 24, No. 3, pp. 1426–1434, Aug. 2009.

[93] Erlich, I., Shewarega, F., Engelhardt, S., Kretschmann, J., Fortmann, J., Koch, F., Effect of wind turbine output current during faults on grid voltage and the transient stability of wind parks, 2009 IEEE Power & Energy Society General Meeting

[94] Pasca, E., Petretto, G., Grillo, S., Marinelli, M., Silvestro, F.: Characterization of wind and solar generation and their influence on distribution network performances, Proceedings of the 44th International Universities Power Engineering Conference, 2009

[95] E. Muljadi, C. P. Butterfield, B. Parsons, and A. Ellis: Effect of variable speed wind turbine generator on stability of a weak grid, IEEE Trans. Energy Convers., Vol. 22, No. 1, pp. 29–35, Mar. 2008

[96] Hamidi, V., Li, F., Robinson, F.: Responsive demand in networks with high penetration of wind power, 2008 IEEE-PES Transmission and Distribution Conference and Exposition

[97] Koch, F.W., Erlich, I., Shewarega, F., Bachmann, U.: Dynamic interaction of large offshore wind farms with the electric power system, Proceedings 2003 IEEE Bologna Power Tech Conference

[98] Seul-Ki K., Eung-Sang K., Jong-Bo A., Modeling and Control of a Grid-connected Wind/PV Hybrid Generation System, 2006 IEEE-PES Transmission and Distribution Conference and Exhibition, pp. 1202 – 1207

[99] K. R. Erlich and F. Shewarega: Impact of large wind power generation on frequency stability, in Proc. 2006 IEEE PES General Meeting, Montreal

[100] J.G. Slootweg, H. Polinder, W.L. Kling: Reduced Order Models of Actual Wind Turbine Concepts, IEEE Young Researchers Symposium, 2002, Leuven

[101] K. Clark, N. W. Miller, J. J. Sanchez-Gasca: Modeling of GE Solar Photovoltaic Plants for Grid Studies, GE Energy report Version 1.1, 2010

[102] F. Fernandez-Bernal, L. Rouco, P. Centeno, M. Gonzalez, and M. Alonso> Modelling of photovoltaic plants for power system dynamic studies, in Proc. Power System Management and Control Conference, Apr. 2002, pp. 341–346

[103] K. Máslo, M. Pistora: Long term dynamics modeling of renewable energy sources, 2011 IEEE EUROCON International Conference, Lisboa

[104] A. Yazdani, A.R. di Fazio, H. Ghoddami, M. Russo, M. Kazerani, J. Jatskevich, K. Strunz, S. Leva, J.A. Martinez (Task Force on Modeling and Analysis of Electronically-Coupled Distributed Resources): “Modeling guidelines and a benchmark for power system

simulation studies of three-phase single-stage photovoltaic systems," IEEE Trans. Power Del., vol. 26, no. 2, pp. 1247–1264, Apr. 2011

[105] CIGRE Technical Brochure No 575, Task Force C6.04.02, Benchmark systems for network integration of renewable and distributed energy resources, 2014

[106] Chobanov, V.Y. : Demand response through grid connected south, east, west PV with energy storage, 2014 IEEE PES T&D Conference and Exposition

[107] W. A. Omran, M. Kazerani, M. M. A. Salama: Investigation of methods for reducing of power fluctuations generated from large gridconnected photovoltaic systems, IEEE Trans Energy Convers, 26 (2011), pp. 318–327

[108] B. Tamimi, C. Ca˜nizares, and K. Bhattacharya: Modeling and performance analysis of large solar photo-voltaic generation on voltage stability and inter-area oscillations, in Proc. IEEE PES General Meeting, Jul. 2011

[109] I. Papaioannou, M. C. Alexiadis, C. S. Demoulias, D. P. Labridis, and P. S. Dokopoulos: Modeling and field measurements of photovoltaic units connected to LV grid. study of penetration scenarios," IEEE Trans. Power Del., Vol. 26, No. 2, pp. 979–987, Apr. 2011

[110] P. P. Dash and M. Kazerani: Dynamic modeling and performance analysis of a grid-connected current-source inverter-based photovoltaic system, IEEE Trans. Sust. Energy, vol. 2, no. 4, 443–450, Oct. 2011

[111] N. Kakimoto, Q. Piao, and H. Ito: Voltage control of photovoltaic generator in combination with series reactor, IEEE Trans. Sust. Energy, Vol. 2, No. 4, 374–382, Oct. 2011

[112] Enslin, J.H.R. Network impacts of high penetration of photovoltaic solar power systems, 2010 IEEE Power and Energy Society General Meeting,

[113] Y. Ueda, S. Suzuki, and T. Ito, Grid stabilization by use of an energy storage system for a large-scale PV generation plant, ECS Transactions, Vol. 16, No. 34, 17–25, Oct. 2009

[114] A. Canova, L. Giaccone, F. Spertino, and M. Tartaglia: Electrical impact of photovoltaic plant in distributed network, IEEE Trans. Ind. Appl., Vol. 45, No. 1,341–347, Jan. / Feb. 2009

[115] R. Baxter, "A call for back-up: How energy storage could make a valuable contribution to renewables," Renewable energy world Mag., Sep. 2007. [Online]. Available: http://www.renewableenergyworld.com

[116] M. Thomson and D. Infield, "Impact of widespread photovoltaics generation on distribution systems," IET Renewable Power Generation, vol. 1, no. 1, 33–40, Mar. 2007

[117] Standard Models for Variable Generation," NERC special report, Feb. 2010, [Online]. Available: http://www.nerc.com/files/Standards%20Models%20for%20Variable%20Generation.pdf

[118] Modeling New Forms of Generation and Storage, CIGRE, Tech. Rep., Nov. 2000, TF 38.01.10

[119] Dallmer-Zerbe, K. ; Bucher, M.A. ; Ulbig, A. ; Andersson, G.: Assessment of capacity factor and dispatch flexibility of concentrated solar power units, 2013 IEEE PowerTech, Grenoble

[120] I. L. Garcia, J. L. Alvarez, and D. Blanco, "Performance model of parabolic solar thermal power plants with thermal storage: Comparison to operating plant data," Solar Energy, vol. 85, pp. 2443- 2460, 2011

[121] Madaeni, S.H. ; Sioshansi, R. ; Denholm, P.: Estimating the Capacity Value of Concentrating Solar Power Plants With Thermal Energy Storage: A Case Study of the Southwestern United States IEEE Transactions on Power Systems, Volume: 28 , Issue: 2 (2013) ,1205 – 1215

[122] Ti Xu ; Gross, G.: A production simulation tool for systems with an integrated concentrated solar plant with thermal energy storage , 2013 Bulk Power System Dynamics and Control Symposium

[123] Sakellaridis, N. ; Mantzaris, J. ; Tsourakis, G. ; Vournas, C. ; Vitellas, I. : Operation and security assessment of the power system of Crete with integration of pumped storage and concentrated solar thermal plants , 2013 Bulk Power System Dynamics and Control Symposium

[124] Xu, Z. ; Kariuki, S.K. ; Chowdhury, S. ; Chowdhury, S.P.: Investigation of thermal storage options for Concentrating Solar Power plants, 2012 47th International Universities Power Engineering Conference

[125] Camm, E.H. ; Williams, S.E.: Solar power plant design and interconnection , 2011 IEEE Power and Energy Society General Meeting

[126] Shah, R. ; Ruifeng Yan ; Saha, T.K.: Performance assessment of solar thermal power plants: A case study in Queensland , 2014 IEEE PES General Meeting | Conference & Exposition

[127] Gonzalez, J.L. ; Dimoulkas, I. ; Amelin, M: .Operation planning of a CSP plant in the spanish day-ahead electricity market, 2014 11th International Conference on the European Energy Market

[128] Andrea Giostri, Marco Binotti, Marco Astolfi, Paolo Silva, Ennio Macchi, Giampaolo Manzolini: Comparison of different solar plants based on parabolic trough technology, Solar Energy, Volume 86, Issue 5,(May 2012), 1208–1221

[129] M.J. Montes, A. Abánades, J.M. Martínez-Val, M. Valdés: Solar multiple optimization for a solar-only thermal power plant, using oil as heat transfer fluid in the parabolic trough collectors, Solar Energy, Volume 83, Issue 12 (December 2009), 2165–2176

[130] Biencinto, M., Bayón, R., Rojas, E., González, L. : Simulation and assessment of operation strategies for solar thermal power plants with a thermocline storage tank Solar Energy 103 (2014), 456-472

[131] Zaversky, F., García-Barberena, J., Sánchez, M., Astrain, D.: Transient molten salt two-tank thermal storage modeling for CSP performance simulations , Solar Energy 93 (2013) , pp. 294-311

[132] M. Medrano, A. Gil, I. Martorell, X. Potau, and L. F. Cabeza, "State of the art on high-temperature thermal energy storage for power generation. part 2: Case studies," Renewable and Sustainable Energy Reviews, vol. 14 (1/2010), 56 – 72

[133] L. Garcia, J. L. Alvarez, and D. Blanco, "Performance model for parabolic trough solar thermal power plants with thermal storage: Comparison to operating plant data," Solar Energy, vol. 85, (10/201), 2443 – 2460

[134] Mertens, N., Alobaid, F., Frigge, L., Epple, B.: Dynamic simulation of integrated rock-bed thermocline storage for concentrated solar power, Solar Energy 110 (2014), 830-842

[135] J.B. Zhang, J.C. Valle-Marcos, B. El-Hefni, Z.F. Wang, G.F. Chen, G.C. Ma, X. Li, R. Soler: Dynamic Simulation of a 1 MWe Concentrated Solar Power Tower Plant System with Dymola®, Energy Procedia, 49 (2014), 1592–1602

[136] P. Viebahn, Y. Lechon, F. Trieb: The potential role of concentrated solar power (CSP) in Africa and Europe–a dynamic assessment of technology development, cost development and life cycle inventories until 2050, Energy Policy, 39 (8/2011), 4420–4430

[137] D. Barlev, R. Vidu, P. Stroeve: Innovation in concentrated solar power, Solar Energy Mater Solar Cells, 95 (10/2011), 2703–2725

[138] M.J. Montes, A. Rovira, M. Muñoz, J.M. Martínez-Val: Performance analysis of an integrated solar combined cycle using direct steam generation in parabolic trough collectors, Appl Energy, 88 (9/2011), 3228–3238

[139] K. Heussen, S. Koch, A. Ulbig, and G. Andersson: Unified system-level modeling of intermittent renewable energy sources and energy storage for power system operation, IEEE Systems Journal, , vol. 6, no. 1 (2012), 140 –151

[140] D3.1. Technology assessment from 2030 to 2050, e-HIGHWAY 2050, Aug.2014

[141] Draft Network Code on Demand Connection, version of 21st December 2012. Available at: http://networkcodes.entsoe.eu/wp-content/uploads/2013/08/121221_final_Network_Code_on_Demand_Connection.pdf

[142] K. Máslo, M. Pistora, T. Linhart: Use of Demand Side Response System Frequency Control in Emergency and Restoration, CIRED Workshop, June 201

[143] IEC 61970: Energy Management System Application Program Interface (EMS-API) – Part 457: Common Information Model (CIM) for Dynamics Profile Draft Edition 1.00 Based on release IEC 61970 CIM16 v24, 2013-08-31

[144] National Energy Technology Laboratory http://www.netl.doe.gov/moderngrid/

[145] Modern Grid Benefits

[146] Barriers to Achieving the Modern Grid

[147] A Compendium of Modern Grid Technologies

[148] The Modern Grid Initiative v2.0

[149] A Vision for the Modern Grid, Khosrow Moslehi, Ranjit Kumar

[150] A Systems View of the Modern Grid v2.0

[151] Appendix A1: Self-Heals v2.0 (Towards self-healing Energy Infrastructure Systems)

[152] Appendix A2: Motivates and Includes the Consumer v2.0

[153] Appendix A4: Provides Power Quality for 21st Century Needs v2.0

[154] Appendix A7: Optimizes Assets and Operates Efficiently v2.0

[155] Appendix B1: Integrated Communications v2.0

[156] Appendix B2: Sensing and Measurement

[157] Appendix B3: Advanced Components

[158] Appendix B4: Advanced Control Methods

[159] Appendix B5: Improved Interfaces and Decision Support

[160] Modern Grid Initiative Vision Summary

[161] Regulatory Funding of Transmission System Research and Development in ENTSO-E Countries WHITE PAPER

[162] Distributed Intelligent Control Systems http://www.sgiclearinghouse.org/Technologies?q=node/2152

[163] ENTSO-E response to the CEER public consultation on the 'Regulatory aspects of the integration of wind generation in European electricity markets'

[164] ENTSO-E Working Draft Network Code on Emergency and Restoration

[165] ENTSO-E Network Code on Electricity Balancing

[166] ENTSO-E Network Code on Load-Frequency Control and Reserves

[167] e-HIGHWAY 2015, WP4, Subtask 4.1.1 Definition of strategy and framework to perform case studies for operational validation report

[168] ENTSO-E SG CSO Solar Eclipse 2015 – Analysis of operational countermeasures

[169] ENTSO-E_spe_pp_solar_eclipse_2015

[170] ENTSO-E Regional Cooperation Paper sketch

Appendix I: Scenarios, Models and Data

A. The Five Scenarios

A.1. Scenario X-5

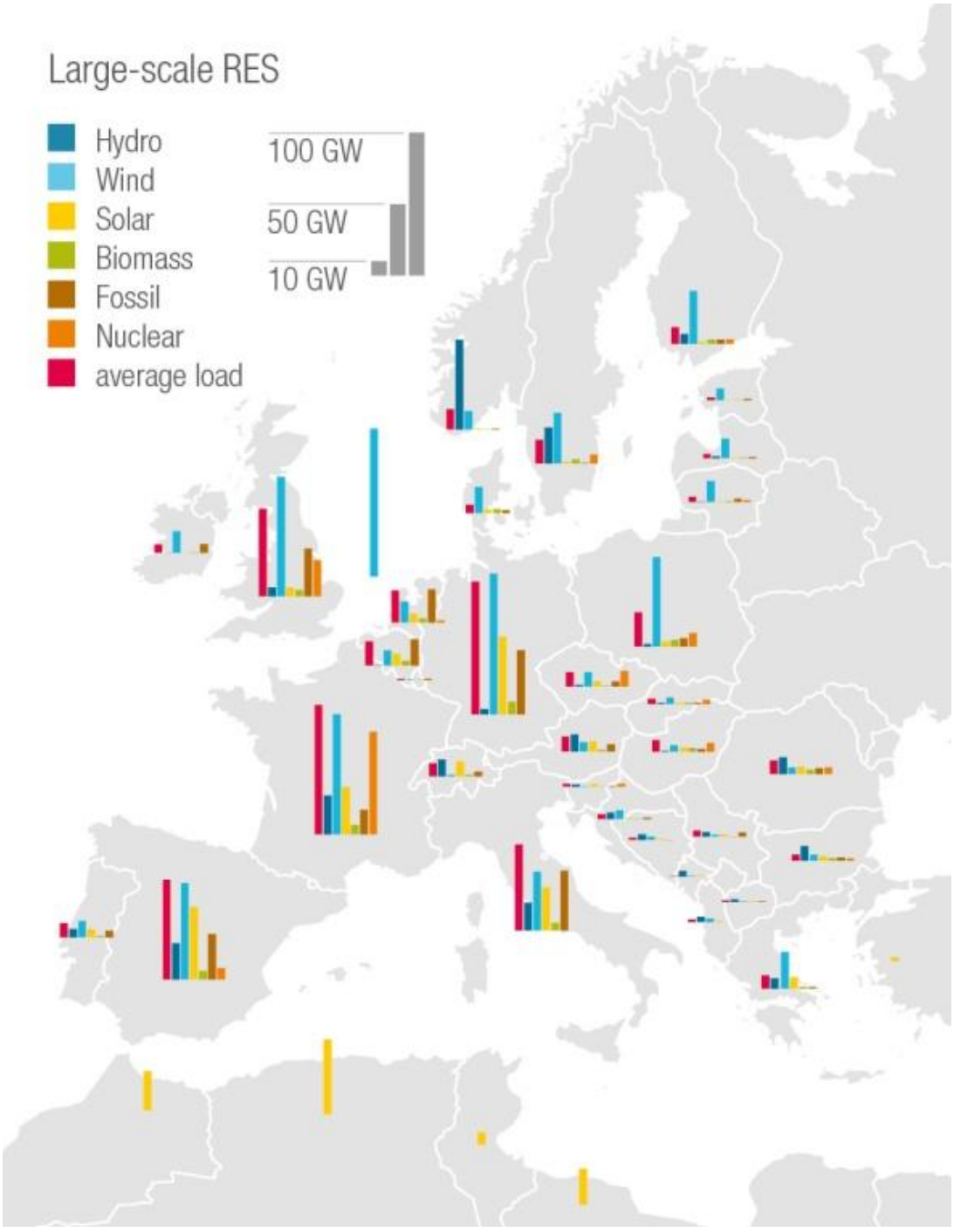

Figure A.1. Overview of the generation and demand in scenario X-5

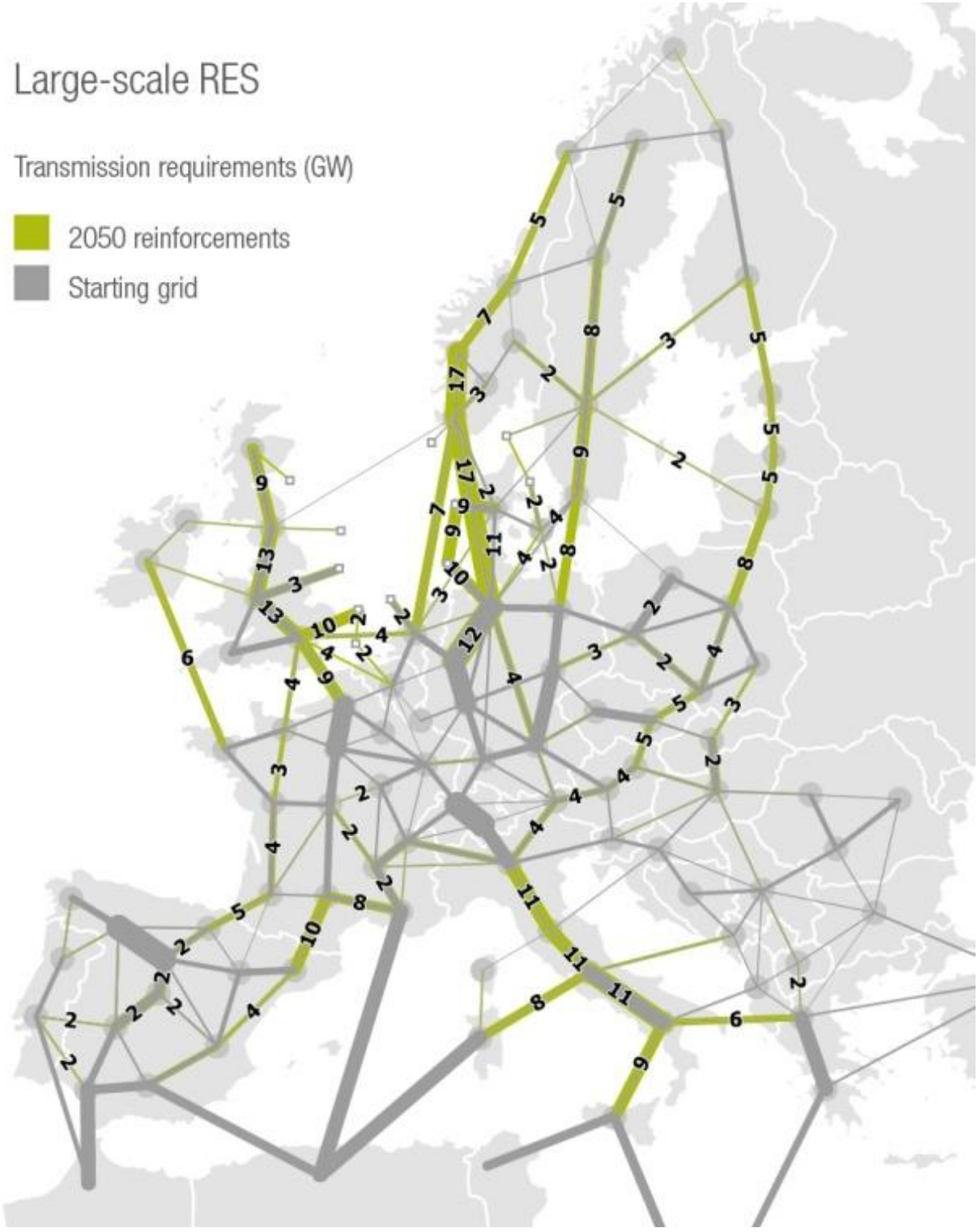

Figure A.2. Overview of the grid architectures in scenario X-5

A.2. Scenario X-7

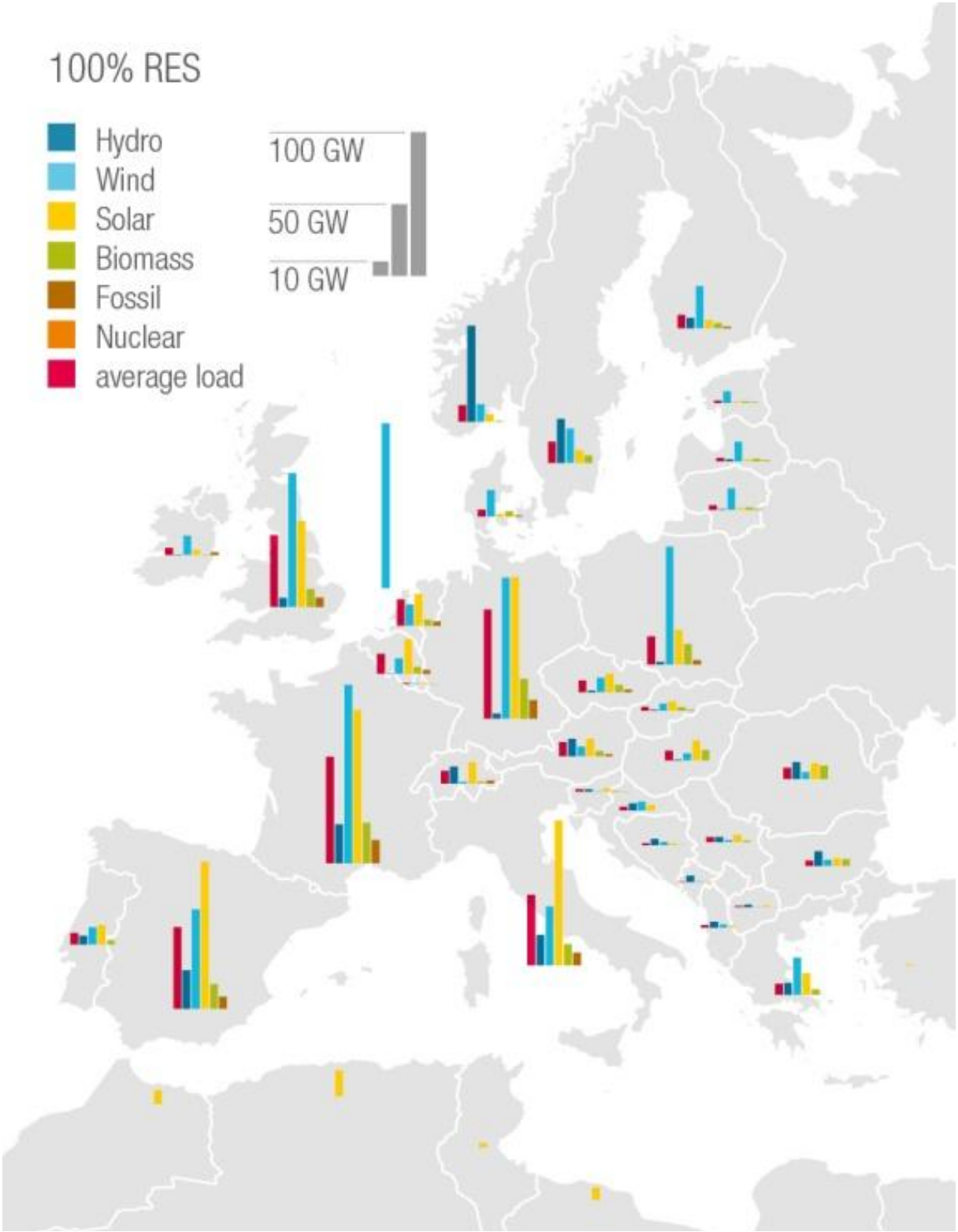

Figure A.3. Overview of the generation and demand in scenario X-7

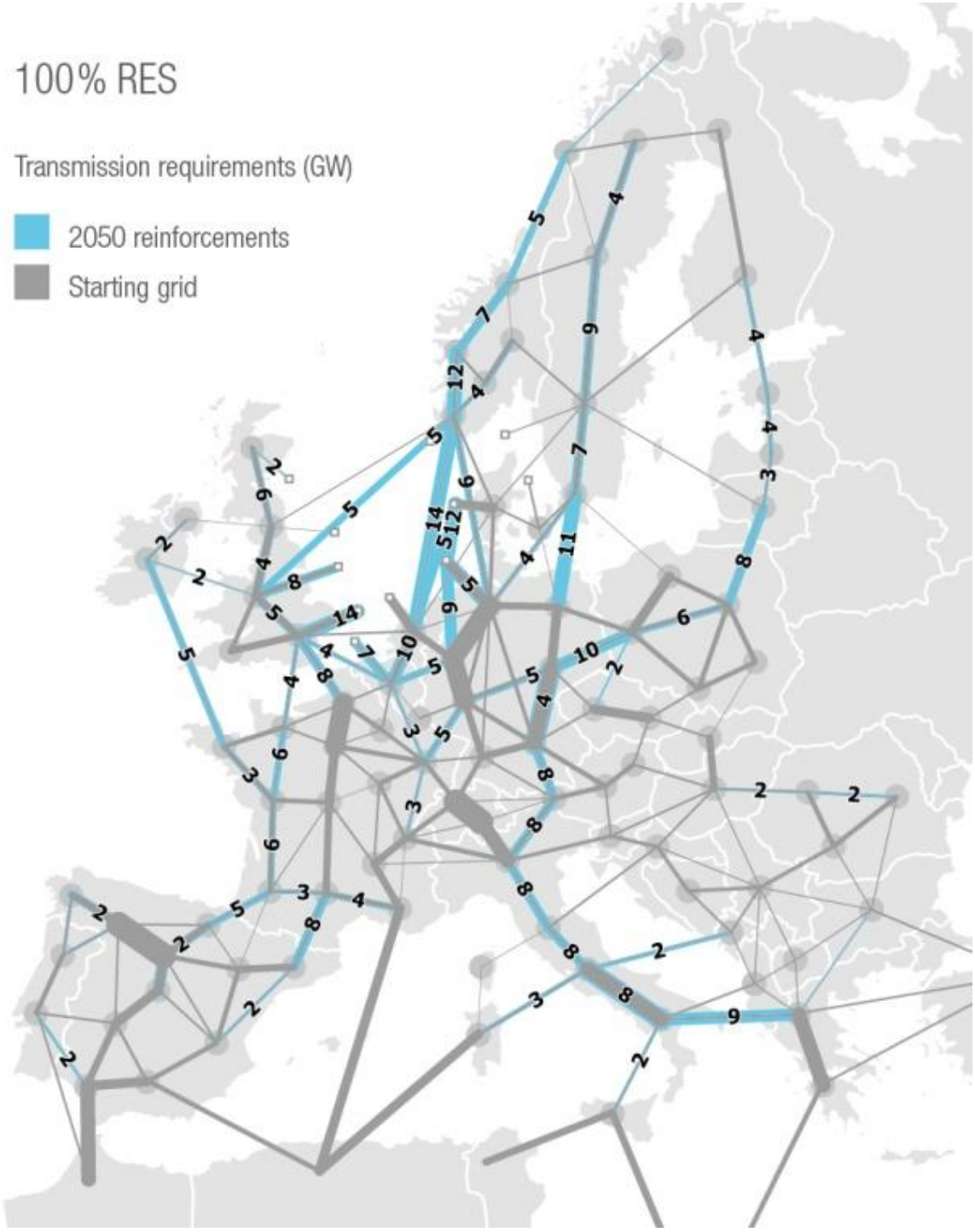

Figure A.4. Overview of the grid architectures in scenario X-7

A.3. Scenario X-10

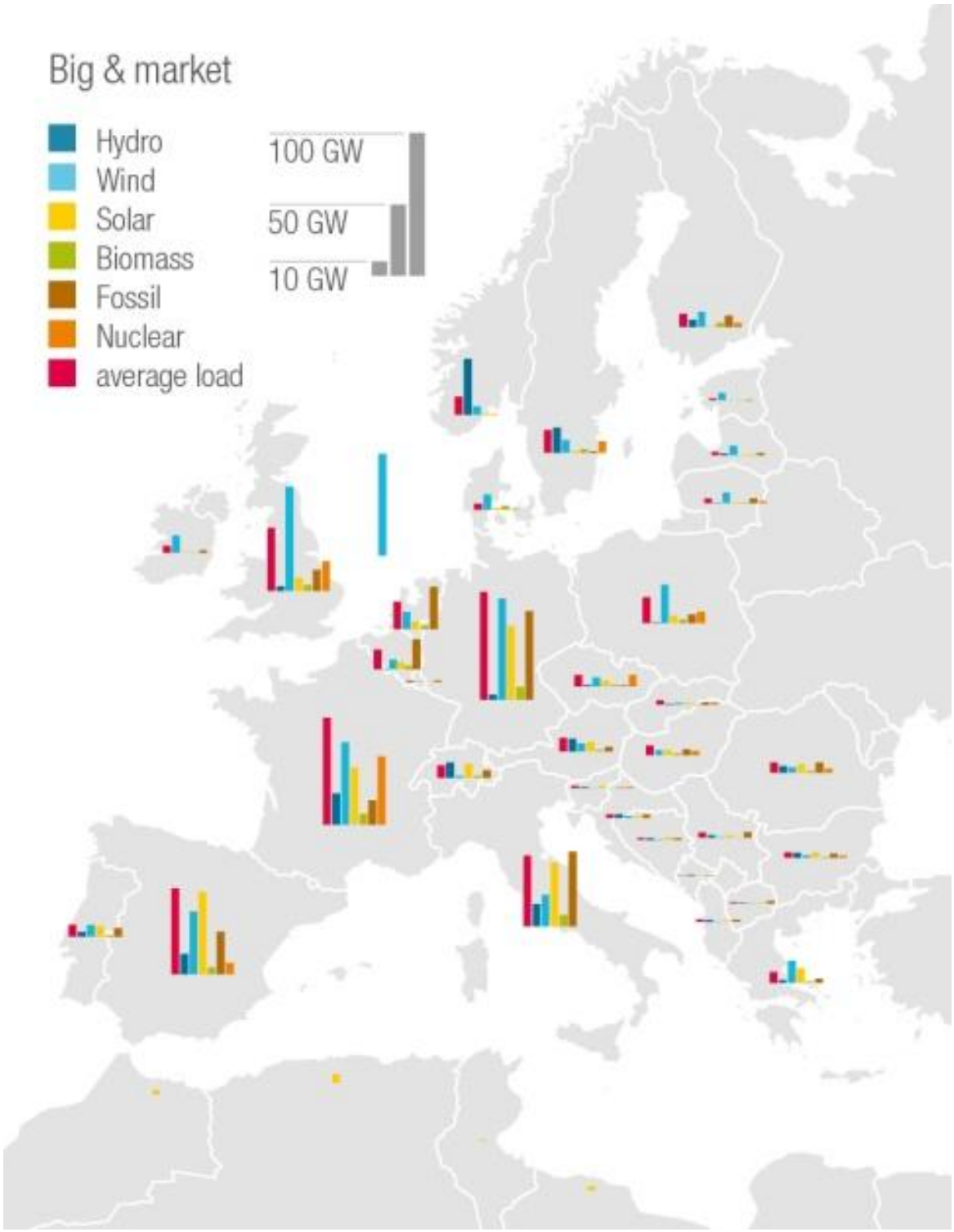

Figure A.5. Overview of the generation and demand in scenario X-10

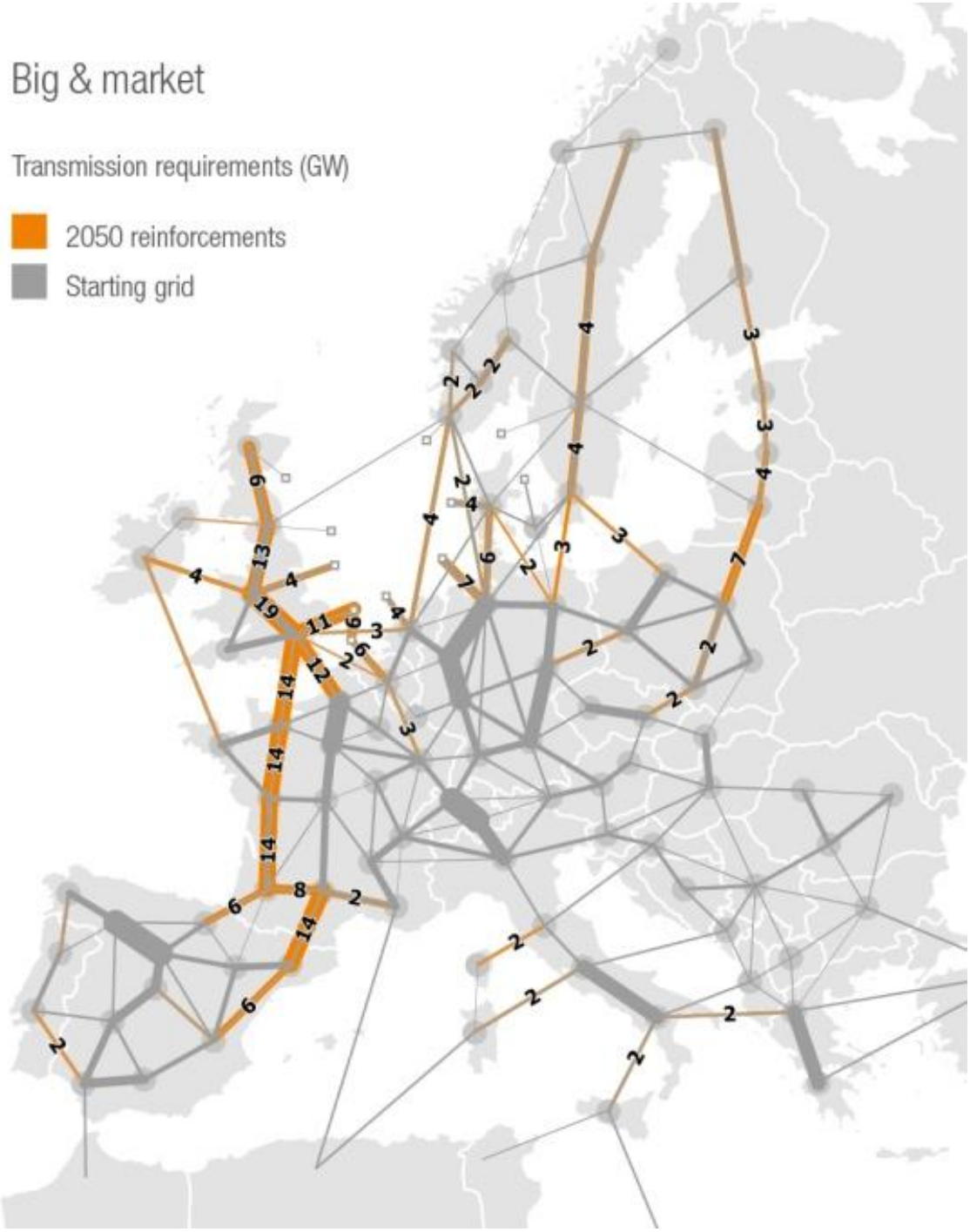

Figure A.6. Overview of the grid architectures in scenario X-10

A.4. Scenario X-13

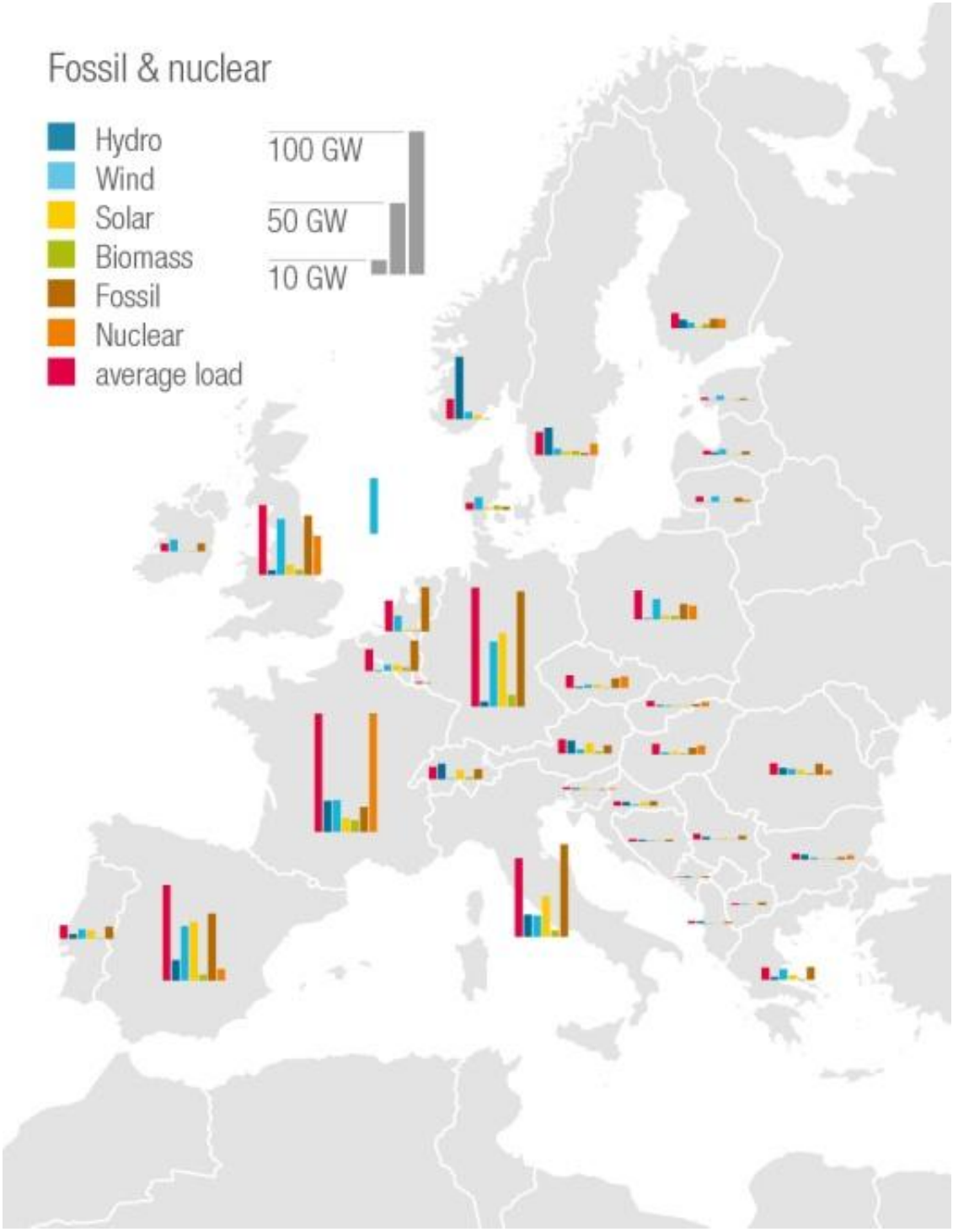

Figure A.7. Overview of the generation and demand in scenario X-13

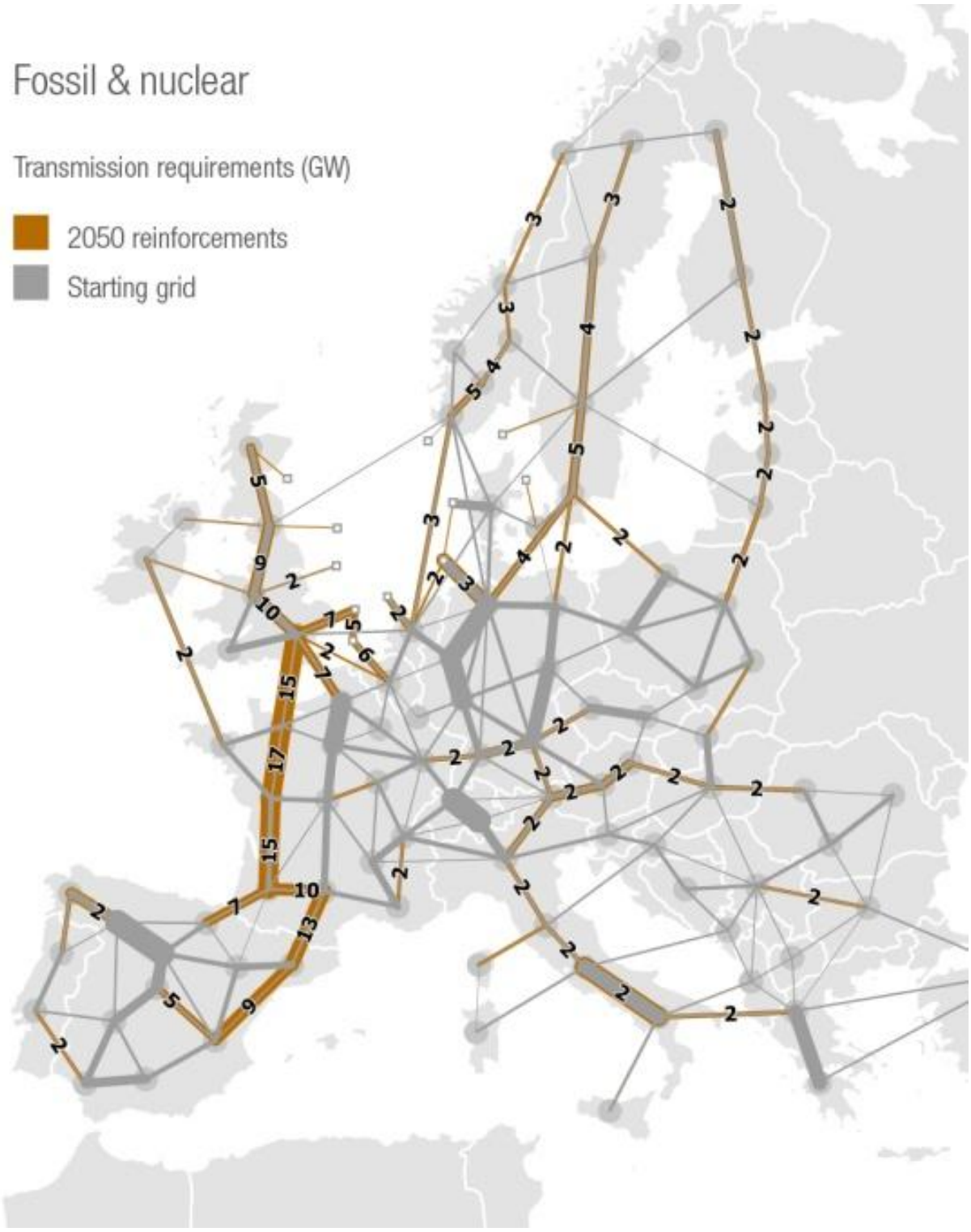

Figure A.8. Overview of the grid architectures in scenario X-13

A.5. Scenario X-16

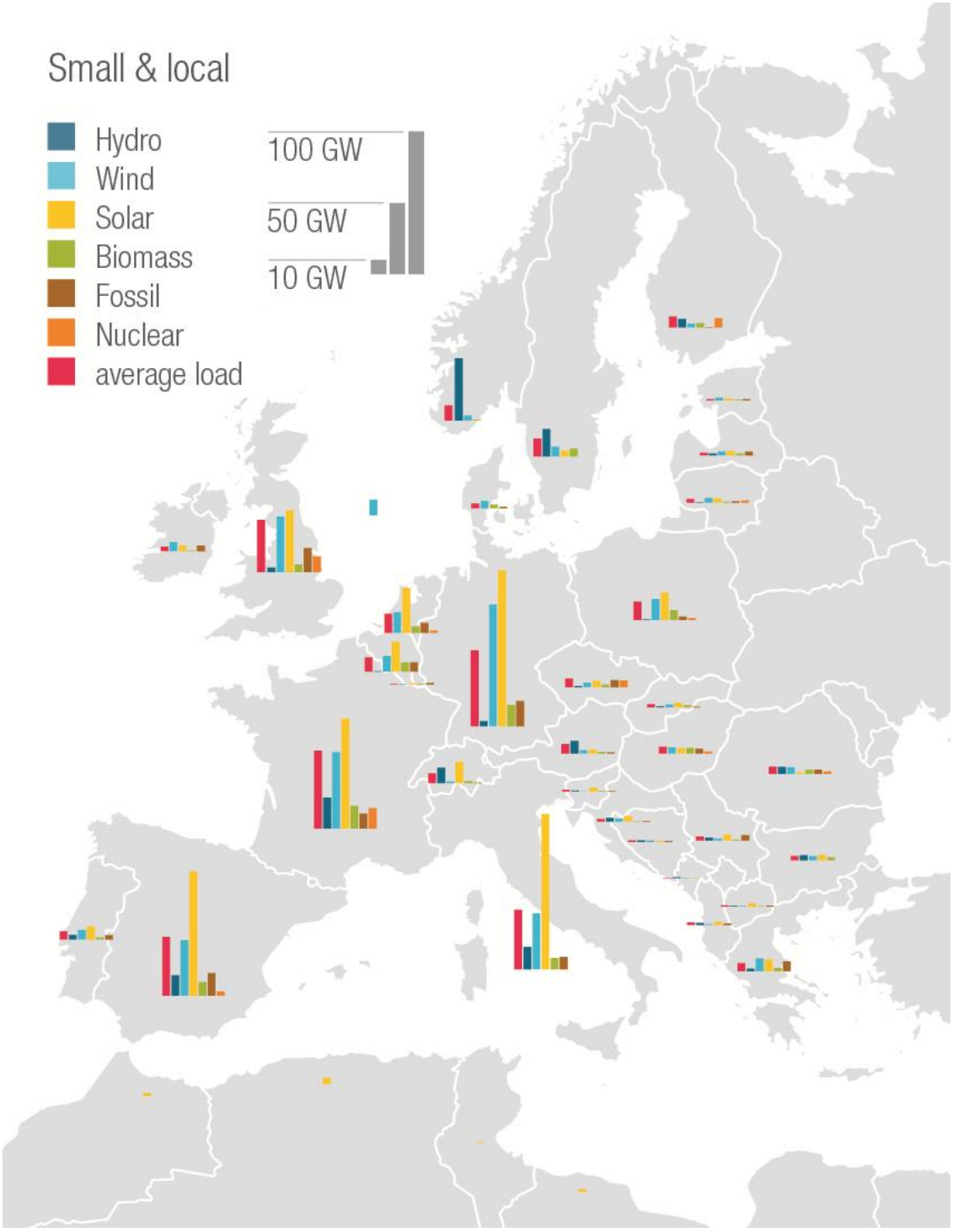

Figure A.9. Overview of the generation and demand in scenario X-16

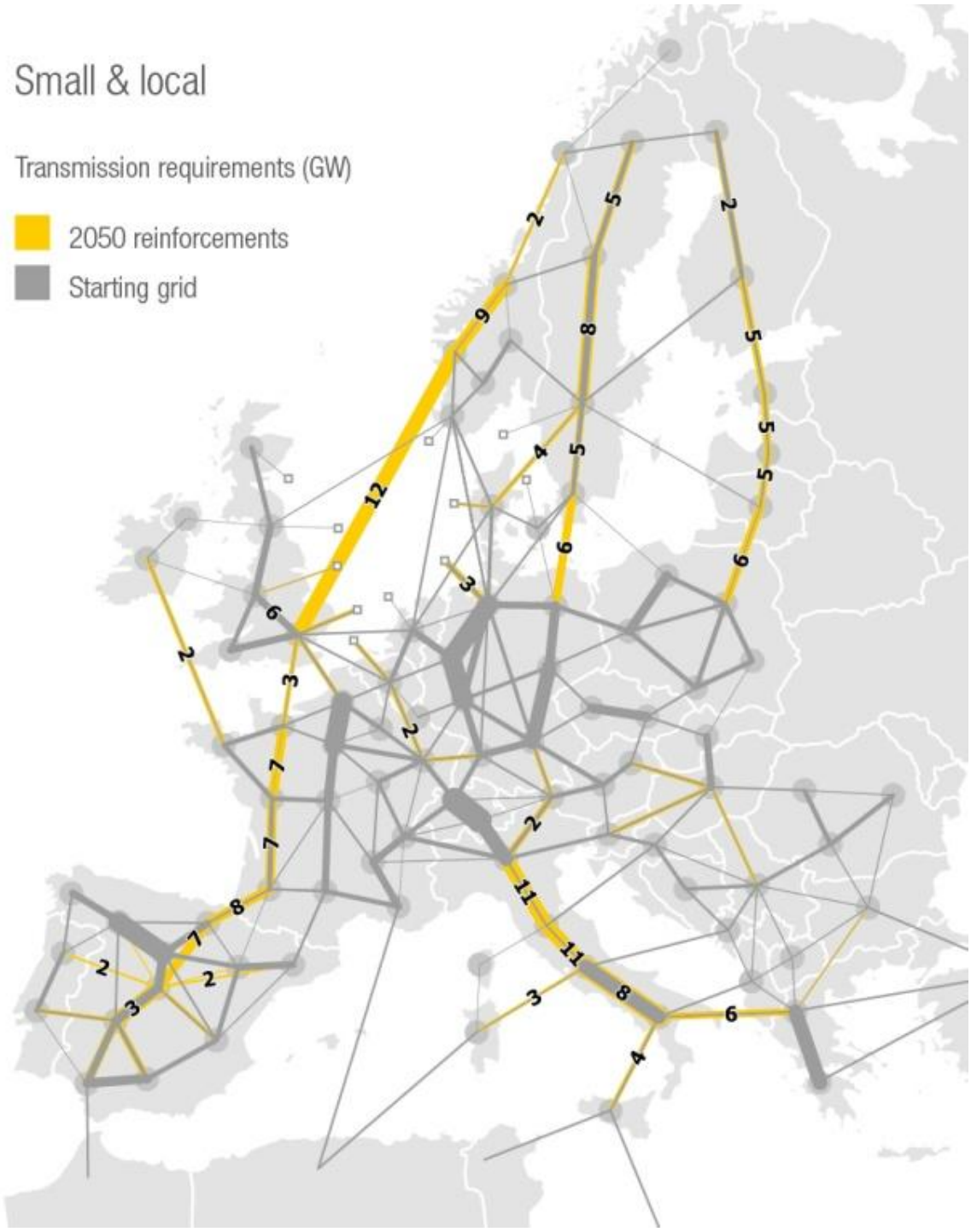

Figure A.10. Overview of the grid architectures in scenario X-16

B. Area Power Balance Data from Market Simulation

The results in Table B.1 and Table B.2 are resulting from market simulations performed with the ANTARES software.

Table B.1. Continental Europe synchronous area

Scenario	X-5		X-7		X-10		X-16	
Regime / Area	Summer Low	Winter Peak	Summer Low	Winter Peak	Summer Low	Winter Peak	Summer Low	Winter Peak
ES	-10461	-25431	**-924**	**-4188**	-4574	-19877	313	-3916
PT	-407	-762	**-1358**	**1382**	-1950	1563	-1791	2236
FR	1240	-13864	**3159**	**-16640**	6114	-13962	1992	-9164
BE	-7669	-7693	**620**	**-9754**	-6329	-2874	822	-435
LU	-926	286	**-586**	**-418**	-897	-96	-309	680
NL	-9845	-11088	**-2454**	**-14098**	-8724	-2170	1554	-3243
DE	-26270	-59624	**-10031**	**-40528**	-16501	-29298	5705	-20283
DK	4431	1581	**861**	**3711**	1929	2237	-366	125
CZ	2123	1116	**60**	**-2513**	1768	-712	-634	1568
PL	893	608	**2299**	**4899**	-1676	-2367	-1904	-2639
SK	384	362	**727**	**380**	-175	-421	12	-425
CH	-3261	-1369	**-2764**	**-1875**	-1641	2013	-2497	4700
AT	-4602	1258	**-6892**	**2784**	-3357	340	-6358	3998
IT	-29971	-22536	**5753**	**-26652**	-5406	-5458	9154	-15809
SI	1511	936	**373**	**-819**	860	132	360	185
H	-1067	-847	**638**	**-941**	-976	-1217	-1291	1869
RO	1273	2039	**193**	**2477**	2108	2475	-2003	2887
HR	-1783	235	**-426**	**-568**	-1226	1009	-53	1135
BA	-59	906	**18**	**3182**	25	169	-489	2
ME	-83	1813	**-165**	**2603**	-110	472	-75	338
RS	-1618	-2937	**150**	**-1701**	-502	-478	-27	717
BG	-543	278	**-812**	**695**	-129	69	-926	256
MK	-760	6	**-195**	**183**	-154	454	225	-6
GR	1325	2747	**469**	**6289**	1537	131	-607	4039
AL	493	478	**190**	**827**	226	-291	539	-699
LT	3110	5912	**1948**	**4006**	3342	4400	-364	4837
TR	0	0	**0**	**0**	0	0	0	0

Table B.2. Export/import to the continental Europe synchronous area

Scenario	X-5		X-7		X-10		X-16	
Regime / Area	Summer Low	Winter Peak	Summer Low	Winter Peak	Summer Low	Winter Peak	Summer Low	Winter Peak
NS	17171	24153	**5362**	**28162**	14852	22494	0	4786
MA	11723	12298	**2046**	**4541**	1839	1366	185	1019
DZ	17554	15562	**2854**	**5901**	1938	1738	464	1026
TN	4059	3852	**497**	**1248**	508	497	116	316
LY	12560	9274	**1530**	**3955**	1708	1232	224	761
IE	-1772	3277	**-848**	**1363**	26	1355	-920	1976
UK	340	17332	**-77**	**9853**	4585	24797	-1621	6947
DKE	3610	4692	**0**	**228**	429	380	0	349
SE	6363	7604	**-263**	**10456**	4020	3696	0	4923
NO	12155	22505	**0**	**22493**	5771	4469	0	3116

C. Data for Dynamic Models

Meaning of parameters is described in [40]. Tuning consist of changing of initial parameters [34] to get similar waveform of frequency deviation for large unit outage (comparing with WAMS) and stable operation for the e-Hihway2050 scenarios in the Pan European dynamic model. Following figures show block schemes of used models for excitation system and turbine.

Meaning of parameters is described in [40], [143]. Tuning consist of changing of initial parameters [34] to get similar waveform of frequency deviation for large unit outage in the Pan European dynamic model. This appendix shows block diagrams of initial models for excitation system and turbine. Tables with parameters consist of initial and tuned parameters. Tuned parameters in the tables are highlighted in red.

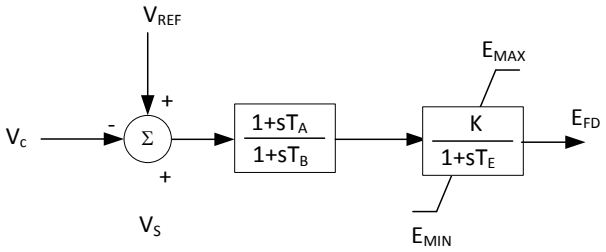

Figure C.1. Block diagram of the SEXS model of excitation system

Table C.1. Initial and tuned parameters of the SEXS model of excitation system

Exciter	T_A	T_B	K	T_E	E_{MIN}	E_{MAX}	Notice
SEXS	3	10	200	0.05	0	4	Initial values
SEXSRD	3	10	100	0.05	0	4	Tuned values for frequency stability calculations

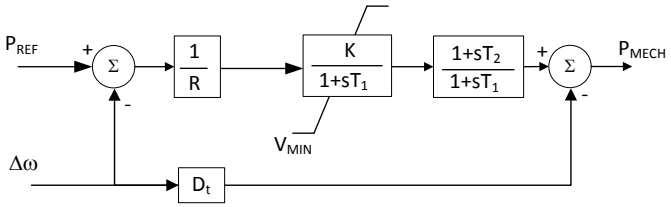

Figure C.2. Block diagram of the TGOV1 turbine model

Table C.2. Initial and tuned parameters of the TGOV1 turbine model

Turbine	R	T_1	T_2	T_3	v_{MIN}	v_{MAX}	Notice
TGOV1	0.380	0.5	3	10	0	1	Initial values
TGOVE	0.3	0.5	6	12	0	1	Tuned values for for frequency stability calculations

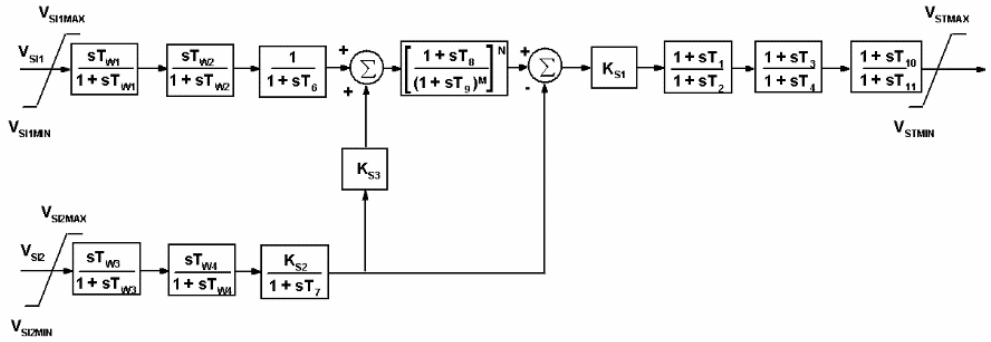

Figure C.3. Block diagram of simplified power system stabiliser model PSS2A

Table C.3. Initial and tuned parameters of simplified power system stabiliser model PSS2A

PSS	$T_{W1}=T_{W2}=T_{W3}=T_7$	$T_6=T_{W4}$	K_{s1}	K_{s2}	K_{s3}	T_9	T_1	T_2	T_3	T_4	$V_{STMX}=-V_{STMin}$	Notice
PSS2A	2	0	10	0.154	1	0.1	0.25	0.03	0.15	0.015	0.1	Initial values
PSS2IB	2	0	40	0.154	1	0.1	0.25	0.03	0.15	0.015	0.1	Tuned values for ES and PT
PSS2CE	2	0	4	0.154	1	0.1	0.25	0.03	0.15	0.015	0.1	Tuned values for the rest of CE

Table C.4. Initial and tuned parameters of synchronous generator

Generator	Xl	Xd	Xq	Xd'	Xd''	Td'	Td''	Xq''	Xq'	Tq''	Tq'	H	Notice
SubtransientRoundRotor	0.15	2	1.8	0.35	0.25	0.9	0.03	0.3	0.5	0.05	0.6	4	Initial values
E500IB	0.15	2	1.8	0.35	0.25	0.9	0.03	0.3	0.5	0.05	0.6	**6**	Tuned values for PT, ES
E500FR	0.15	2	1.8	0.35	0.25	0.9	0.03	0.3	0.5	0.05	0.6	**5.5**	Tuned values for BE, FR and TR
E500CE	0.15	2	1.8	0.35	0.25	0.9	0.03	0.3	0.5	0.05	0.6	**3**	Tuned values for the Balkan
E500E	0.15	2	1.8	0.35	0.25	0.9	0.03	0.3	0.5	0.05	0.6	**5**	Values for the rest of CE

Table C.4. Initial and tuned parameters of synchronous generator

Generator	Xl	Xd	Xq	Xd'	Xd''	Td'	Td''	Xq''	Xq'	Tq''	Tq'	H	Notice
SubtransientRoundRotor	0.15	2	1.8	0.35	0.25	0.9	0.03	0.3	0.5	0.05	0.6	4	Initial values
SubtransientRoundRotor	0.15	2	1.8	0.35	0.25	0.9	0.03	0.3	0.5	0.05	0.6	**8**	Tuned values for PT, ES
SubtransientRoundRotor	0.15	2	1.8	0.35	0.25	0.9	0.03	0.3	0.5	0.05	0.6	**5.5**	Tuned values for BE, FR
SubtransientRoundRotor	0.15	2	1.8	0.35	0.25	0.9	0.03	0.3	0.5	0.05	0.6	**1.5**	Tuned values TR
SubtransientRoundRotor	0.15	2	1.8	0.35	0.25	0.9	0.03	0.3	0.5	0.05	0.6	**3**	Tuned values for the rest of CE

D. Parameters for Dynamic Models used for the benchmark test systems

IEC standard models were used if they exist.

D.1. Synchronous Generators Models

This model is according to the IEC standard.

Table D.1. IEC synchronous machine parameters (without saturation)

name [unit]	Objects			description
	G1,G2	**G3,G4**	**SG**	
	Test A,B		**TestC**	
rotorType	Round	Round	Salient	Type of rotor on physical machine.
modelType				Type of synchronous machine model
Xd	1.8	1.8	2.642	Direct-axis synchronous reactance
X'd	0.3	0.3	0.377	Direct-axis transient reactance (unsaturated)
X''d	0.25	0.25	0.21	Direct-axis subtransient reactance (unsaturated
Xq	1.7	1.7	2.346	Quadrature-axis synchronous
X'q	0.55	0.55		Quadrature-axis transient reactance
X''q	0.25	0.25	0.18	Quadrature-axis subtransient reactance
T'do [s]	8	8	4.45	Direct-axis transient rotor time constant
T''do [s]	0.03	0.03	0.0269	Direct-axis subtransient rotor time constant
T'qo [s]	0.4	0.4	0.2	Quadrature-axis transient rotor time
T''qo [s]	0.05	0.05	0.05	Quadrature-axis subtransient rotor time
tc [s]	0	0	0	Damping time constant for “Canay” reactance.
D	0	0	0	Damping torque coefficient
H[s]	6.5	6.175	4	Inertia constant of generator and mechanical load
Xl	0.2	0.2	0.18	Stator leakage reactance
Rs	0.0025	0.0025		stator Resistance

D.2. Excitation System Models

This model is according to the IEC standard.

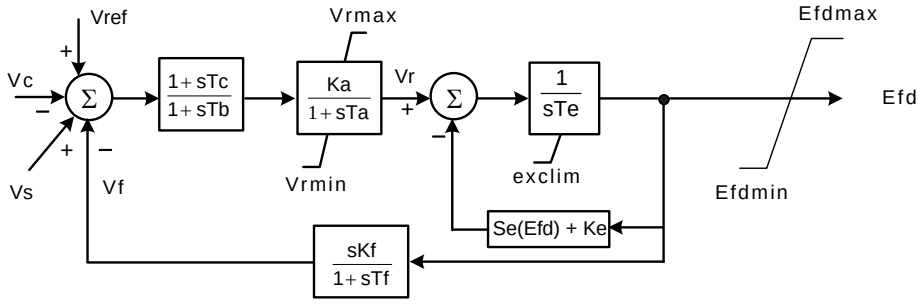

Figure D.1. IEC Excitation System Dynamics: ExcIEEEDC1

Table D.2. IEC Excitation System Dynamics: ExcIEEEDC1

name[unit]	Objects		description
	G1-G4		
	Test A,B		
KA	20		Voltage regulator gain
TA[s]	0.05		Voltage regulator time
TB[s]	0		Voltage regulator time constant
TC[s]	0		Voltage regulator time constant
VRMAX	10		Maximum voltage regulator output
VRMIN	-10		Minimum voltage regulator
KE	1		Exciter constant related to self-excited field
TE[s]	0.36		Exciter time constant,
KF	0.07		Excitation control system stabiliser gain
TF[s]	1.8		Excitation control system stabiliser time constant (
EFD1	3.2		Exciter voltage at which exciter saturation is defined
SEEFD1	0.055		Exciter saturation function value aEFD1
EFD2	2.2		Exciter voltage at which exciter saturation is defined
SEEFD2	0.027		Exciter saturation function value at EFD2

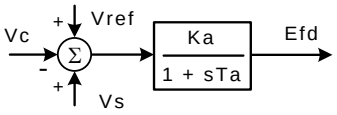

Figure D.2. IEC Excitation System Dynamics: ExcAVR5

Table D.3. IEC Excitation System Dynamics: ExcAVR5

name	Object	description
	SG	
	TestC	
Ka	400	Gain
Ta	0.01	Time constant
rex	0	Effective Output Resistance

D.3. Prime Mover Models

This model is according to the IEC standard.

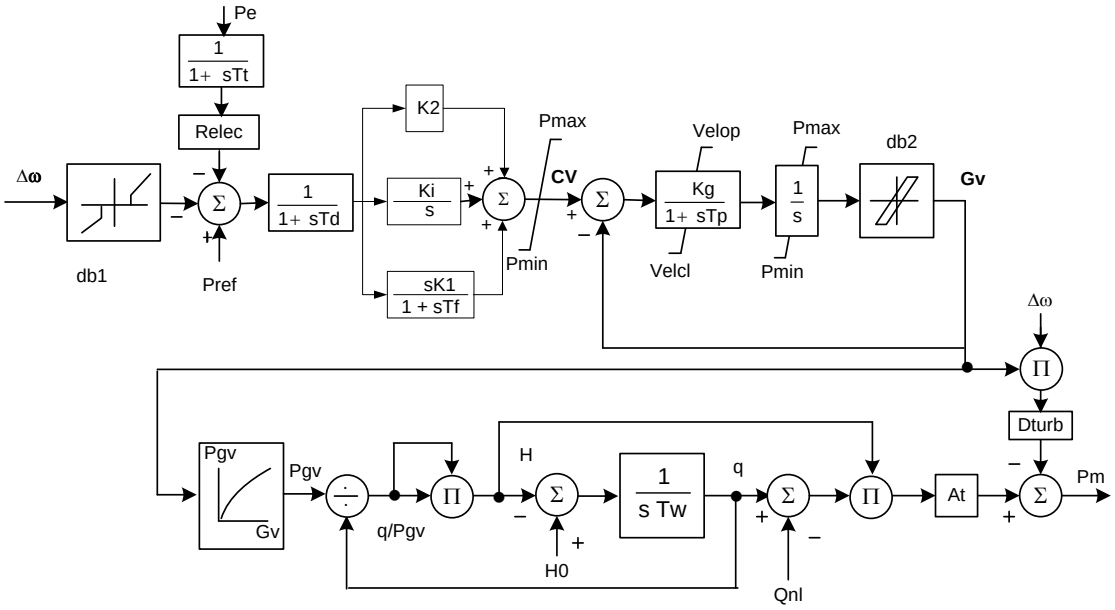

Figure D.3. IEC Turbine Governor Dynamics: GovHydro3 (without nonlinear flow-gate relationship)

Table D.4. IEC Turbine Governor Dynamics: GovHydro3 (without nonlinear flow-gate relationship)

name	mult	description
	SG	
	TestC	
MWbase [MW]	353	Base for power values (MWbase) (> 0). Unit = MW.
Pmax	1	Maximum gate opening,
Pmin	0	Minimum gate opening
Cflag	true	Governor control flag true = PID control is active
Rgate	0	Steady-state droop,
Relec	0.04	Steady-state droop for electrical power feedback
Td [s]	0	Input filter time constant
tf		Washout time constant
tp	0	Gate servo time constant
Velop [1/s]	0.066	Maximum gate opening velocity
Velcl [1/s]	-0.14	Maximum gate closing velocity
K1	0	Derivative gain.
K2	2	Gain,
Ki	0.33	Integral gain
Kg	2	Gate servo gain
tt		Power feedback time
db1	0	Intentional dead-band
eps	0	Intentional db hysteresis
db2	0	Unintentional dead-band
Tw[s]	1	Water inertia time constant.
At	1.2	Turbine gain.
Dturb	0	Turbine damping factor
Qnl	0.17	No-load turbine flow at nominal head
H0	1	Turbine nominal head

D.4. Wind Turbine +PMG with FPC Models for TESTC

This model has been implemented in the MODES network simulator.

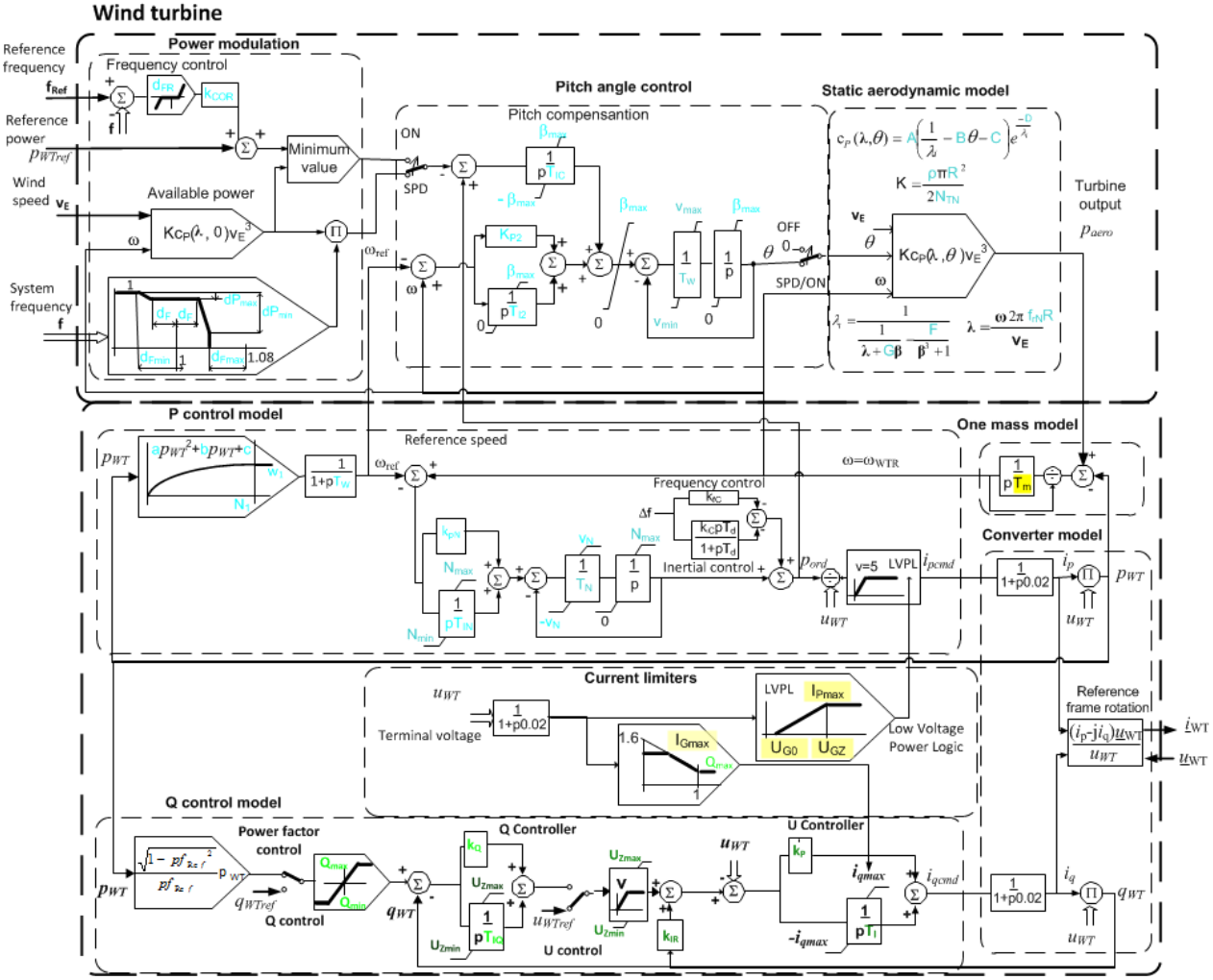

Figure D.4. Model of Wind turbine with Permanent Magnet Generator and Full Power Converter

p_{WT}, q_{WT}, p_{aero} terminal active and reactive power (generation sign convention), aerodynamic power (P_n)

$\Theta, \omega_{gen}, \omega_{WTR}$ pitch angle (deg), generator and turbine rotational speed (□base)

i_{pcmd}, i_{qcmd} active and reactive current command to generator system (gen. and cap. sign convention) (I_n)

i_{pmax}, i_{qmax} maximum active and reactive current (generation and capacitive sign convention) (I_n)

q_{WTmin}, q_{WTmax} minimum and maximum reactive power (capacitive sign convention) (P_n)

$\underline{u}_{WT}, \underline{i}_{WT}$ terminal voltage and current phasor in power system coordinates (U_n, I_n)

Table D.5. Limits of converter

IGmax(-)	IPmax(-)	Ug0(-)	UgZ(-)
1.1	1.11	0.4	0.9

Table D.6. Voltage control parameters

Uzmin	Uzmax	Kp	TI(s)	v(%/s)	KIR	kQ	TIQ	Qmin	Qmax
0.8	1.2	0	0.008	10	0	0	0	-0.4	0.4

Table D.7. Power control parameters

N_1	w_1	T_{IN}	T_W	T_N	T_D	k_{pN}	K_{fC}	K_{IC}	a	b	c	v_N	dP_{min}	d_{Fr}	d_F	d_{Fmin}	d_{Fmax}	dP_{max}
		s	s	s	s							1/s						
1	1.47	0.6	50	0.05	0.05	6	20	30	-0.75	1.59	0.63	0.45	0.21	0	0	0.012	0.03	0.05

Table D.8. Pitch control parameters

βmax(^{O})	Kp2	TIC(s)	TI2(s)	V_{min}(^{o}/s)	V_{max}(^{o}/s)
27	150	0.2	0	-10	10

Table D.9. Turbine parameters

k_N	T_W(s)	A	B	C	D	G	F	ρ(kg/m^3)	N_{min}	N_{max}	R(m)	vE_n(m/s)	f_{rn}(Hz)
1.11	0.3	80	0.00384	0.065	18.4	-0.02	-0.003	1.225	0	1.11	50	12.5	0.263

D.5. UPFC Dynamic Model

This model has been implemented in the MODES network simulator.

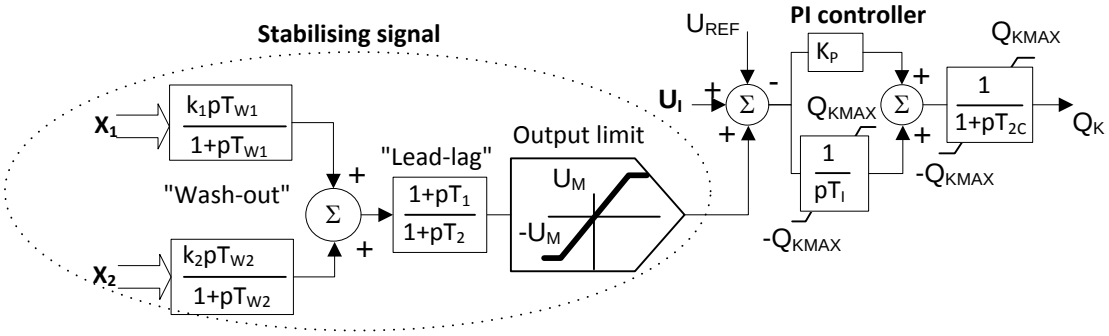

Figure D.5. Block diagram of the voltage regulator with supplementary stabiliser signal

Voltage regulator is complemented by two inputs stabiliser (this stabiliser has the same purpose as the power system stabiliser in excitation control of the synchronous generators - especially damping of inter-area oscillations). Inputs are active power flows of the lines V13-102 and V13-101A in MW.

Table D.10. UPFC dynamic parameters

kp	Ti (s)	T_{2C}(s)	TW1(s)	TW2(s)	k1	k2	T1(s)	T2(s)	UM
2	0.25	0	4	4	5	5	0	1	0.08

D.6. VSC HVDC Dynamic Model

This model has been implemented in the MODES network simulator.

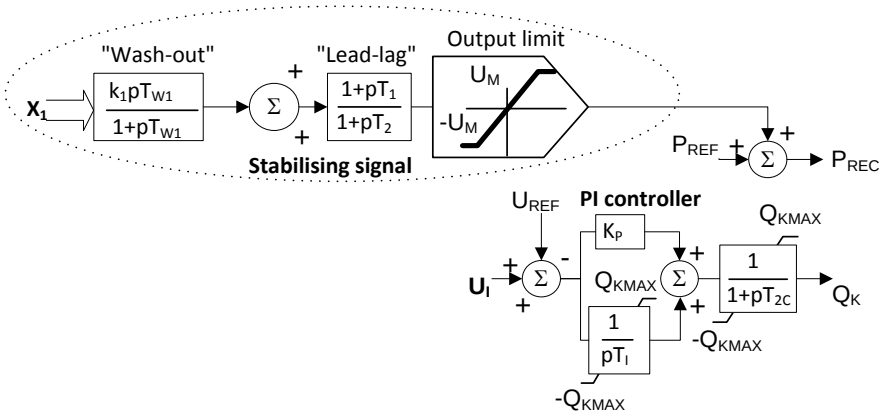

Figure D.6. Block diagram of the voltage regulator and power control with stabiliser

Transmitted power control is complemented by stabiliser. Input is active power flow of the line V13-101A in [MW].

Table D.11. VSC HVDC dynamic parameters

kp	Ti (s)	T_{2C}(s)	TW1(s)	k1	T1(s)	T2(s)	UM
2	0.25	0	10	25	0.55	0.2	0.25

Appendix II: Model Validation

E. Validation of the Reduced Model

The reduced dynamic model was verified by simulation of an outage of a 1400 MW unit is Spain. WAMS records were compared with simulation results of:

- full and reduced models for MODES network simulator and
- reduced models for PSS/E simulator.

The following figures show simulation results (from full and reduced model) with measured frequency waveforms:

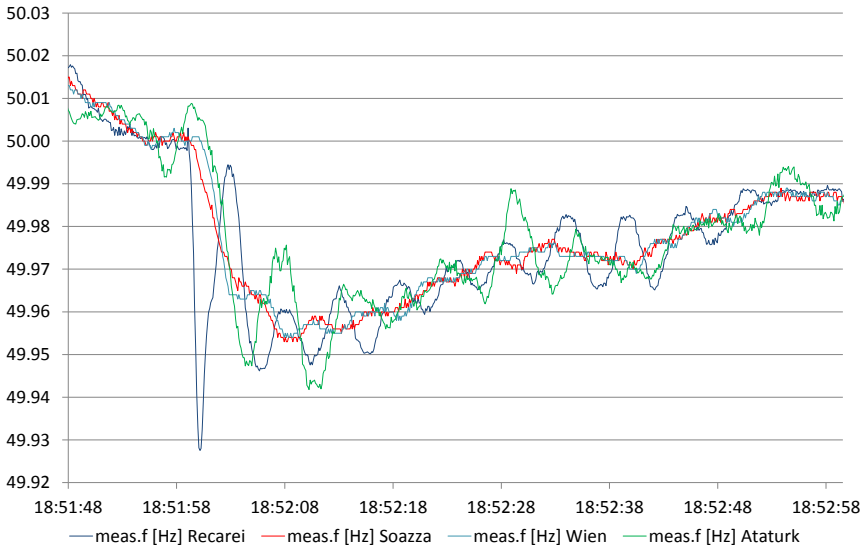

Figure E.1. Frequency waveforms for WAMS in Portugal, Switzerland, Austria and Turkey

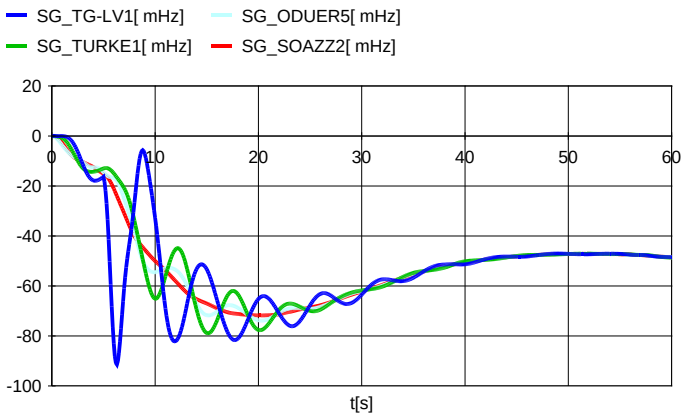

Figure E.2. Frequency deviations waveforms of the MODES simulations full model

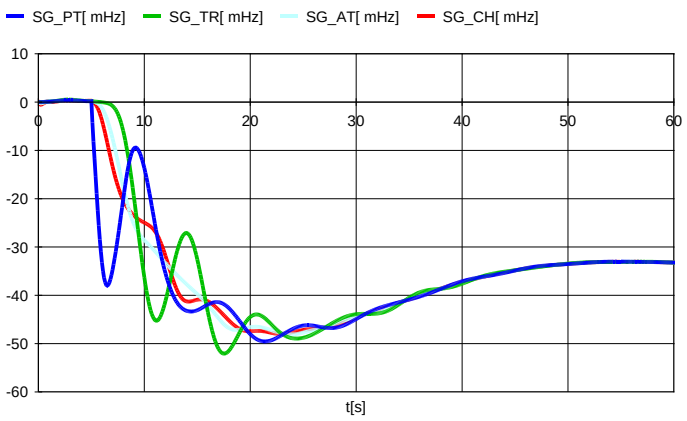

Figure E.3. Frequency deviations waveforms of the MODES simulations reduced model

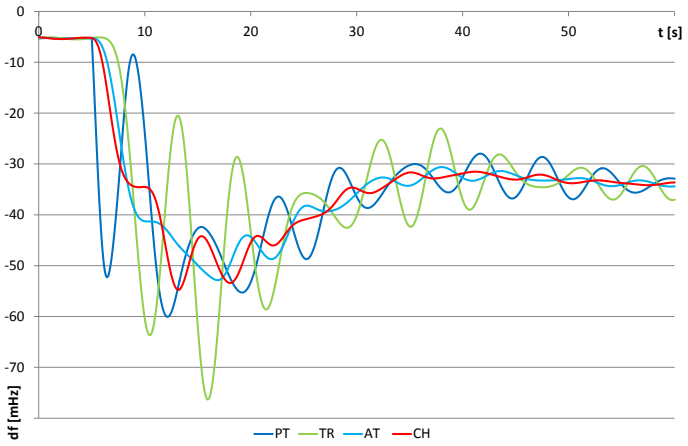

Figure E.4. Frequency deviations waveforms of the PSS/E simulations on reduced model

Mean frequency deviation for simulation corresponds to the measured data. Inter-area oscillations are more damped for the MODES simulations. Reduced CE 2030 dynamic model is able to simulate frequency stability with simplified inter-area oscillations (e.g. for inertia and load frequency shedding analysis). Moreover it enables investigation of island operation of control areas (e.g. splitting of the interconnection). Plug-in nodes and external HVDC terminal are complemented as well. Reduced CE 2030 dynamic model can be used as starting data set for frequency and small signal stability calculations.

F. Validation of Dynamic Models – Benchmark test systems

This appendix deals with dynamic models of non-standard technologies like UPFC, VSV-HVDC, RES, ESS and DSR with focus on small disturbance stability (inter area oscillations), frequency stability (primary frequency and inertia controls) and angle stability (short circuits on (U)HVAC lines). Demand Side Response possibilities are investigated as well.

Simple benchmark systems are prepared to present the dynamic performance of the new technologies. These "stand-alone" benchmark systems are used for testing in the framework of this deliverable.

The MODES network simulator was used for new technologies demonstration. It is important to mention that no mature standard dynamic models exist for the new technologies, so that available models in the different tools are somehow user-defined and more or less compatible. However, they should be tuned to provide consistent reproduction of dynamic behaviour for the simple benchmark systems.

F.1. Power Electronics Systems

Power electronic interface is widely used for distributed energy resources (DER) connection into network and from new transmission equipment. Figure F.1 shows common structure of such interface for DER.

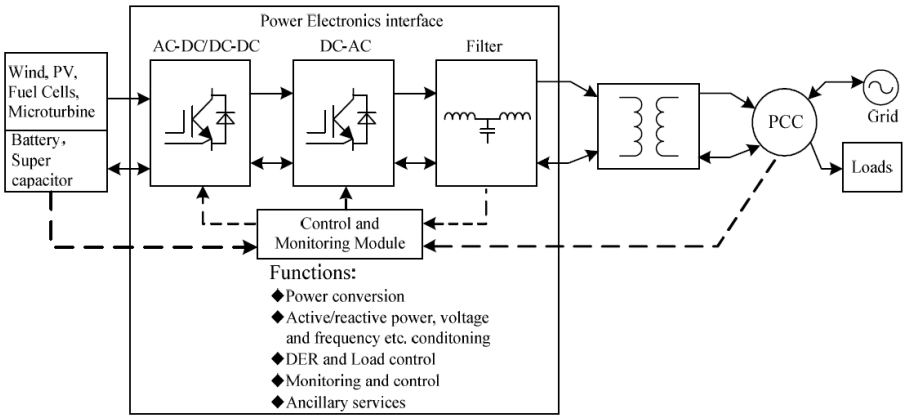

Figure F.1. General block diagram of typical power electronic system (according to [42])

There are four main parts:

- Source input converter
- Inverter module
- Output interface module
- Controller module

More information on power electronics is in references [43]- [51]. This section deals with the following two power electronic systems:

- Unified Power Flow Controller - UPFC.
- VSC-HVDC.

F.1.1. Unified Power Flow Controller

The Unified Power Flow Controller (UPFC) is a member of the FACTS equipment's, which are able to increase power system operation flexibility and controllability. Figure F.2 shows scheme for UPFC according to [52] .

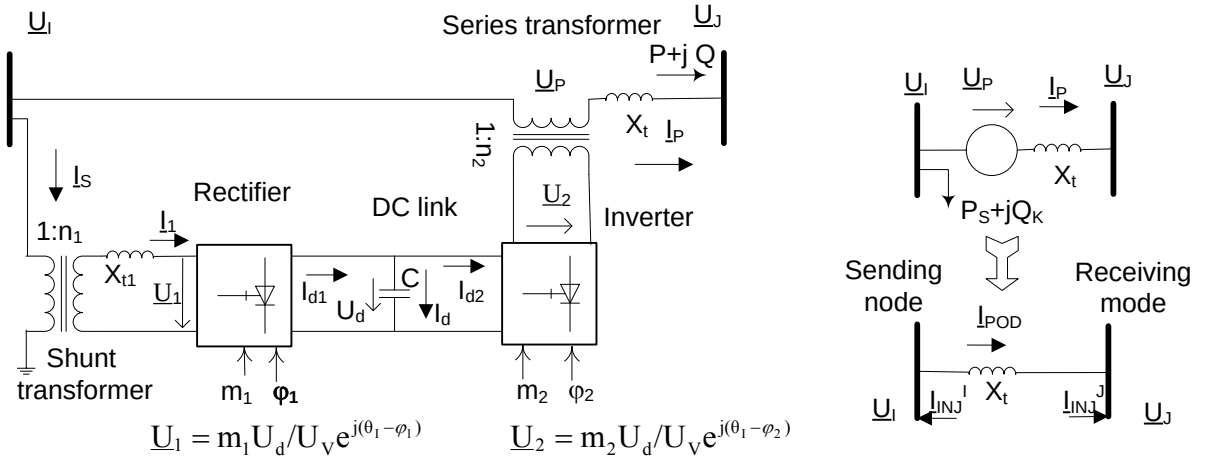

Figure F.2. Scheme of UPFC connected between nodes I and J

The network model is depicted in the right side of the figure. Reactive power Q_K injected into sending node controls voltage in this node (see e.g. [53]). A PI controller depicted in Figure D.2 in Appendix D can be used for this purpose. The transmitted power is controlled by inverter side of the UPFC.

Simple test system (taken over from [52]) was used to present UPFC transmission capability.

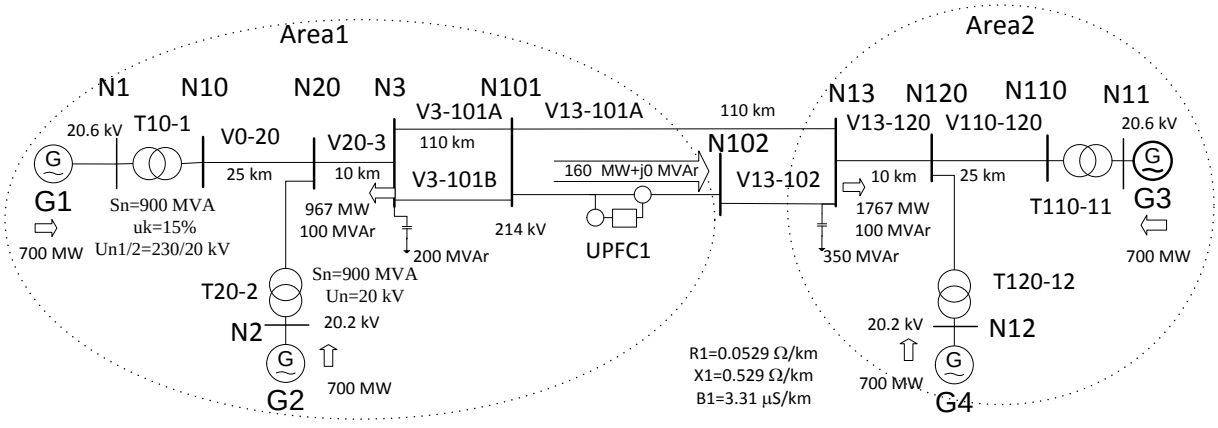

Figure F.3. One line scheme for simple test system with UPFC (test system A)

Original test system comes from [54] (Example 12.6) and it consists of two areas connecting by double 230 kV tie line with transfer more than 400 MW. UPFC is connected into one of the parallel lines.

Three cases were simulated:

- original system without UPFC,
- installed UPFC in conventional control (active power and voltage control),

- installed UPFC in conventional control with additional stabilising signal (with tie line active power flows as input variables).

A 100 ms three phase short circuit in the node N3 was applied as initial disturbance. Following figure shows waveforms of difference between rotor angles of generators G1 and G3.

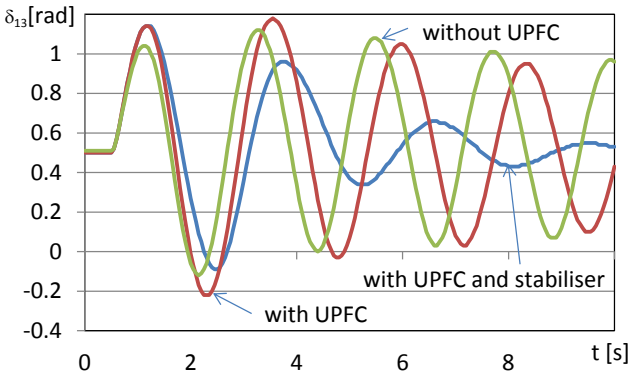

Figure F.4. Results of simulations for cases without and with UPFC and for UPFC with stabiliser signal

Similarly as in the reference [52] the UPFC installation (red curve) can damp system oscillations, but it increases the first swing comparing with system without UPFC (green curve). Introducing stabiliser signal improves oscillations damping significantly (blue curve), but the first swing is still greater than in the system without UPFC. The UPFC installation improves the static stability (damping of oscillations), but it worsens dynamic stability. Of course the UPFC enables power flows control and decreasing loop flows in the system.

F.1.2. VSC-HVDC

VSC-HVDC is based on fully controllable valves, which make possible the flexible control, voltages, power flows and oscillations in the power system. The injection model depicted in Figure F.5 is possible to use for simulation of electromechanical transients (see e.g. [55]).

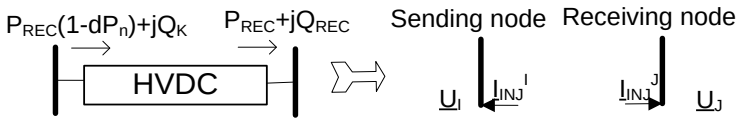

Figure F.5. Scheme of HVDC connected between nodes I and J and injection model

VSC-HVDC controls voltage (by injection of reactive power Q_K) in the sending node and transferred active and reactive power P_{REC} and Q_{REC} in the receiving node. HVDC losses dPn is taken into account. HVDC control model is depicted in Figure D.3 in Appendix D.

Simple test system depicted in Figure F.6 was used to illustrate the HVDC capability. This test system comes from the reference [54] (page 1151).

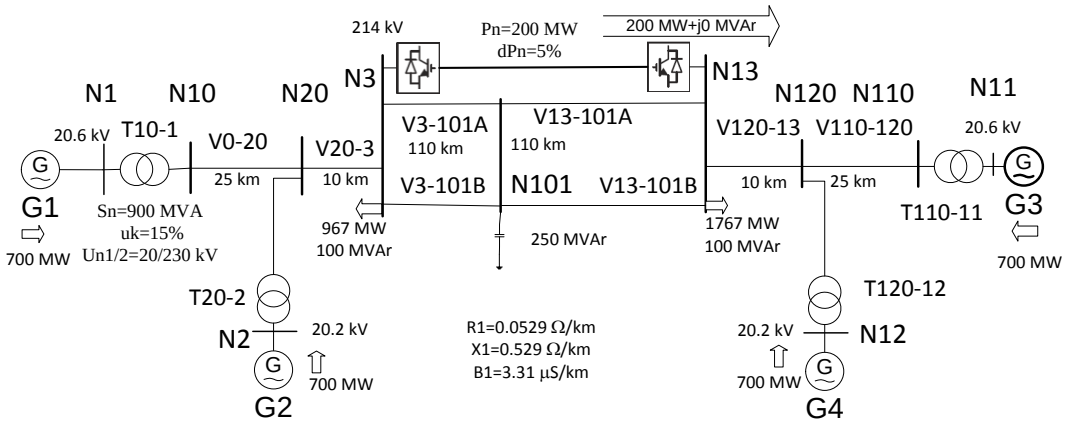

Figure F.6. One line scheme for simple test system with HVDC (test system B)

Three cases were simulated (similar as in the reference to [54]):

- original system without HVDC,
- installed HVDC in conventional control (active power and voltage control),
- installed HVDC in conventional control with additional stabilising signal (added to the reference transferred active power).

A 100 ms three phase short circuit on line V13-101B near the node N13 was applied as initial disturbance. The fault was cleared by switching off the line. Following figure shows waveforms of difference between rotor angles of generators G1 and G3.

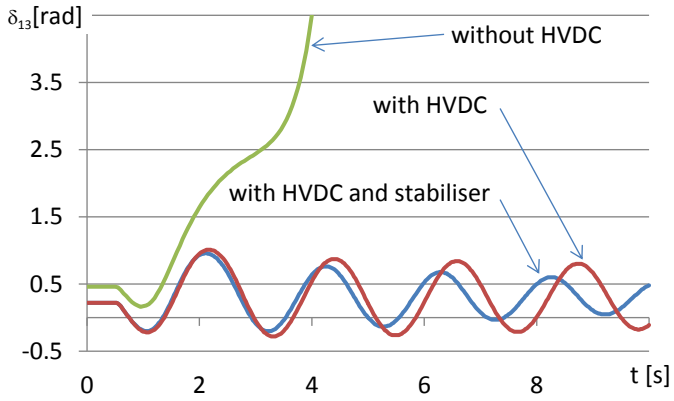

Figure F.7. Results of simulations for cases without and with UPFC and fro UPFC with stabiliser signal

The system is unstable for original system without HVDC (green curve). After system reinforcement by HVDC installing, the system is stable, but oscillations are poor damped (red curve). With supplementary stabilisation signal the damping was improved (blue curve). These results are similar as in the reference [54]. The more information about VSC-HVDC models are in [56]-[55].

F.2. Energy Storage System

There is a variety of technologies for Energy Storage Systems (ESS):

- Pumped hydro-storage
- Compressed Air Energy Storage (CAES)

- Regular batteries
- Redox flow batteries
- Hydrogen storage
- Molten Salt
- Power to gas
- Pumped Heat Energy Storage
- Liquid Air Energy Storage
- Superconducting magnetic energy storage (SMES)
- Super capacitors
- Fly wheels

Energy Storage Systems (ESS) can be classified as either centralised or decentralised [65]. Some technologies are better suitable for centralised storage systems (e.g. pumped hydro) and others are better suitable for decentralised storage (e.g. SMES) An overview of performances for selected ESS is given in the following Table.

Table F.1. Specification of selected ESS (according to [66])

Categories	Storage Technology	Power Range (MW)	Response Time	Efficiency (%)	Category
Mechanical Energy Storage	Pumped hydro-storage	100~2000	4h~10h	60~70	Centralised
	CAES	100~300	6h~20h	40~50	Centralised
	flywheel	0.005~5	15s~15min	70~80	Decentralised
Electromagnetic Energy Storage	SMES	0.01~20	1ms~15min	80~95	Decentralised
	super capacitors	0.001~0.1	1s~1min	70~80	Decentralised
Chemical Energy Storage	lead-acid battery	0.001~50	1min~3h	60~70	
	Li-ion and NaS battery	0.001~10	1min~3h	70~80	

The simplest ESS dynamic model could be described by relation between storage energy E_s and charge and discharge powers P_C and P_D [67]:

$$\frac{dE_S}{dt} = \frac{-P_D}{\eta_D} \qquad E_S < E_{MAX} \quad P_D < P_{DMAX}$$
$$\frac{dE_S}{dt} = -\eta_C P_C \qquad P_{CMIN} < P_C < P_{CMAX} \tag{1}$$

P_{CMAX}, P_{DMAX}, S_{MAX} maximum charge and discharge powers and energy capacity,
η_C, η_D charge and discharge efficiencies.

Storage power is controlled depending on desired objective. For example: peak shaving loads, removing line overloads, frequency control and/or synthetic inertia providing. More information about ESS is in [68]-[86].

F.3. Sustainable Energy Sources

Wind energy has become one of the most important RES, which has the most influence on transmission system operation (large wind power plants are connected directly into

transmission network). Hence we focus on wind turbines firstly. Other important RES are solar plants. There are two main types: Concentrated solar thermal power plants (CSP) and Photovoltaics modules (PV).

F.3.1. Wind Turbines

A simple test system depicted on Figure F.8 was prepared for demonstration of up to date wind modules capabilities. The system was inspired by the reference [87], only instead of DFIG modules connected by one VSC-HVDC into an AC island system, permanent magnet generators (PMG) with full power converter (FPC) was used (Type 4 according to [89]). The model of PMG-FPC was complemented by additional signals to enable frequency and inertial control.

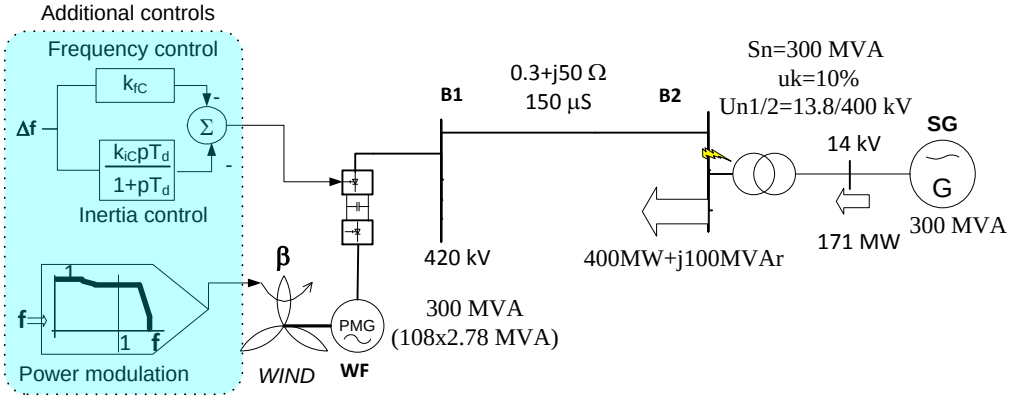

Figure F.8. Simple test system with wind turbine and synchronnous generator (test system C)

Three cases were simulated for different disturbances:

- 10% step increasing of load connected to node B2,
- increasing of wind speed,
- short circuit in the node B2.

The following figure shows results of the first simulation cases for 10% step load change.

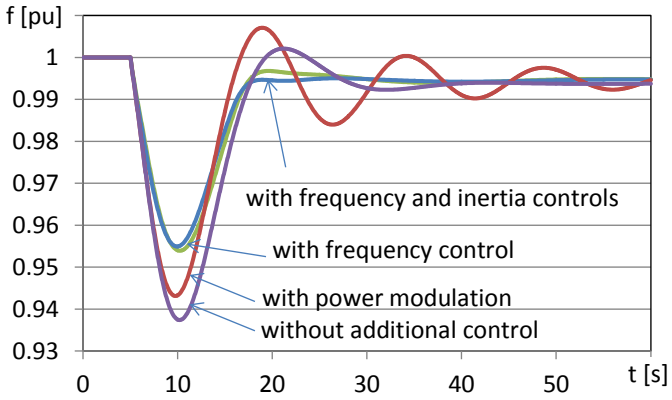

Figure F.9. Frequency waveforms for simulation of load step change

Four different control modes were tested:

- conventional wind power plant control without additional controls,
- simple frequency modulation of turbine power to enable the Frequency Sensitive Mode (FSM) according to prepared NC RfG [88] (wind turbine operates with a primary control reserve to provide response to network frequency deviations by pitch angle control),
- extended FPC grid side inverter control for frequency control and
- inertial control to enable so called Synthetic Inertia according to [88].

Figure F.9 shows significant improving of the frequency response for combination of turbine pitch angle control and extended inverter controls.

The following figure shows results of the second simulation case for the wind speed changes with conventional wind power plant control and with additional frequency control (all (b),c),d) control modes activated):

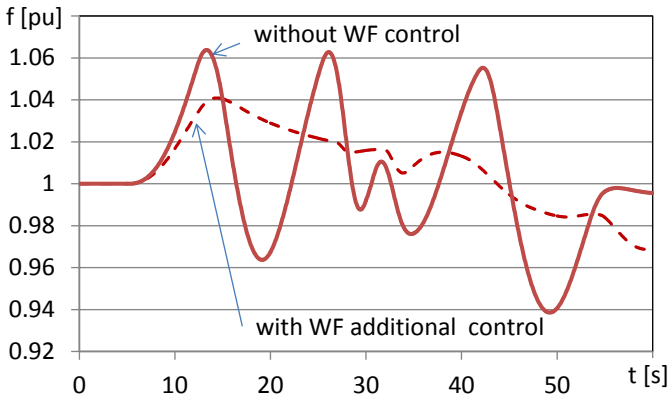

Figure F.10. Frequency waveforms for simulation of the wind speed

Additional frequency control of wind power plant module can improve frequency stability especially in the power system island operation.

The following figure shows results of the third simulation case for the short circuit.

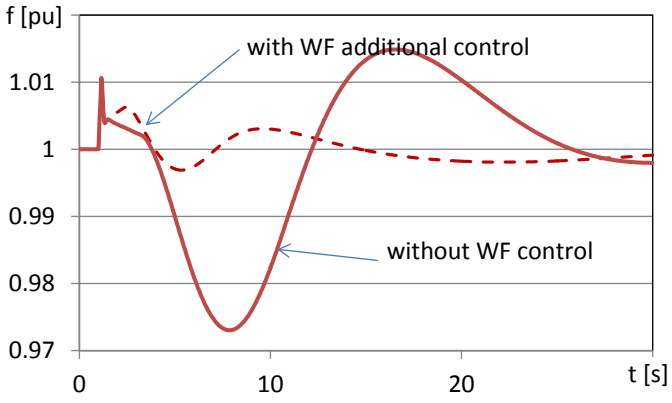

Figure F.11. Frequency waveforms for simulation of the short circuit

Additional frequency control of wind power plant can improve frequency stability after short circuit as well. References [90]-[100] deal with wind modules modelling in more details.

F.3.2. Photovoltaic Modules

PV model for system stability studies are described in [101]. Basically this model contains two main parts: Electric control and Converter models – see Figure F.12.

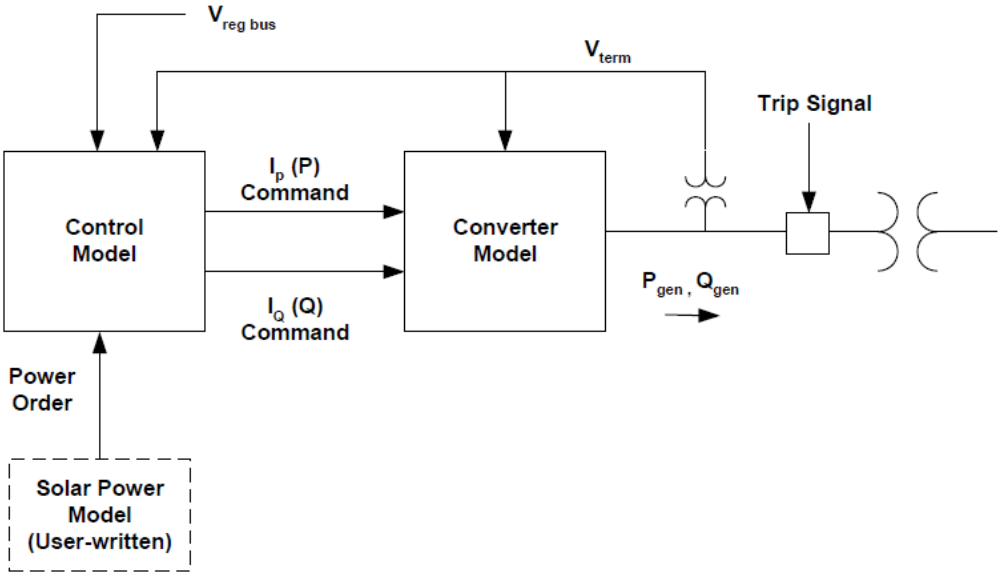

Figure F.12. Basic structure of PV dynamic model according to [101]

Electric control model should contain some important parts like Reactive Power Control and Limited Over-frequency Sensitive Mode. Converter model should contain at least Low Voltage Power Logic and it provides interface between PV and the network (usually implemented by a controlled current source injected into the network. Trip signal is controlled by a switched and reconnection logic, which is based on frequency and voltage relays. Solar power model may contain a dependency of PV power on solar irradiation (see reference.[102]). This irradiation may be either constant or variable in dependency on daytime (see reference [103]).

A simple test system depicted on was prepared for demonstration of up to date PV modules capabilities. The system was inspired by the reference [104] and data description is in [105].

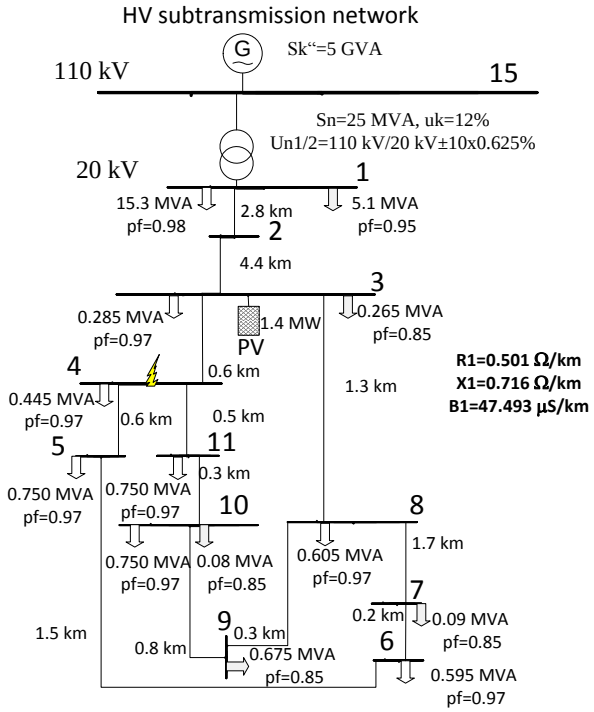

Figure F.13. One line scheme for simple test system with PV (test system D)

100 ms three phase short circuit at node 3 was applied as initial disturbance. The fault was cleared, but at t=0.9 s occurred again as permanent. PV was disconnected by under voltage protection at t=1.013 s. Following figure shows waveforms of PV current I (violet curve) and active power P (red curve).

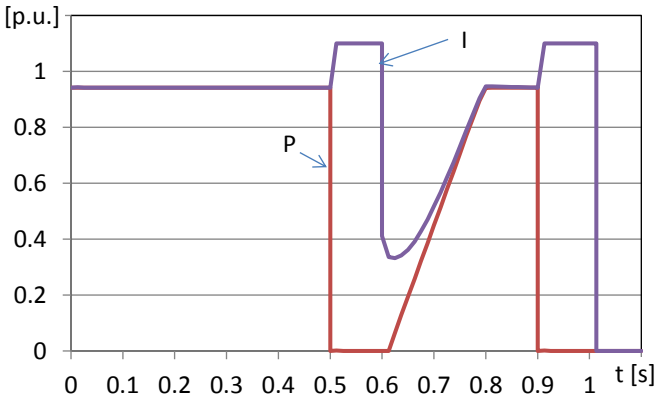

Figure F.14. Results of simulation of short circuit near PV for Test system D

The active power P decreased to zero due to a low voltage power logic during the short circuit and it is restored to the initial value after short circuit clearing. Current I increased to 110 % of nominal value (defined short term overloading value). P and I decreased to zero after disconnection.

References [106]-[118] deal with wind modules modelling in more details.

Additional benchmark system was developed to test PV and decentralised ESS (batteries). This system comes from [105] and one line diagram is shown in the following figure:

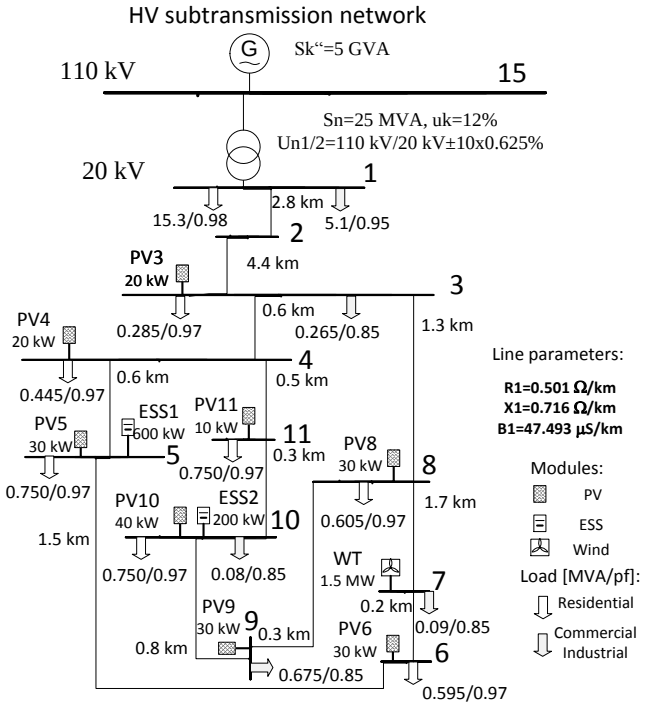

Figure F.15. One line scheme for simple test system with PV and decentralised ESS (test system E)

Whole day simulation was carried to present performance of the ESS. Load was changed according to daily load profiles from [105], production of PVs was changed according Direct normal insolation curve (model is described in [103]) and wind speed was changed as well.

Three cases were simulated:

- without RES and ESS
- with RES
- with RES and ESS

Figure F.16 shows simulated time profiles of active powers of PV (yellow curve), wind turbine (blue curve), residential and commercial loads (red and brown curves).

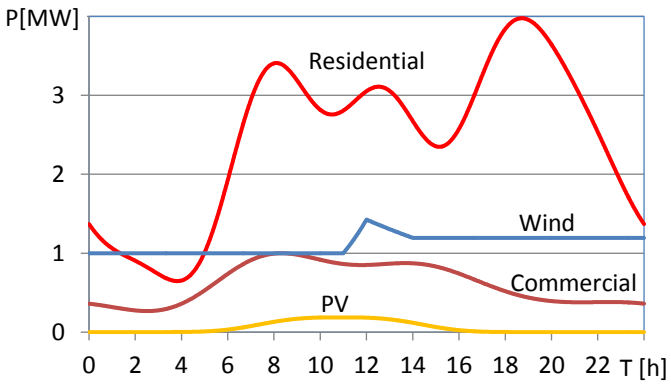

Figure F.16. Active powers of load and generation

Figure F.17 shows active powers of the line 2-3 for three cases (blue curve for the first case without RES and ESS, green curve for the second case without RES, brown curve for the third

case with RES and ESS). ESS power (in [MW]) and stored energy (in per unit [ ]) are depicted by dashed and dotted lines.

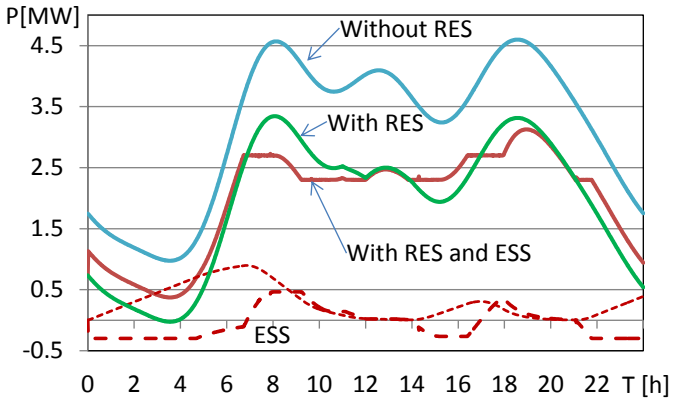

Figure F.17. Active powers of line 2-3 and ESS

The batteries charging/discharging were adjusted to maintain the line 2-3 power flow to 2.5±0.2 MW (for the third case with RES and ESS). When the power flow of the line 2-3 is smaller than setup value 2.5 MW, the batteries were charged (P_{ESS} is negative and stored energy increased) and reversely. Figure F.18 shows voltages waveforms:

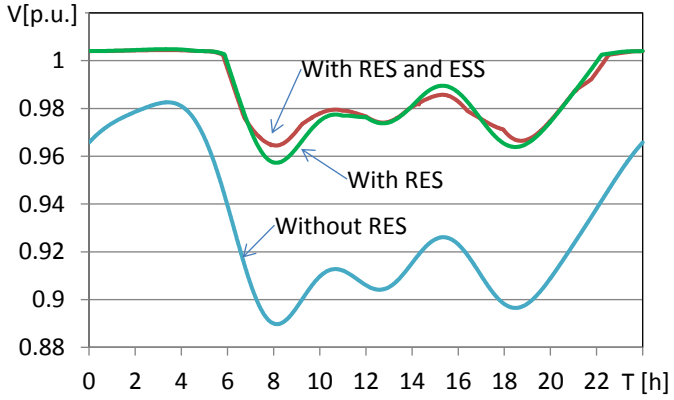

Figure F.18. Voltage of the node 1

Installation of RES can significantly improve voltage deviations during the day (of course RES modules have to be able to control voltage). ESS Installation can smooth out power flows from sub-transmission network (load peak shaving).

F.3.3. Concentrated Solar Thermal Power Plants

Concentrated solar thermal power plants (CSP) produce electricity with conventional synchronous generators combined with steam turbines, but they use solar radiation as energy source instead of fossil fuel. This means the solar field is the heat source instead of boiler. A basic model for CSP with Thermal Energy Storage (TES) is depicted in Figure F.19.

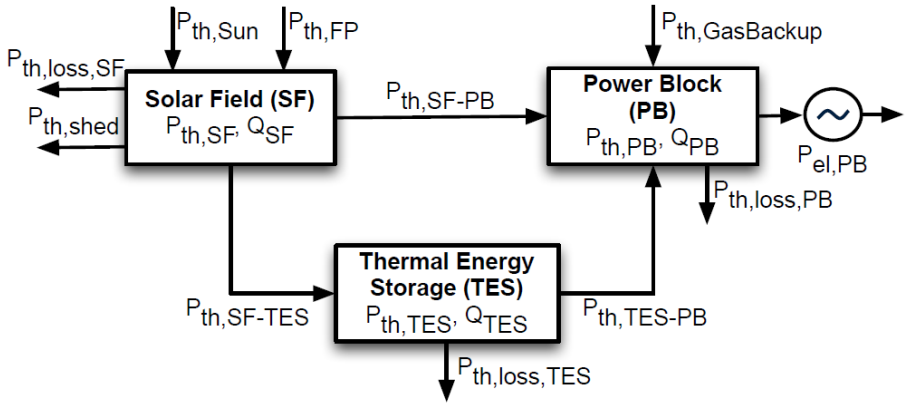

Figure F.19. Basic structure of CSP with Thermal Energy (according to [119])

The simplest solar field and TES dynamic model could be described by relation between heat transfer fluid temperatures T_{SF} and T_{TES} charge and thermal powers (see reference [119]):

$$C_{SF}\frac{dT_{SF}}{dt} = -P_{SF-PB} - P_{SF-TES} + P_{Sun} \qquad C_{TES}\frac{dT_{TES}}{dt} = +P_{SF-TES} - P_{TES-PB} \qquad (2)$$

C_{SF}, C_{TES} are thermal capacities and T_{SF}, T_{TES} are per unit temperatures. Thermal losses are neglected. More detailed model was published in [120].

Thermal input power to the power block model P_{PB} can be changed into turbine mechanical power with efficiency η_{PB}:

$$\eta_{PB} = a_1 + a_2 e^{-\frac{P_{PB}}{a_3}} \qquad (3)$$

According to [120] the parameters for 50 MW_e CSP are $a_1 = 0.397$, $a_2 = -0.243$ and $a_3 = 28.23$ $MW_{t,}$.

F.4. Demand Side Response

Deliverable 3.1 [140] defines three the most impacting demand-side technologies: heat pumps, electric vehicles and LED/OLED lightning. The heat pumps as typical representatives of the temperature-controlled devices are interesting from the dynamic analysis point of view.

One form of Demand Side Response (DSR) specified in the Network Code on Demand Connections [141] is a System Frequency Control (SFC) with decreasing or increasing set temperature proportionately to frequency deviation. Temperature controlled devices are for example fridges, freezers, heat pumps, water heaters, air conditioning and electric heating. Appropriate dynamic model was published e.g. in [142].

F.5. Summary

Features of the possible new technologies are demonstrated on the simple benchmarks test systems:

- Test system A with UPFC
- Test system B with HVDC
- Test system C with wind power plant
- Test system D with PV modules

- Test system E with PV and decentralised ESS.

Namely, UPFC, VSC-HVDC and Wind and PV modules were investigated. The test cases were focused mainly on small disturbance and frequency stability.

Since no consolidated standard dynamic models exist for these new technologies, these benchmark test systems for all potentially used SW tools (Powerfactory, PSS/E and DSA). These benchmark test system calculations may help to prepare suitable models, align dynamic responses, provide reliable and consistent results and facilitate future implementing of these models into the European grid architecture model.

Examples of the dynamic input data were introduced in Appendix D.

Different simple benchmark systems have been developed where these new features have been modelled. Their impact on the system Operational Security has been investigated by means of dynamic simulations.

The described test systems:

- provide suitable models to test grid and generation technologies for future European power system
- allow the comparison and benchmark of the dynamic response of different available tools and
- provide reliable and consistent results to facilitate future implementation of these models into pan-European grid architecture model.

Appendix III: Result Details

G. Geographical Mode Shape Scatter Plots

The geographical mode shape scatter plots are displayed. The modes are numbered starting at the lowest frequency mode. Only the lowest three frequency modes are displayed.

G.1. Scenario X-10

G.1.1. Mode 1

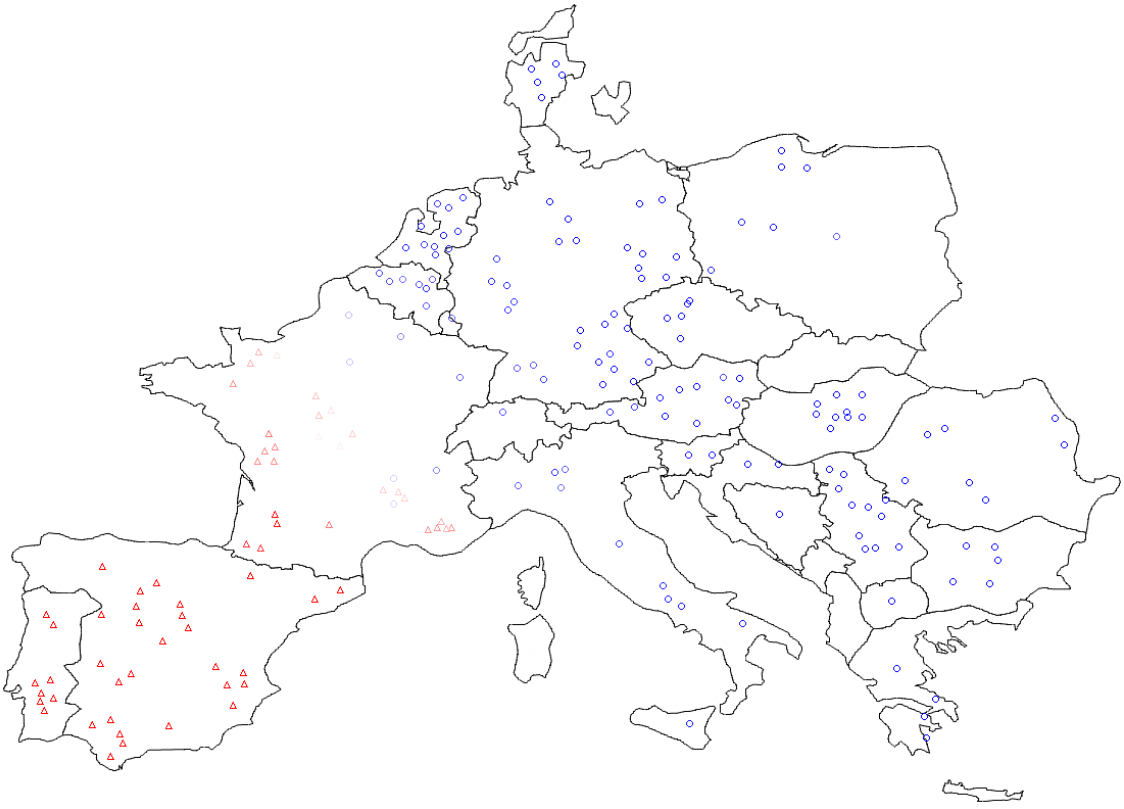

Figure G.1. Mode 1 - frequency 0.3458 Hz, damping 2.51, scenario X-10, strategy 2, Summer Low

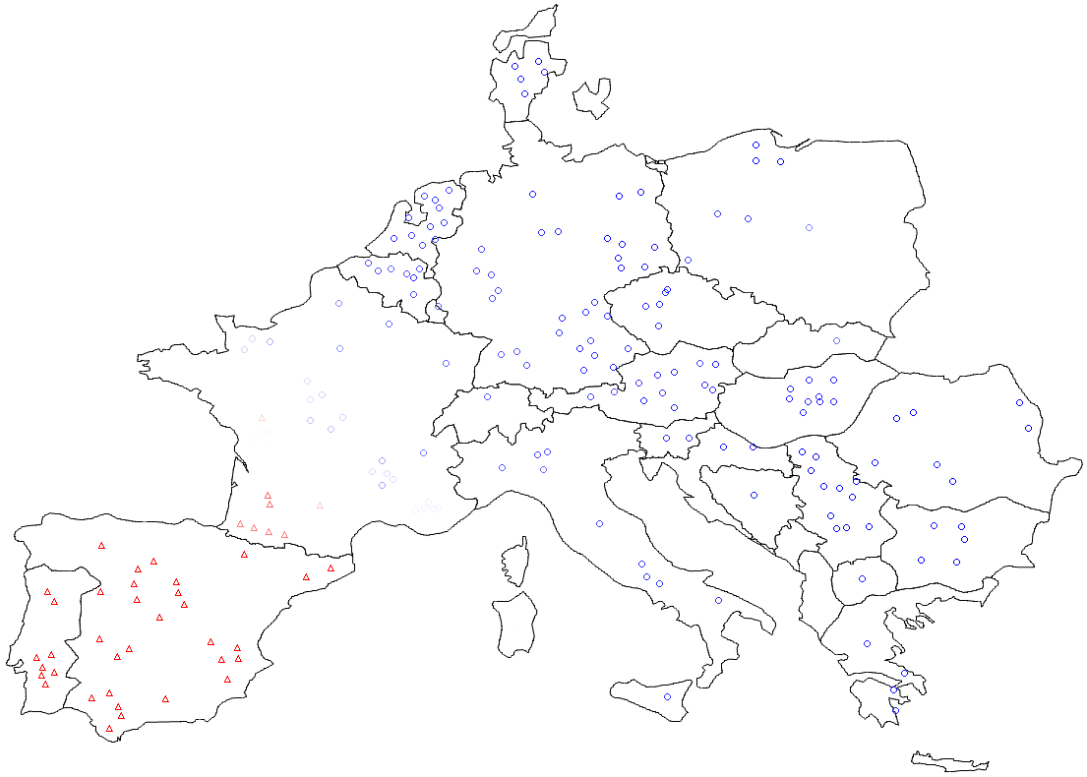

Figure G.2. Mode 1 - frequency 0.2935 Hz, damping 2.72, scenario X-10, strategy 3, Summer Low

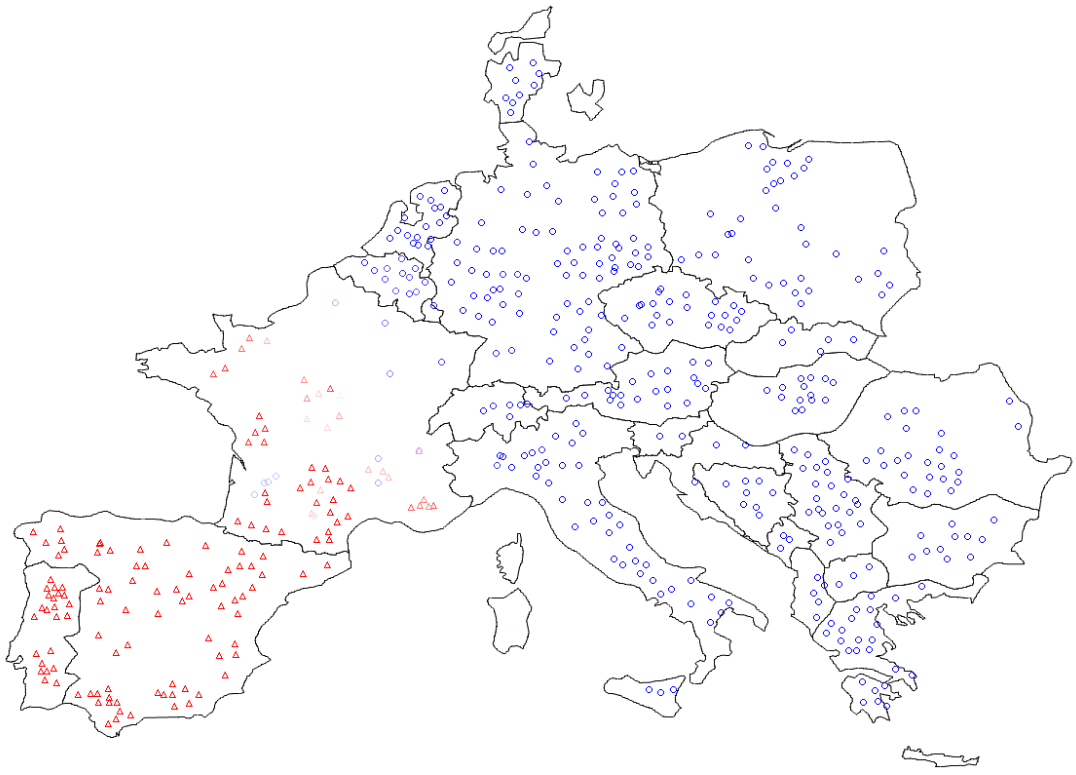

Figure G.3. Mode 1 - frequency 0.2331 Hz, damping 2.08, scenario X-10, strategy 2, Winter Peak

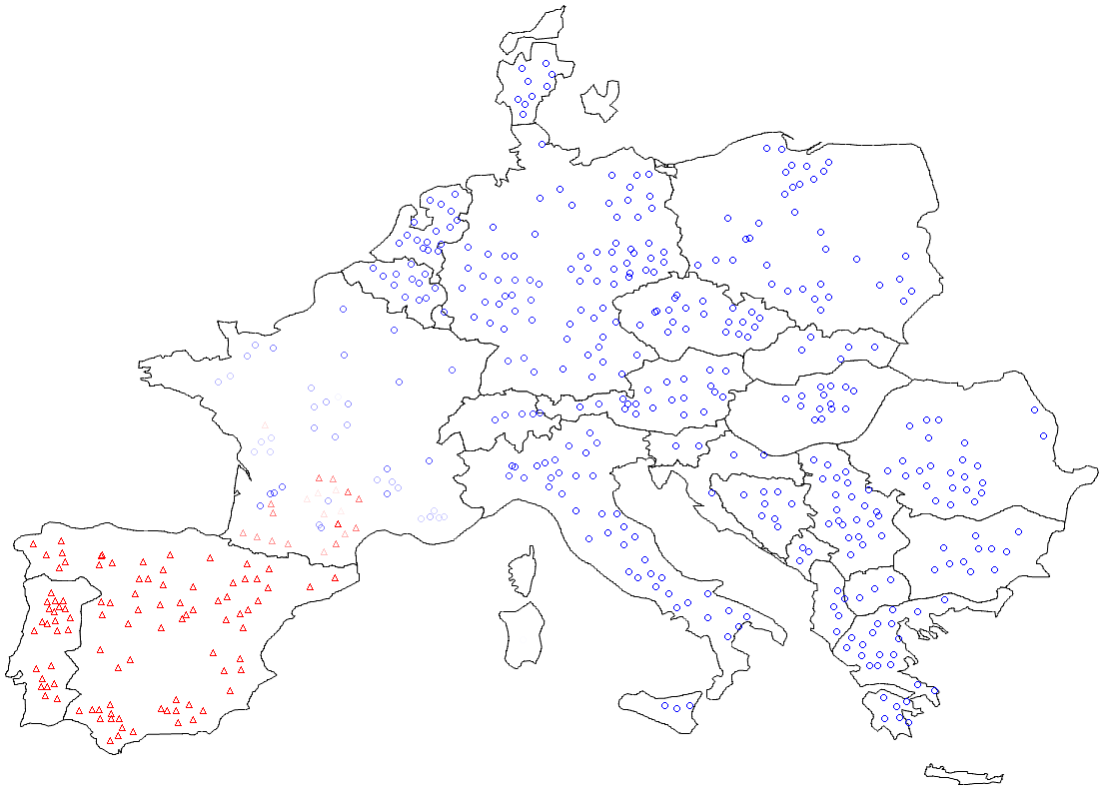

Figure G.4. Mode 1 - frequency 0.1864 Hz, damping 3.28, scenario X-10, strategy 3, Winter Peak

G.1.2. Mode 2

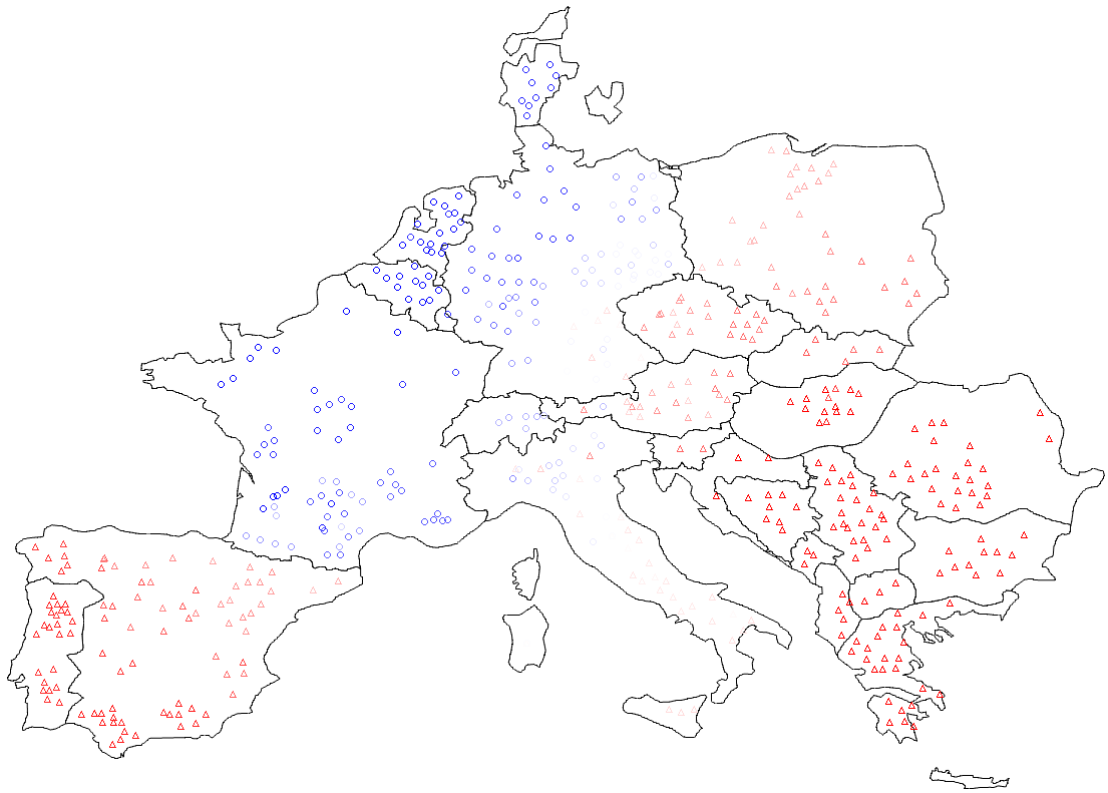

Figure G.5. Mode 2 - frequency 0.3764 Hz, damping 0.62, scenario X-10, strategy 2, Winter Peak

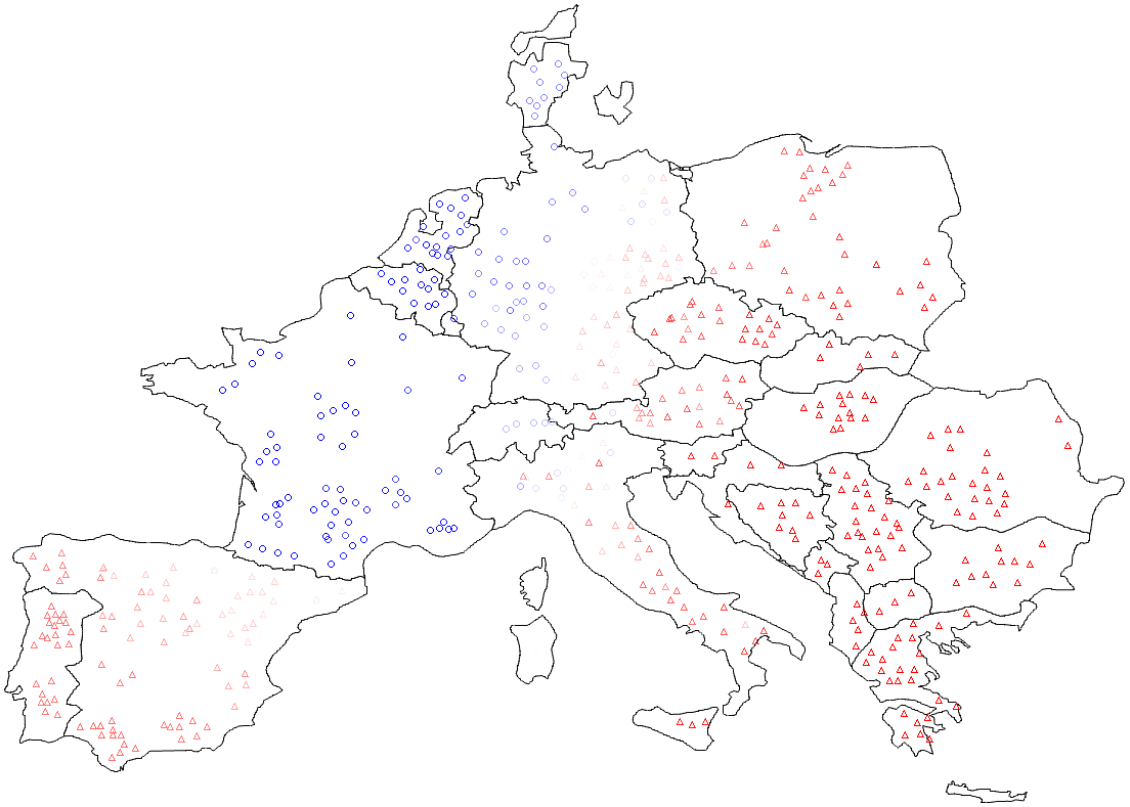

Figure G.6. Mode 2 - frequency 0.3626 Hz, damping 1.33, scenario X-10, strategy 3, Winter Peak

G.1.3. Mode 3

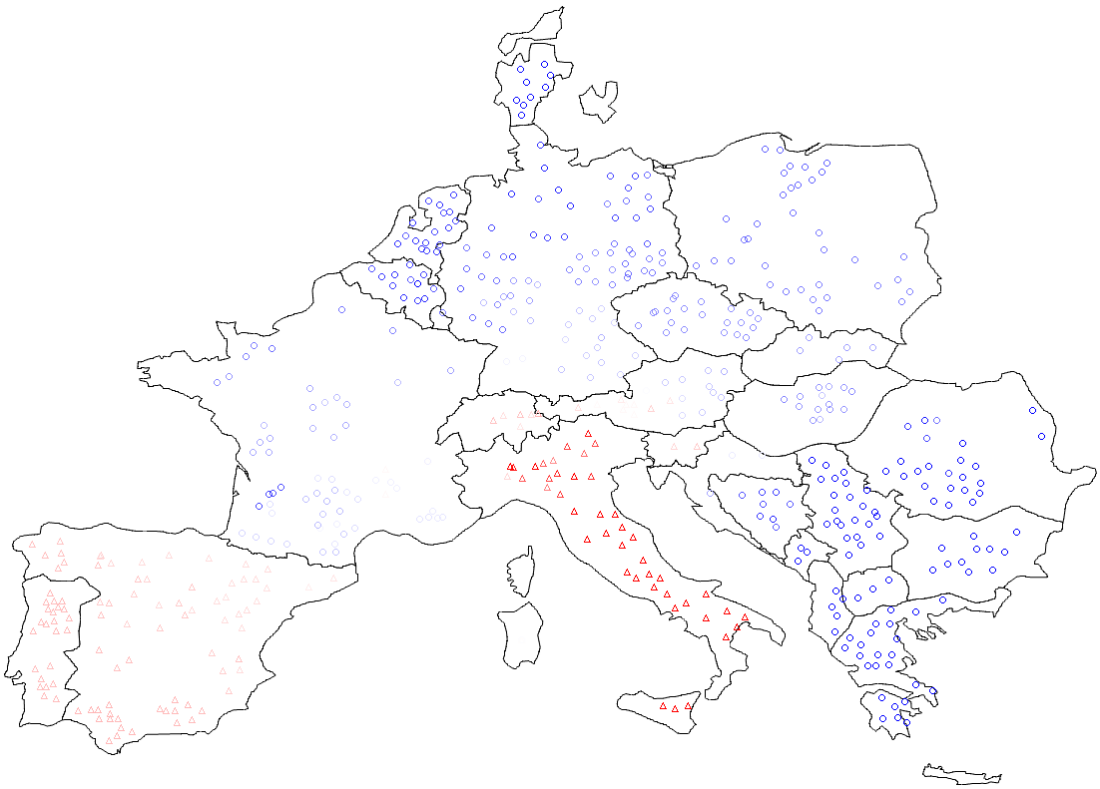

Figure G.7. Mode 3 - frequency 0.3842 Hz, damping 2.70, scenario X-10, strategy 2, Winter Peak

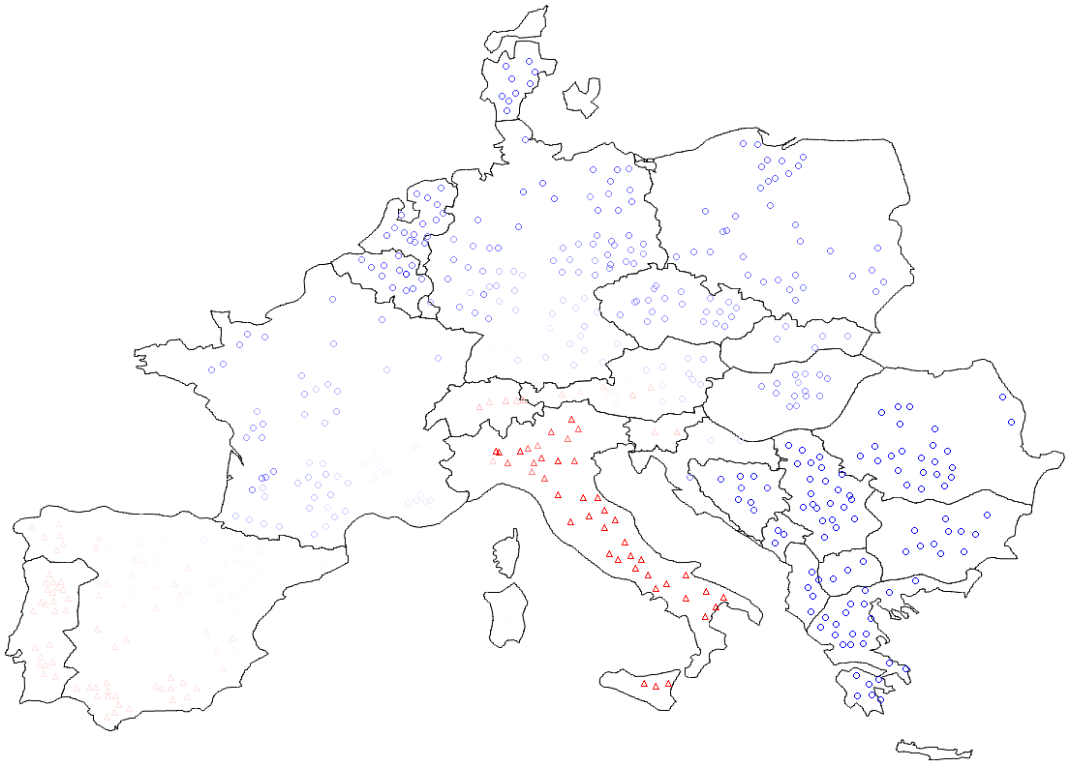

Figure G.8. Mode 3 - frequency 0.3836 Hz, damping 2.67, scenario X-10, strategy 3, Winter Peak

G.2. Scenario X-13

G.2.1. Mode 1

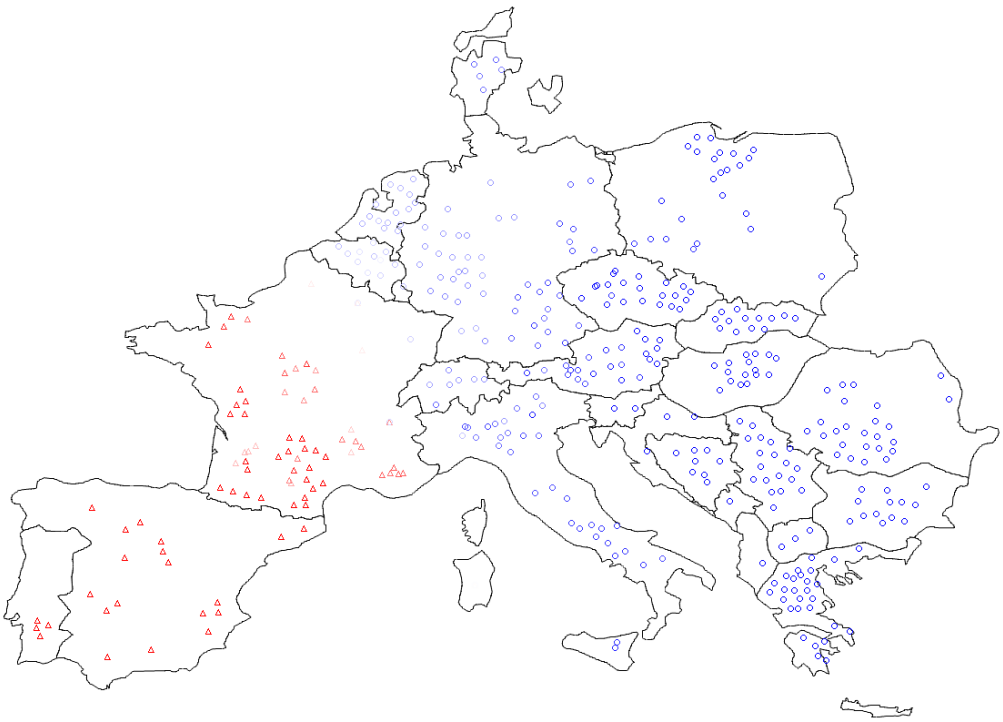

Figure G.9. Mode 1 - frequency 0.3187 Hz, damping 1.83, scenario X-13, strategy 2, Summer Low

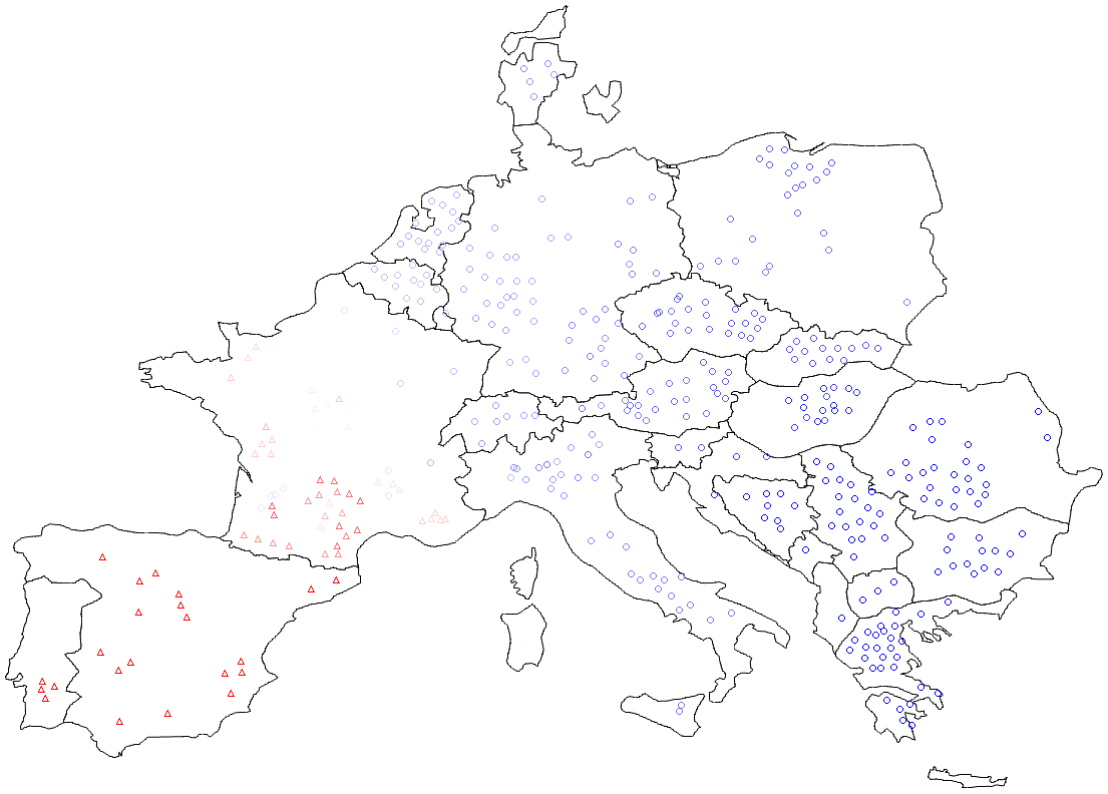

Figure G.10. Mode 1 - frequency 0.2600 Hz, damping 3.59, scenario X-13, strategy 3, Summer Low

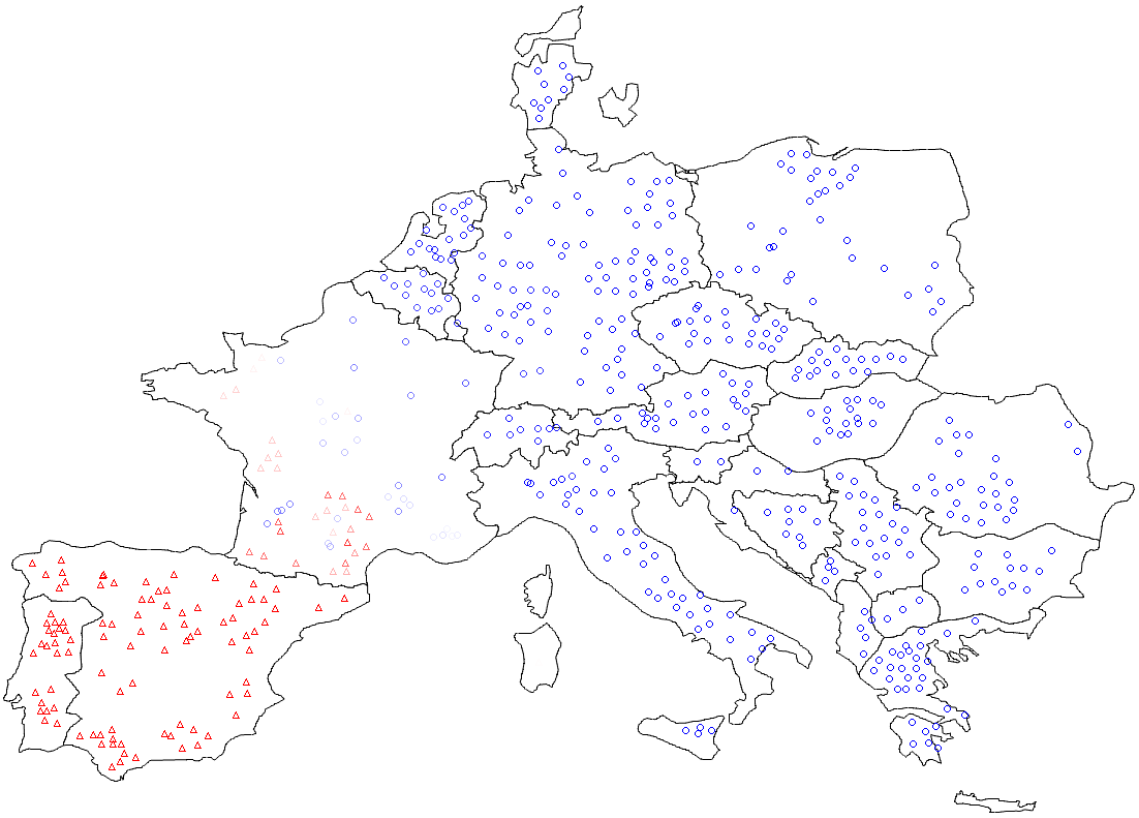

Figure G.11. Mode 1 - frequency 0.2147 Hz, damping 3.51, scenario X-13, strategy 2, Winter Peak

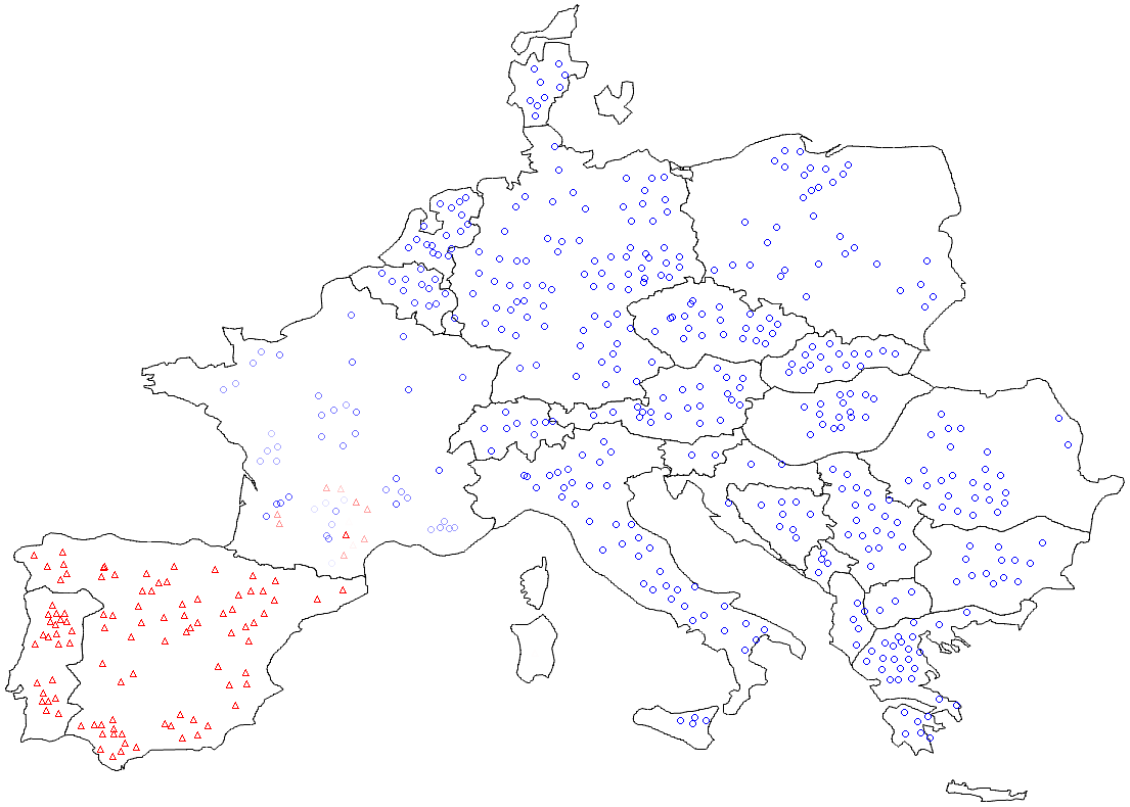

Figure G.12. Mode 1 - frequency 0.1576 Hz, damping 5.04, scenario X-13, strategy 3, Winter Peak

G.2.2. Mode 2

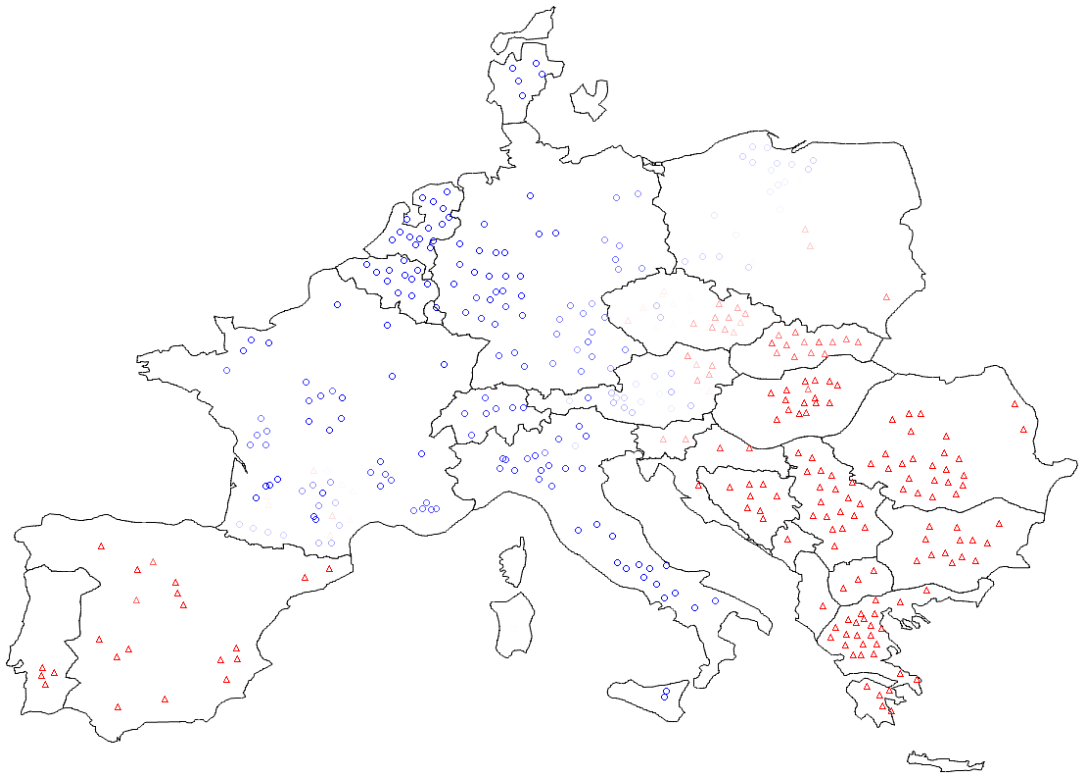

Figure G.13. Mode 2 - frequency 0.4333 Hz, damping 1.82, scenario X-13, strategy 2, Summer Low

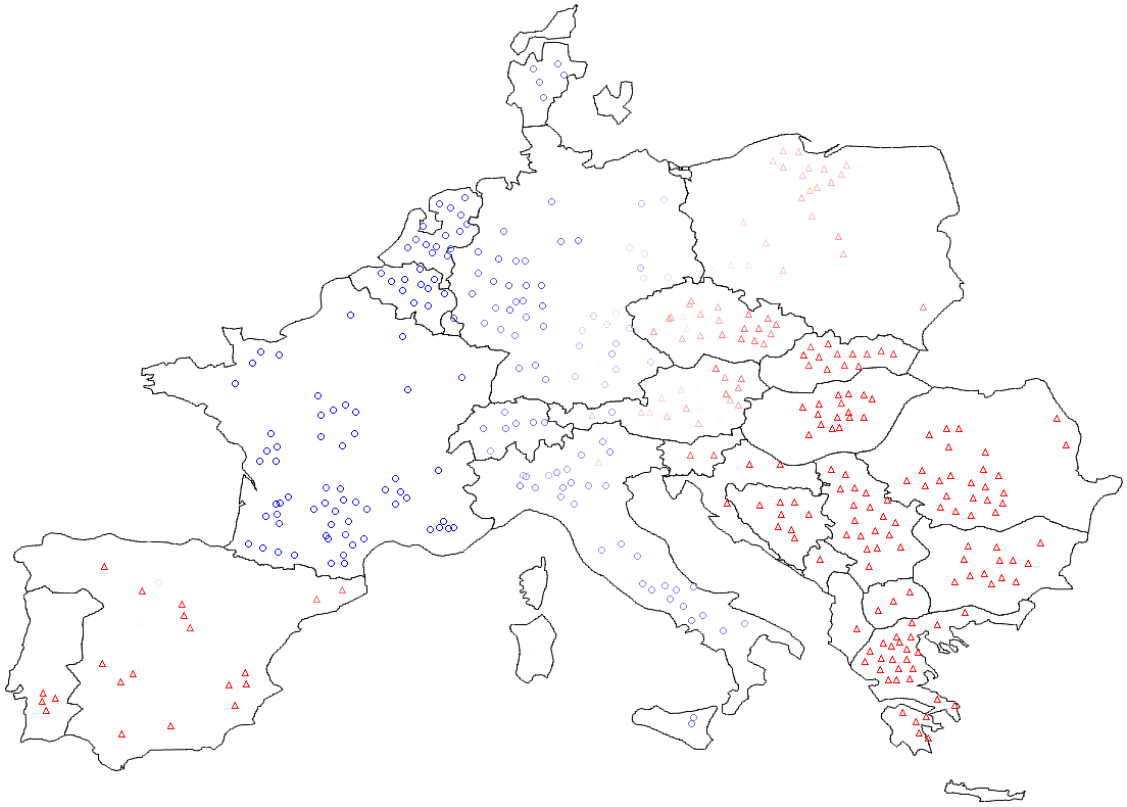

Figure G.14. Mode 2 - frequency 0.3628 Hz, damping 1.87, scenario X-13, strategy 3 Summer Low

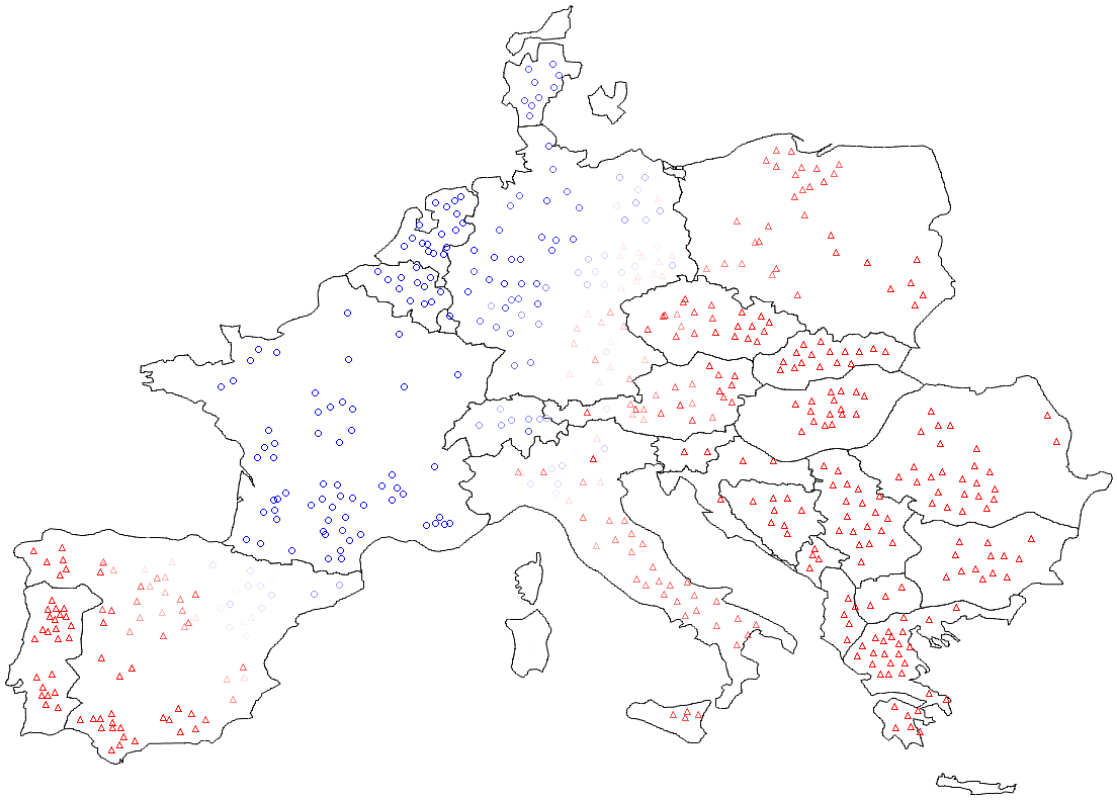

Figure G.15. Mode 2 - frequency 0.3794 Hz, damping 1.48, scenario X-13, strategy 2, Winter Peak

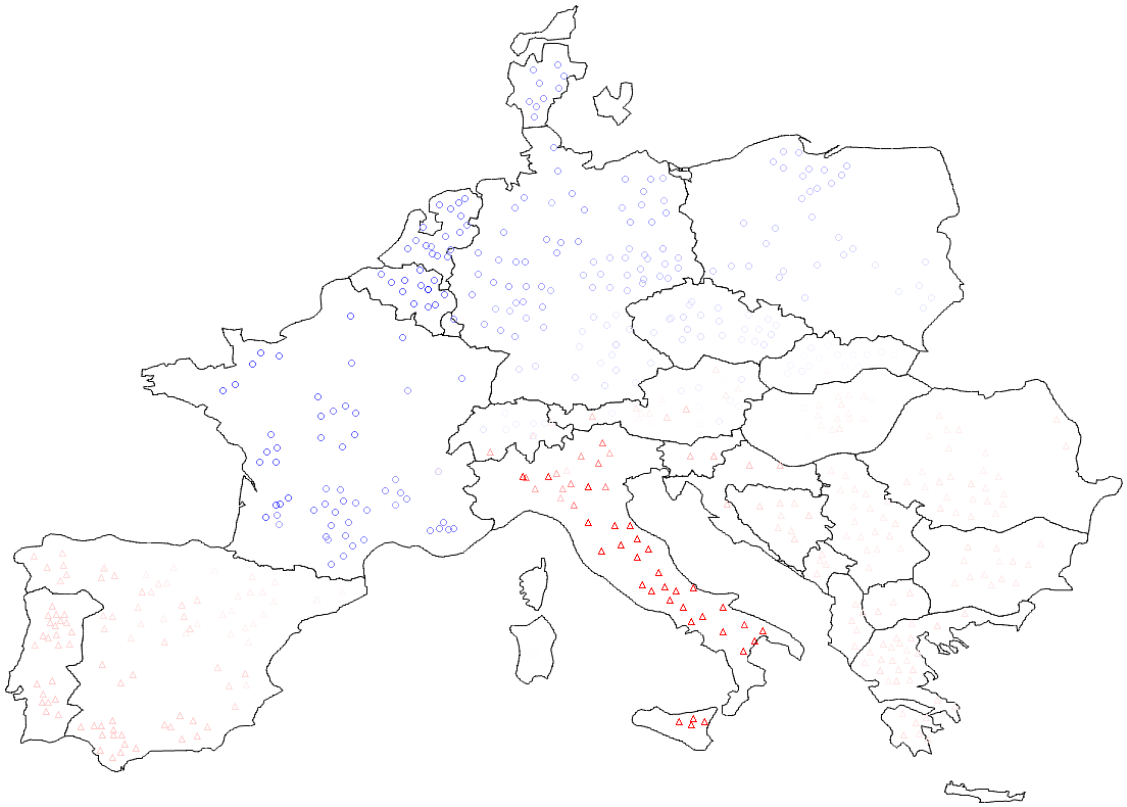

Figure G.16. Mode 2 - frequency 0.3382 Hz, damping -0.50, scenario X-13, strategy 3, Winter Peak

G.2.3. Mode 3

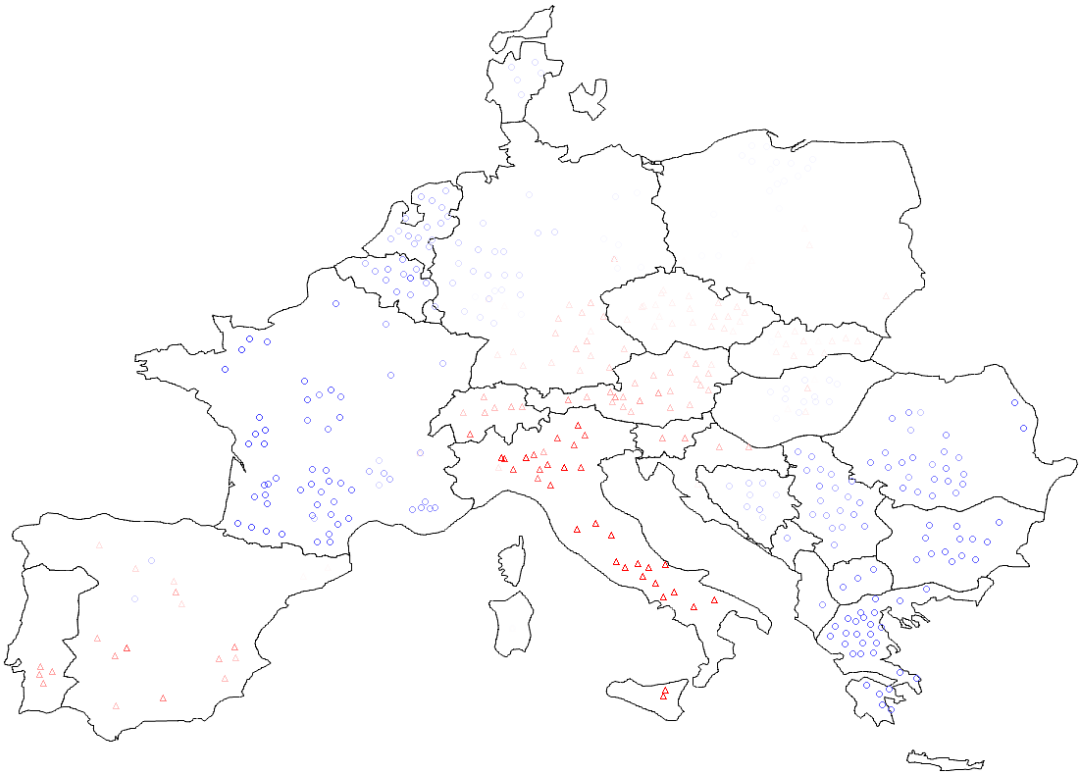

Figure G.17. Mode 3 - frequency 0.4665 Hz, damping 0.51, scenario X-13, strategy 3, Summer Low

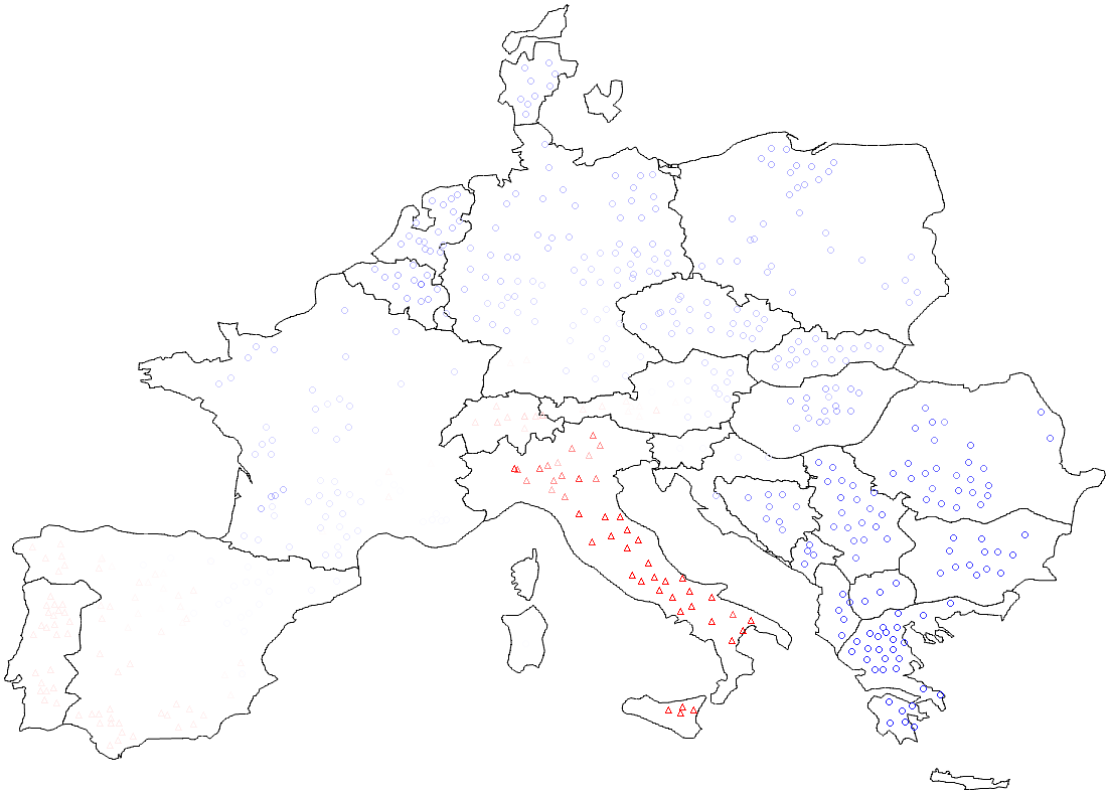

Figure G.18. Mode 3 - frequency 0.4053 Hz, damping 2.02, scenario X-13, strategy 2, Winter Peak

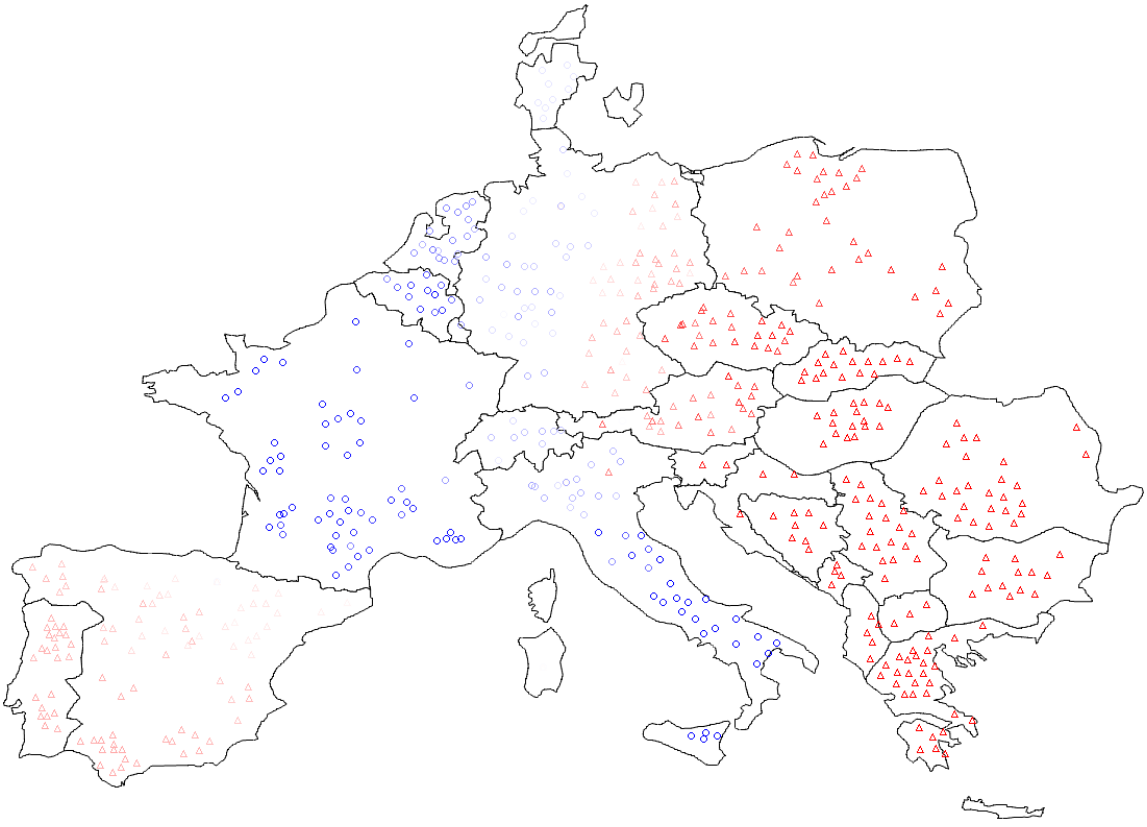

Figure G.19. Mode 3 - frequency 0.3439 Hz, damping 1.91, scenario X-13, strategy 3, Winter Peak

G.3. Scenario X-16

G.3.1. Mode 1

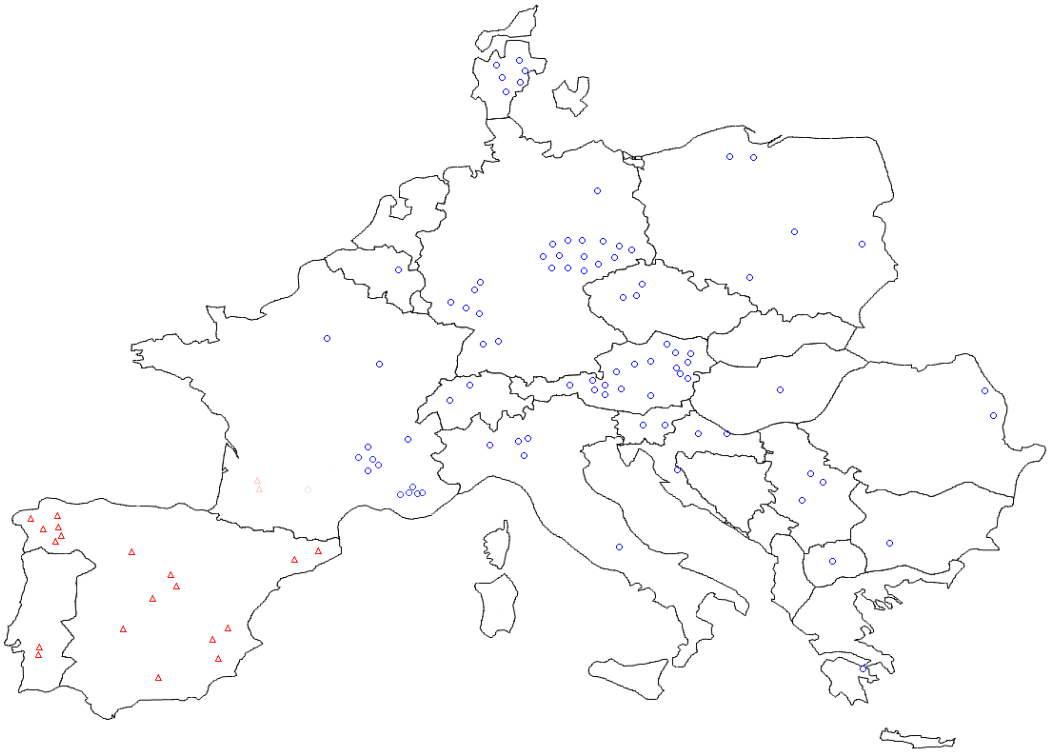

Figure G.20. Mode 1 - frequency 0.3648 Hz, damping 1.35, scenario X-16, strategy 2, Summer Low

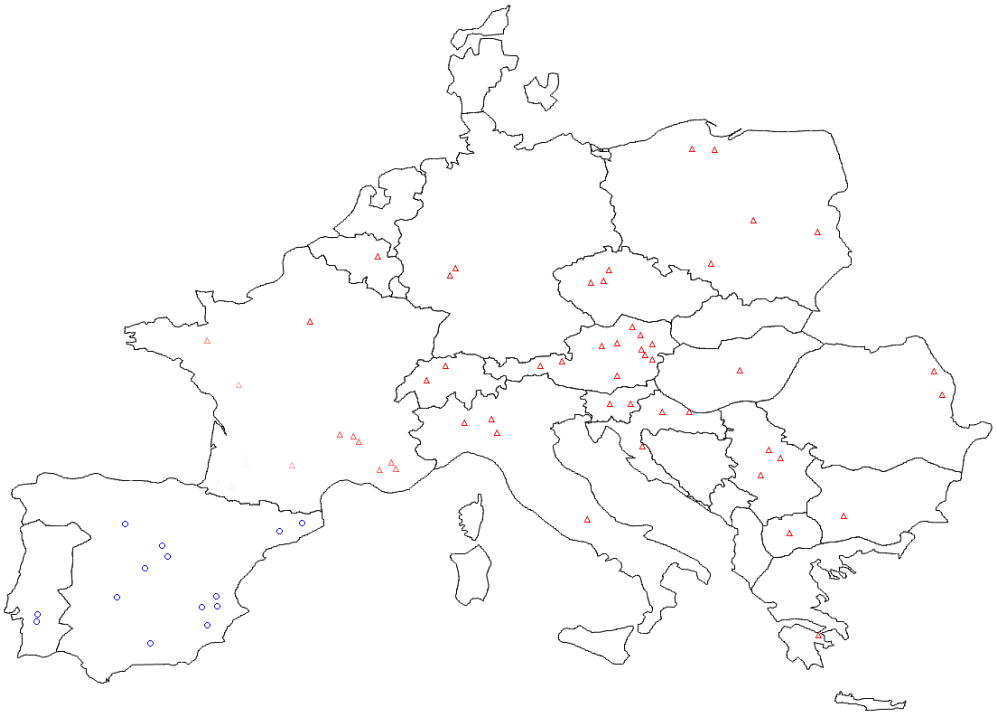

Figure G.21. Mode 1 - frequency 0.3816 Hz, damping 2.15, scenario X-16, strategy 3, Summer Low

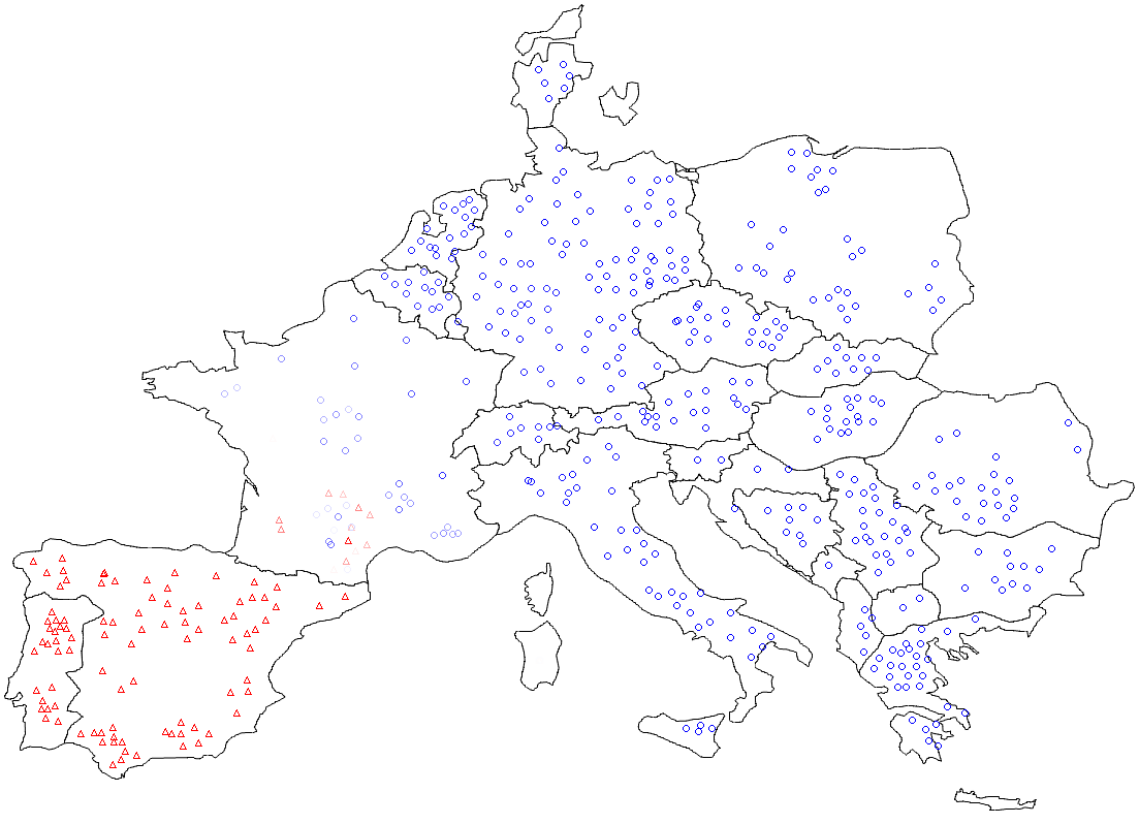

Figure G.22. Mode 1 - frequency 0.2026 Hz, damping 3.33, scenario X-16, strategy 2, Winter Peak

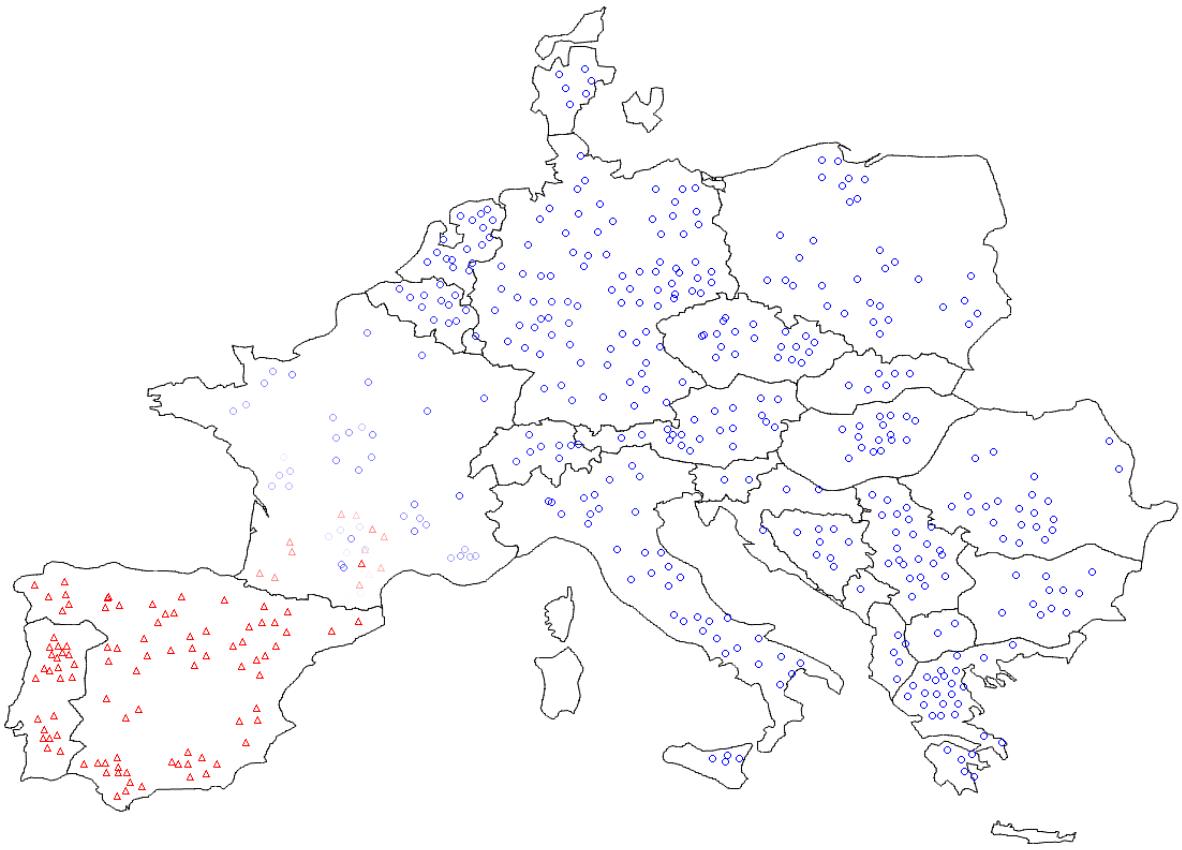

Figure G.23. Mode 1 - frequency 0.1937 Hz, damping 3.80, scenario X-16, strategy 3, Winter Peak

G.3.2. Mode 2

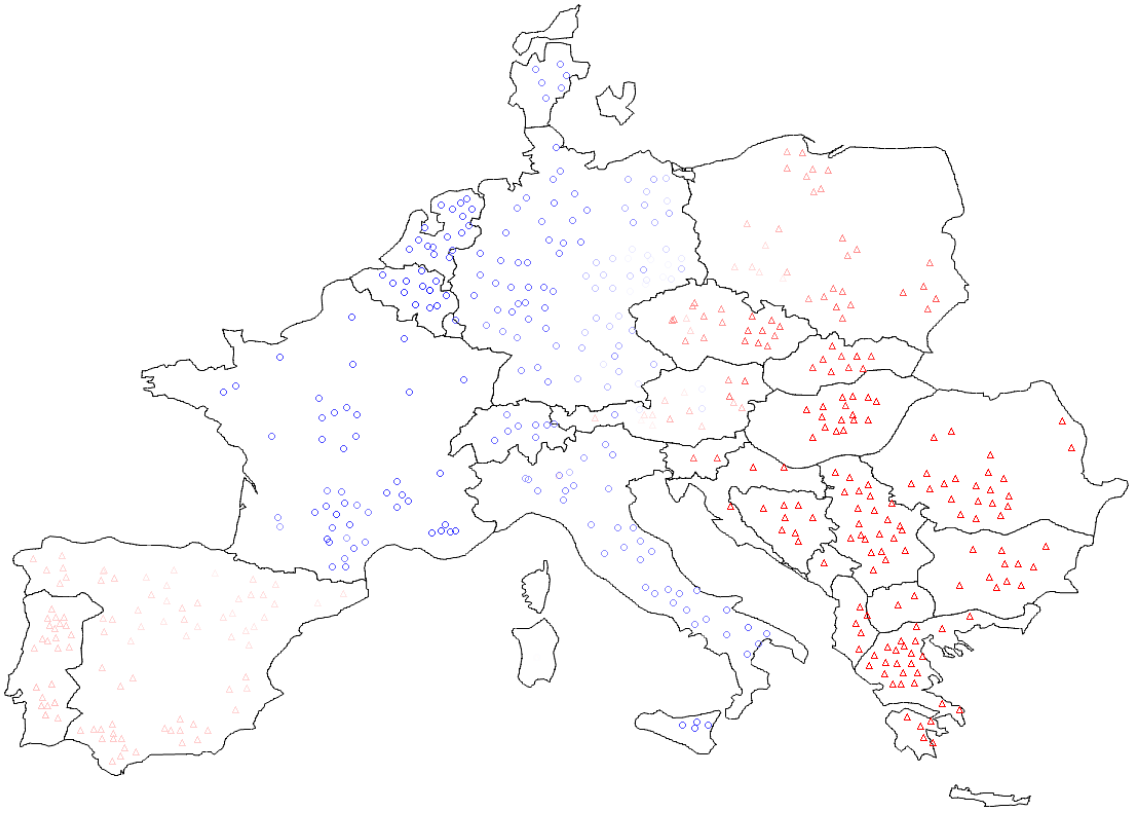

Figure G.24. Mode 2 - frequency 0.4060 Hz, damping 0.48, scenario X-16, strategy 2, Winter Peak

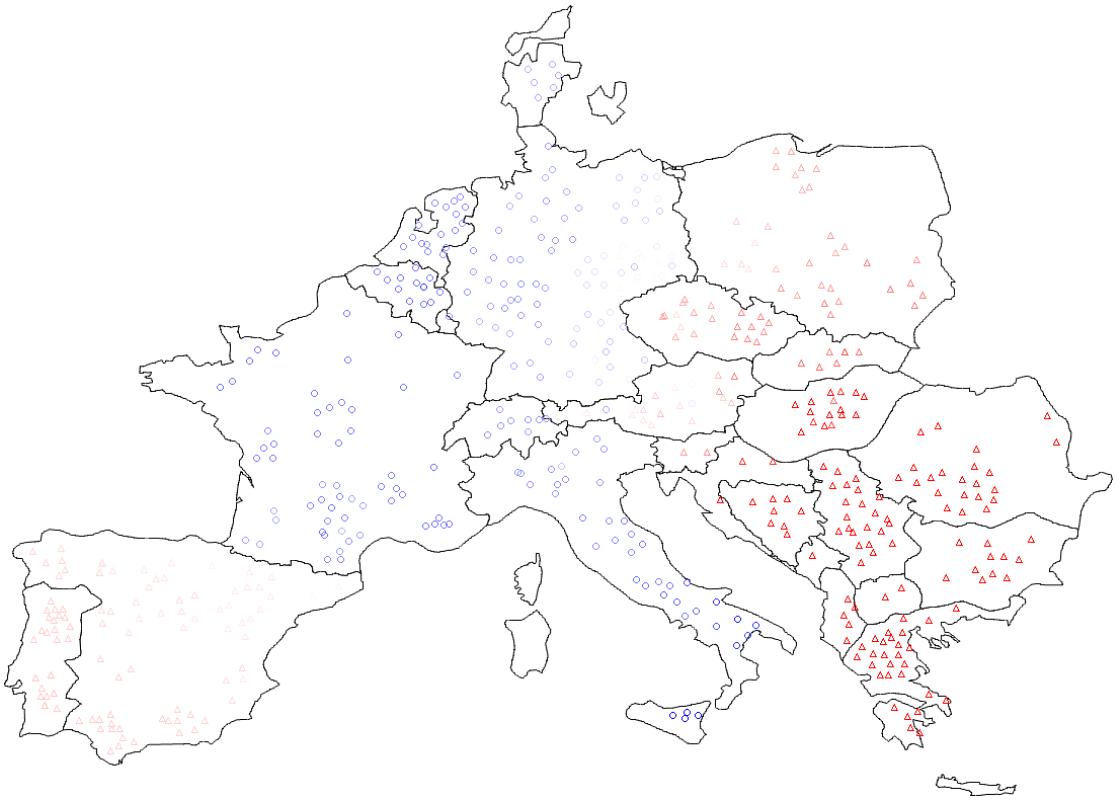

Figure G.25. Mode 2 - frequency 0.3753 Hz, damping 0.63, scenario X-16, strategy 3, Winter Peak

G.3.3. Mode 3

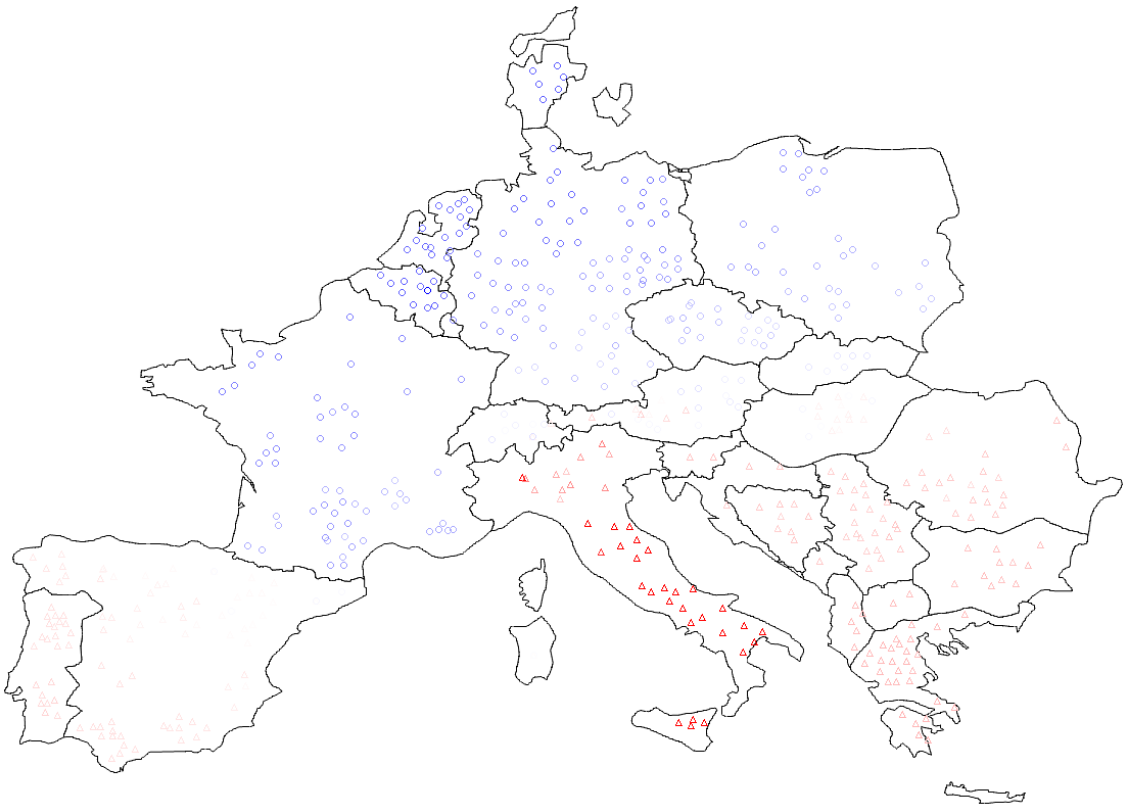

Figure G.26. Mode 3 - frequency 0.4325 Hz, damping 1.07, scenario X-16, strategy 3, Winter Peak

H. Detailed Voltage Analysis Plots

Voltage analysis has been performed by simulating the loss of every transmission grid reinforcement, using the base case (N) voltage as the normalised voltage. The horizontal axis is the Very High Voltage bus number for continental Europe. In the figures in this appendix, X7 refers to X-7, X10 to X-10, X13 to X-13 and X16 to X-16. S2 refers to Strategy 2 and S3 to Strategy 3. SL refers to Summer Low and WP to Winter Peak. This is not to be confused with WP as Work Package.

H.1. Scenario X-7

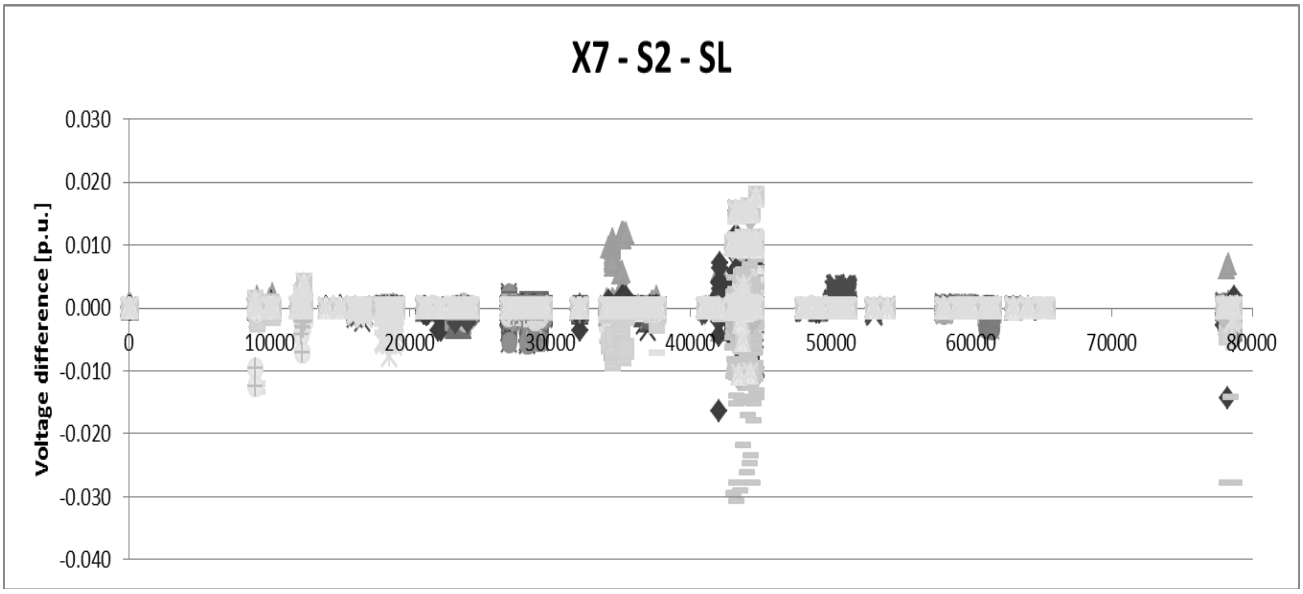

Figure H.1. Voltage difference of the n-1 grid reinforcements for X-7 – Strategy 2 – Summer Low

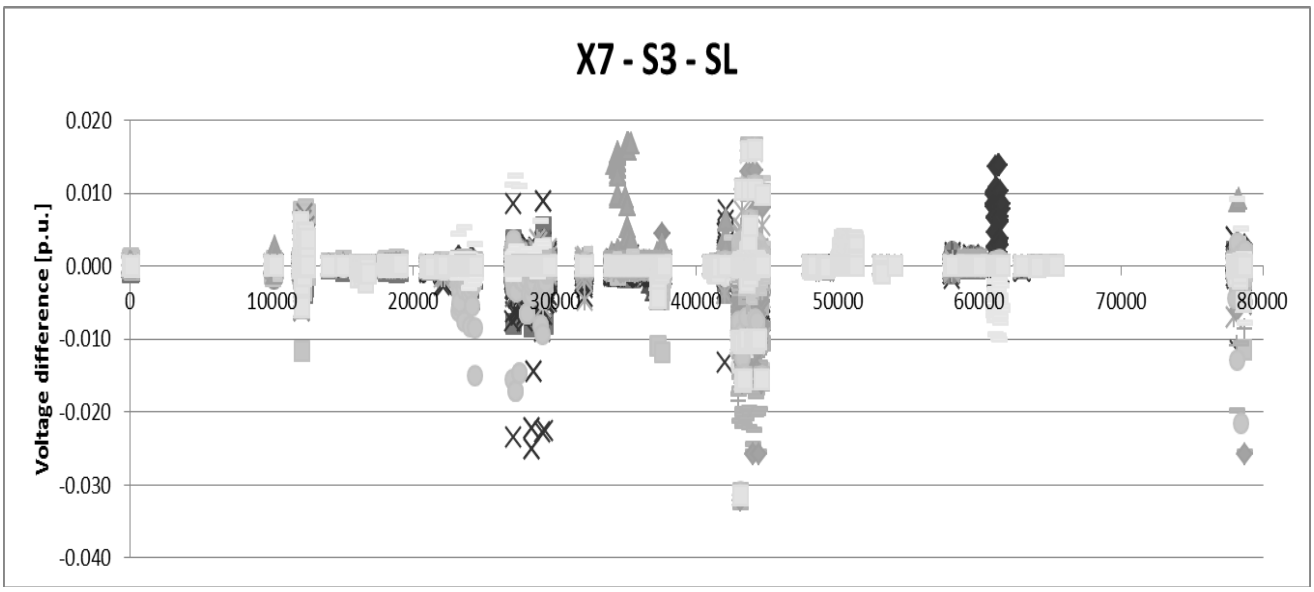

Figure H.2. Voltage difference of the n-1 grid reinforcements for X-7 – Strategy 3 – Summer Low

H.2. Scenario X-10

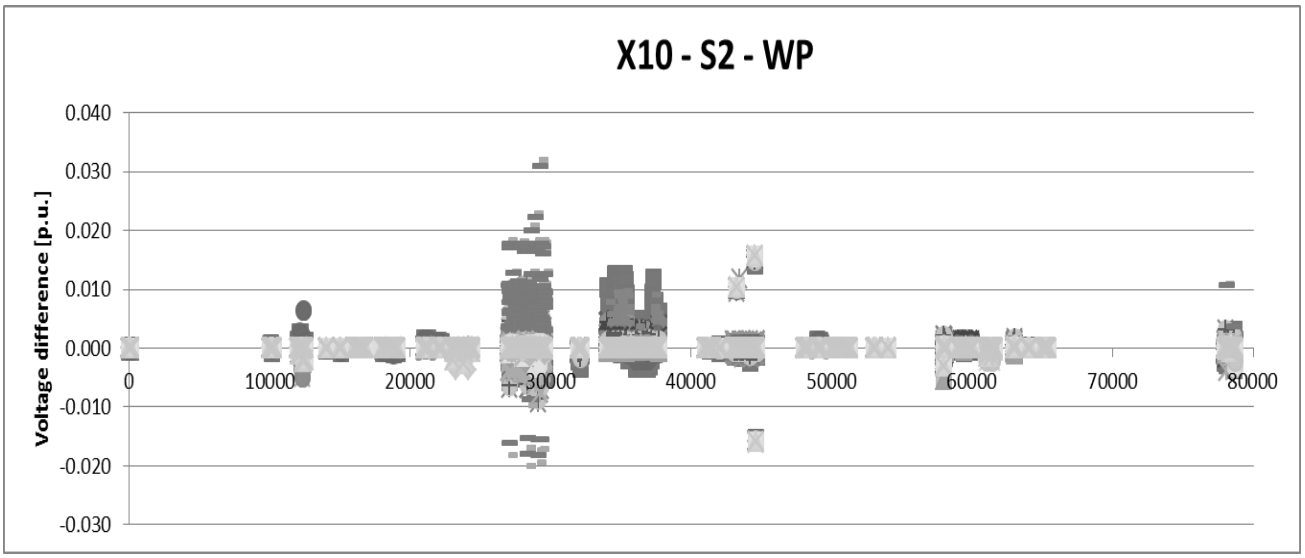

Figure H.3. Voltage difference of the n-1 grid reinforcements for X-10 – Strategy 2 – Winter Peak

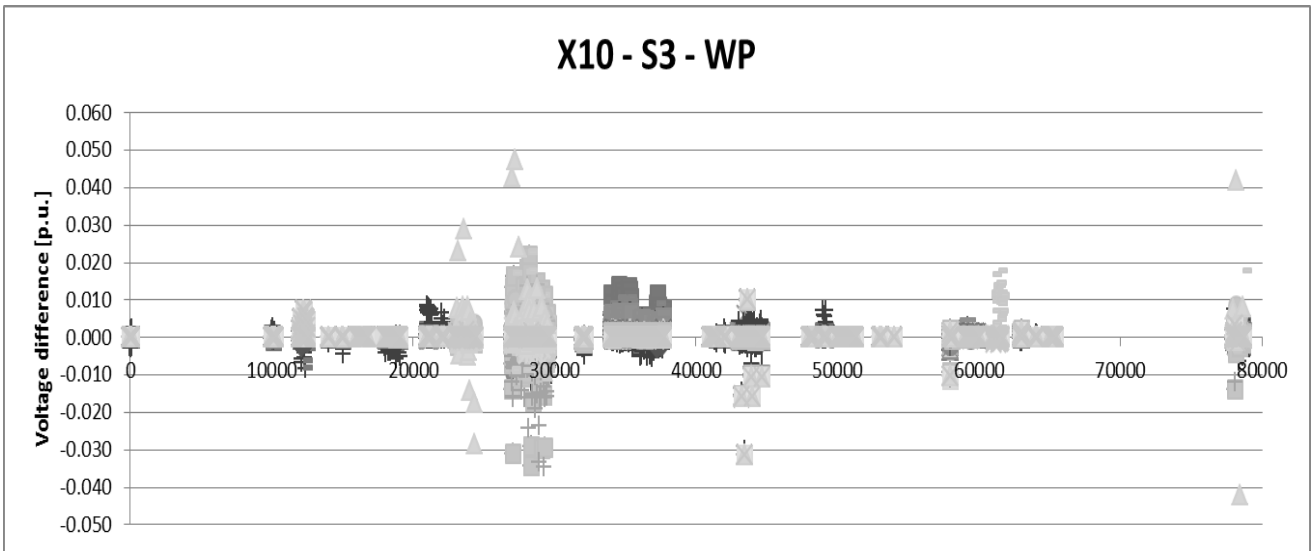

Figure H.4. Voltage difference of the n-1 grid reinforcements for X-10 – Strategy 3 – Winter Peak

H.3. Scenario X-13

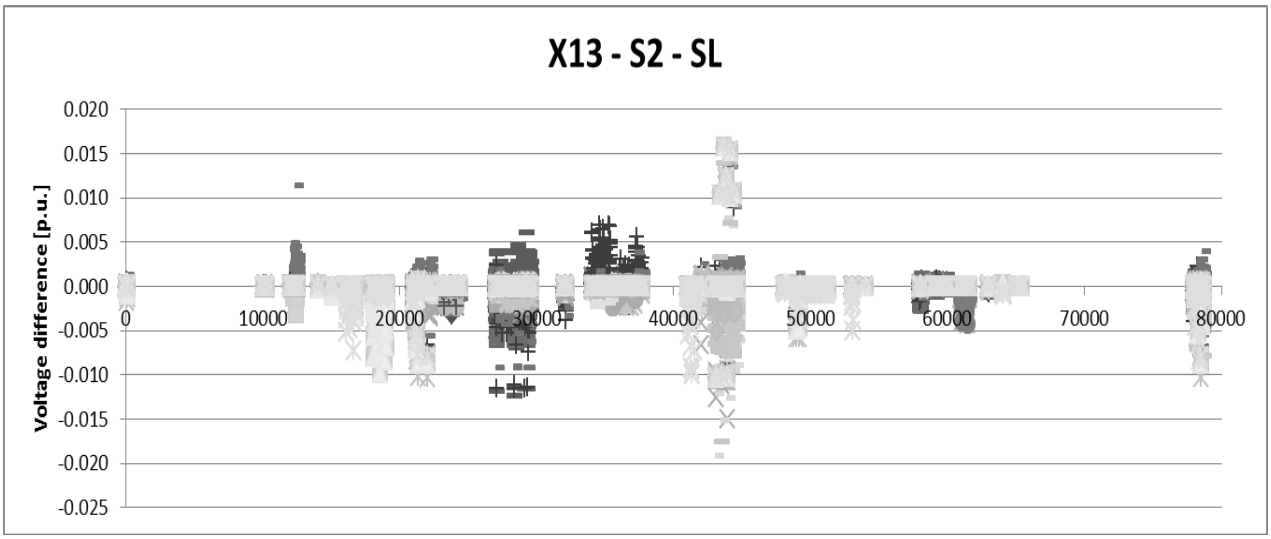

Figure H.5. Voltage difference of the n-1 grid reinforcements for X-13 – Strategy 2 – Summer Low

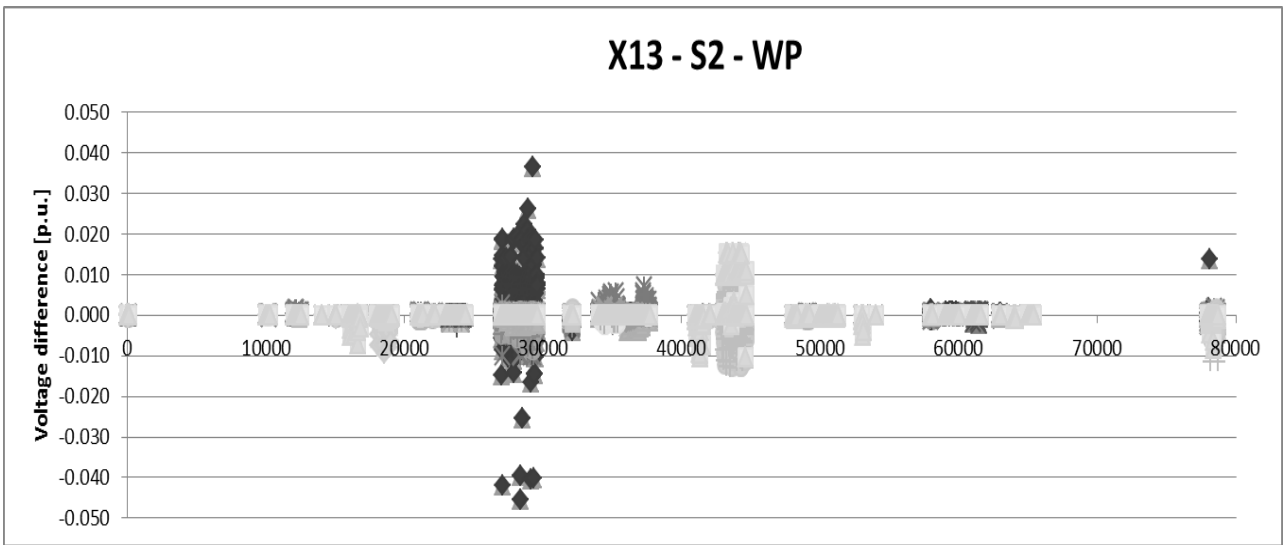

Figure H.6. Voltage difference of the n-1 grid reinforcements for X-13 – Strategy 2 – Winter Peak

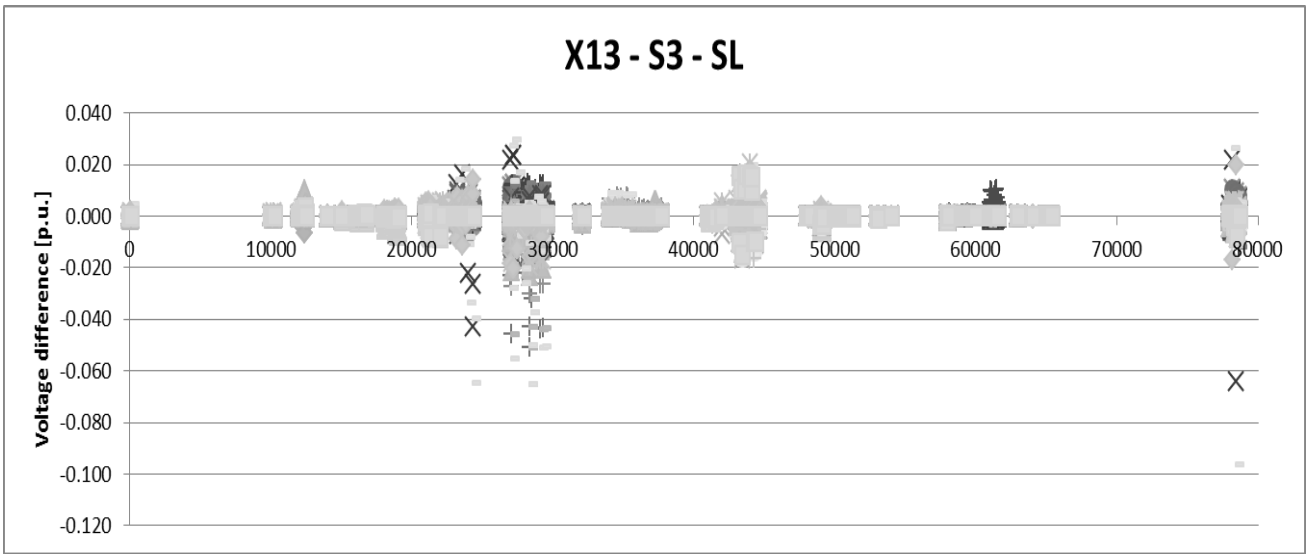

Figure H.7. Voltage difference of the n-1 grid reinforcements for X-13 – Strategy 3 – Summer Low

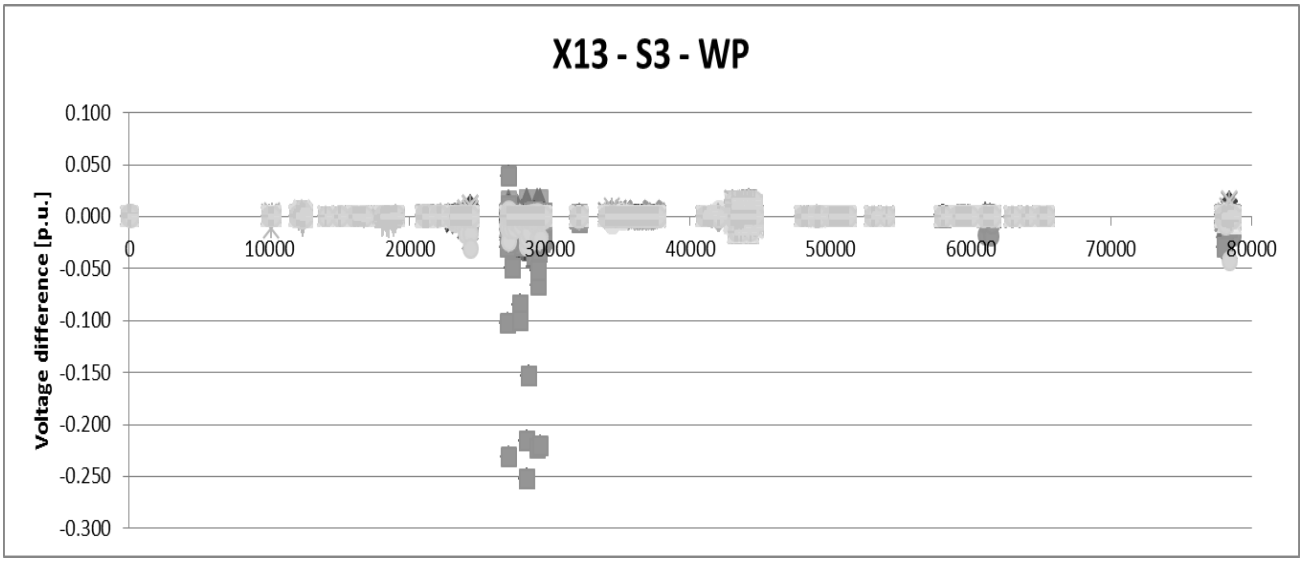

Figure H.8. Voltage difference of the n-1 grid reinforcements for X-13 – Strategy 3 – Winter Peak

H.4. Scenario X-16

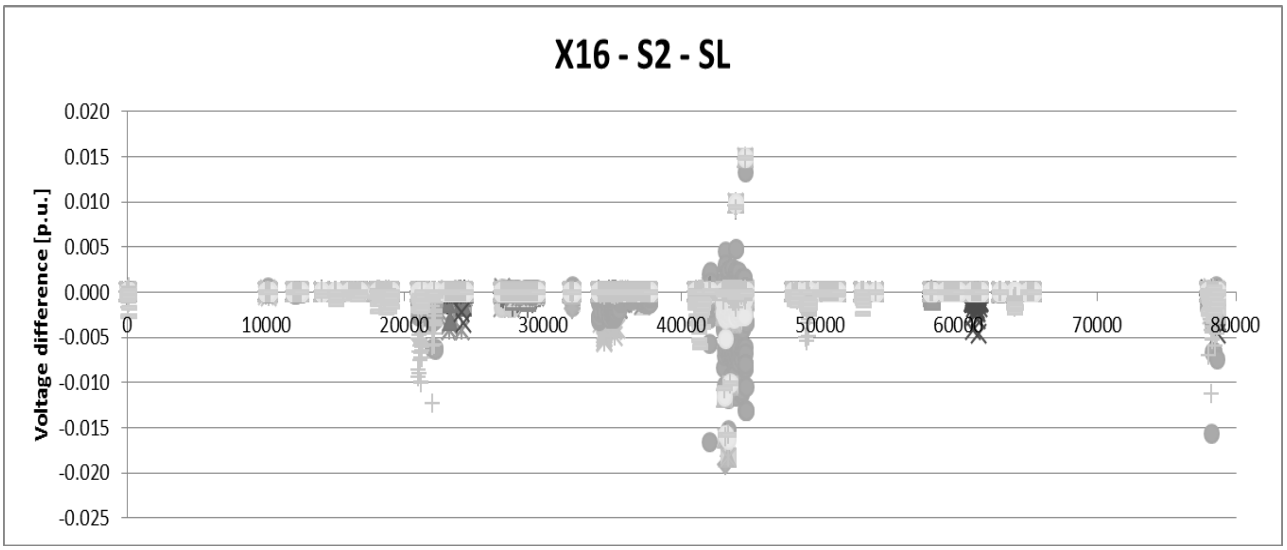

Figure H.9. Voltage difference of the n-1 grid reinforcements for X-16 – Strategy 2 – Summer Low

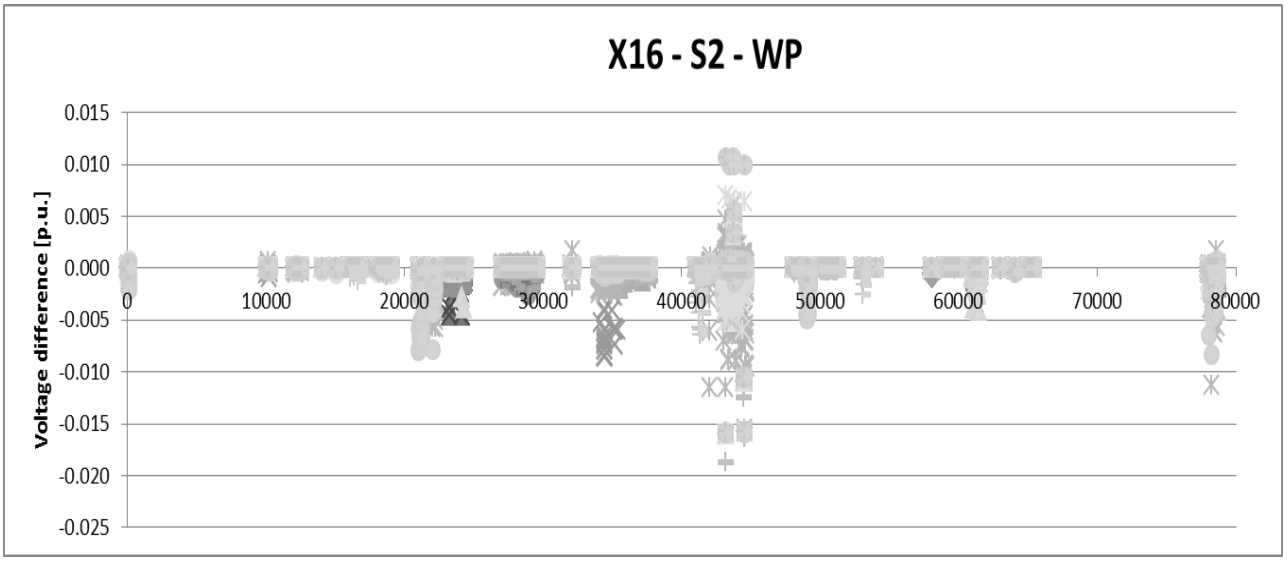

Figure H.10. Voltage difference of the n-1 grid reinforcements for X-16 – Strategy 2 – Winter Peak

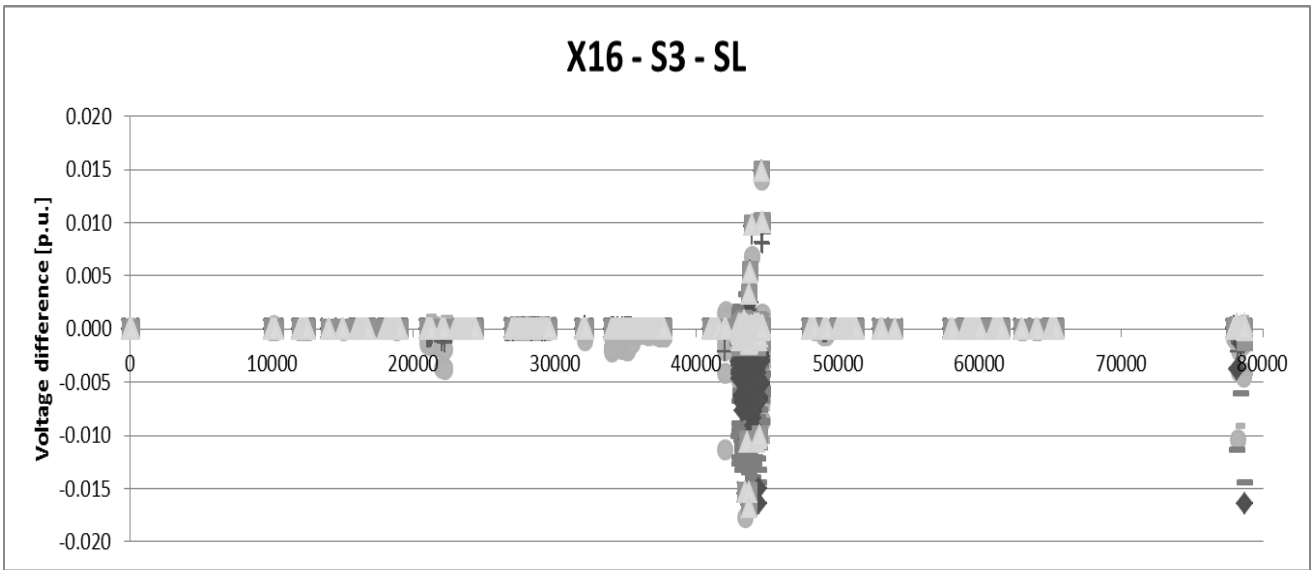

Figure H.11. Voltage difference of the n-1 grid reinforcements for X-16 – Strategy 3 – Summer Low

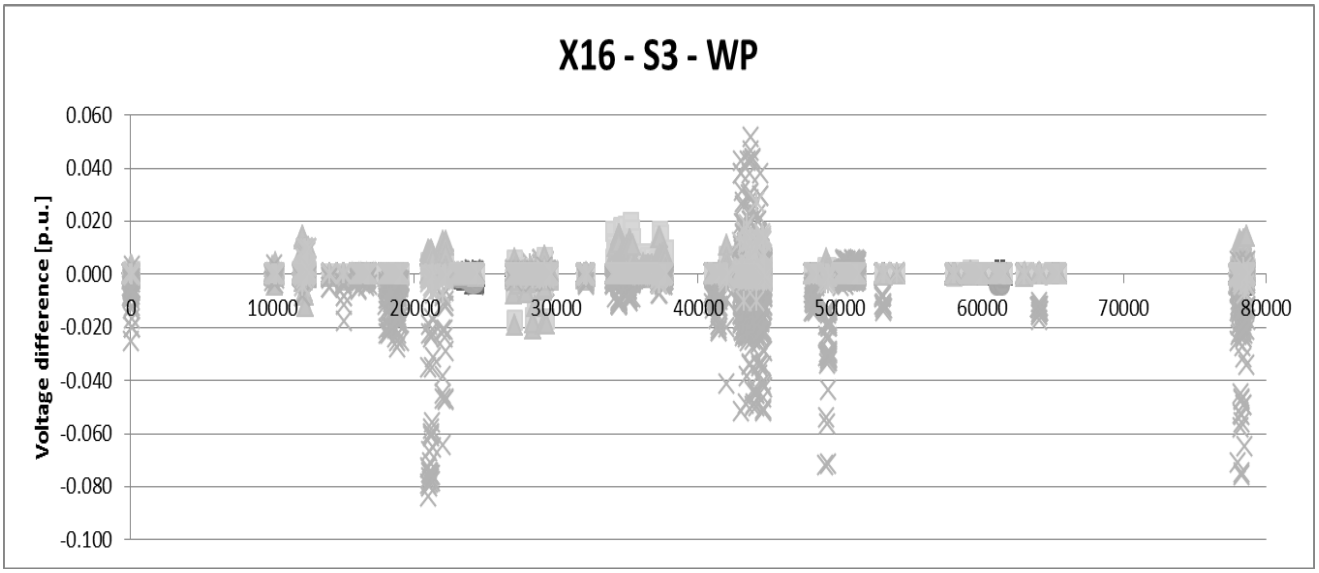

Figure H.12. Voltage difference of the n-1 grid reinforcements for X-16 – Strategy 3 – Winter Peak